A STUDY OF WATERFLOOD SWEEP EFFICIENCY IN A COMPLEX VISCOUS OIL RESERVOIR

By

Marc Daniel Jensen

GRADUATE ADVISORY COMMITTEE

Dr. Santanu Khataniar (Advisory Committee Chair)

Dr. Abhijit Dandekar (Advisory Committee Co-Chair)

Dr. Shirish Patil (Advisory Committee Member)

A STUDY OF WATERFLOOD SWEEP EFFICIENCY IN A COMPLEX VISCOUS OIL RESERVOIR

A
PROJECT

in Partial Fulfillment of the Requirements
for the Degree of

MASTER OF SCIENCE

By
Marc Daniel Jensen, B.S.

Fairbanks, AK

December 2014

ABSTRACT

West Sak is a multi-billion barrel viscous oil accumulation on the North Slope of Alaska. The unique geologic complexities and fluid properties of the West Sak reservoir make understanding ultimate sweep efficiency under waterflood a challenge. This project uses uncertainty modeling to evaluate the ultimate sweep efficiency in the West Sak reservoir and honors a rich dataset gathered from 30 years of development history.

A sector model encompassing the area of the West Sak commercial pilot was developed and a sensitivity analysis conducted to determine the most important parameters affecting sweep efficiency. As part of this process unique constraints were incorporated into the model including measured saturations at the end of history, and observed completion performance.

The workflow for this project was documented and can be adapted for use in larger scale models. The workflow includes the development of static cell properties which accurately represent field behavior, a preliminary history match using conventional methods and a sensitivity analysis employing a multi-run visualization tool to effectively navigate and process large amounts of data.

The main contributions of this work include the identification of key parameters affecting sweep efficiency in the West Sak oil field, a documented workflow, and increased insight into observed production behavior.

TABLE OF CONTENTS

SIGNATURE PAGE i
TITLE PAGE iii
ABSTRACT v
TABLE OF CONTENTS vi
LIST OF FIGURES vii
LIST OF TABLES viii
LIST OF APPENDICES ix
ACKNOWLEDGEMENTS x
CHAPTER 1.0 INTRODUCTION 1
CHAPTER 2.0 LITERATURE SURVEY 5
CHAPTER 3.0 PROJECT BACKGROUND 7
CHAPTER 4.0 SIMULATION STUDY 11
CHAPTER 5.0 RESULTS AND DISCUSSION 36
CHAPTER 6.0 CONCLUSION 38
CHAPTER 7.0 RECOMMENDATIONS 39
CHAPTER 8.0 REFERENCES 40
CHAPTER 9.0 APPENDICES 43
Appendix A: Well-level Match Quality Plots 43

LIST OF FIGURES

Figure 1-1: Alaska North Slope Location Indicator (after Burton et al. 2005; Davis et al. 2005; Peirce et al. 2014) 2
Figure 1-2: Simulation Study Workflow 3
Figure 3-1: West Sak Type Log 8
Figure 3-2: West Sak Pilot Area Bottomhole Locations (after Targac et al. 2005) 10
Figure 4-1: Plan View of Geostatistical Model 11
Figure 4-2: 3D Simulation View of West Sak Pilot 13
Figure 4-3: D Sand Permeability Distribution, Model Layer 4 14
Figure 4-4: B Sand Permeability Distribution, Model Layer 24 15
Figure 4-5: A Sand Permeability Distribution, Model Layer 77 16
Figure 4-6: Comparison of Actual and Calculated Model Cumulative Oil Volumes 17
Figure 4-7: Comparison of Actual and Calculated Model Cumulative Produced Water Volumes 18
Figure 4-8: Comparison of Actual and Calculated Model Cumulative Gas Volumes 18
Figure 4-9: Comparison of Actual and Calculated Model Injection Water Volumes 19
Figure 4-10: Saturation Change Snapshot and Location of Conduit 20
Figure 4-11: Comparison of Actual and Calculated Model Oil Rates in West Sak Pilot Producer 12 21
Figure 4-12: Comparison of Actual and Calculated Model Water Rates for West Sak Pilot Producer 12 21
Figure 4-13: D Sand Suppressed Resistivity in Offset Well Log 23
Figure 4-14: Comparison of Heritage and Project Model Results 24
Figure 4-15: Base Case Fractional Flow Curve 28
Figure 4-16: Modified Fractional Flow Curve 30
Figure 4-17: Contribution to Variance Tornado Diagram 34

LIST OF TABLES

Table 3-1: Summary of West Sak Reservoir Properties 9
Table 4-1: Average Properties for West Sak Pilot 8i (McGuire et al. 2005).....12
Table 4-2: Summary of History Matched Model Adjustments 17
Table 4-3: Comparison of Heritage and Project Model Results 24
Table 4-4: Summary of Uncertainty Parameters.....26
Table 4-5: Updated Summary of Uncertainty Parameters 31

LIST OF APPENDICES

Appendix A: Well-level Match Quality Plots.....43

ACKNOWLEDGEMENTS

I would like to thank ConocoPhillips Alaska, Inc., BP Exploration (Alaska) Inc., Chevron USA Inc., and ExxonMobil Alaska Production Inc. for the opportunity to submit this work as partial fulfillment of the requirements for a Master of Science Degree in Petroleum Engineering. This paper reflects my views which are not necessarily the views of the owner companies. I would like to thank the 30 years' worth of lab and field personnel who contributed directly and indirectly to the data used in this project. Many special thanks to Scott Redman for his patient mentorship and expertise in guiding this project. I would like to thank my manager, James Rodgers, and supervisor, Brian Seitz, for their detailed proof reading, continued encouragement, and help with the approval process. Also, I am grateful for the support of Mark Scheihing, Brian Ludolph, and Hari Sudan and the time the donated to this project through the answering of my questions. I would like to thank my graduate advisory committee at UAF consisting of Dr. Santanu Khataniar, Dr. Abhijit Dandekar, and Dr. Shirish Patil for their support during my time as a graduate student.

CHAPTER 1.0
INTRODUCTION

1.1 Background

Heavy and viscous oil assets located on the North Slope of Alaska represent a development target with as much as 25 billion stock tank barrels (STB) of original oil in place (OOIP). Two low- API gravity oil zones are the main development targets, informally called Ugnu and West Sak (Werner 1987). The West Sak field is the subject of this project. Figure 1-1 on the next page illustrates the location of the West Sak field in relation to other developments on the North Slope of Alaska.

Development of the field began with a three year multi-well pilot which spanned the years of 1983 through 1986. The results of the pilot provided the foundation for future development of the West Sak field. Following the pilot, full-scale commercial development began in the early 1990's. Commercial development of the field occurred in phases beginning with vertical producers and injectors in a traditional five-spot pattern. The second phase incorporated horizontal producers with offset vertical injectors. The third and current phase of development consists of horizontal, multi-lateral producers and injectors (Burton et al. 2005; Foerster et al. 1997; Targac et al. 2005).

New and unforeseen challenges arise from the ever changing development landscape. Innovative ideas are in constant demand to optimize well designs and reservoir management practices. Recent surveillance data has prompted a relook into the way reservoir modeling is approached in the West Sak field. This project focuses on the fundamental assumptions of the current modeling approach by revisiting the West Sak Pilot.

The West Sak commercial-scale pilot was successful in many ways, one of which was the mass amounts of data collected and recorded. The goal of this project is to integrate all of these data and incorporate learnings from the subsequent developments into an integrated reservoir simulation study. The primary outcome sought in this project is to better understand reservoir sweep efficiency under waterflood in the West Sak field. An improved understanding will be achieved through determining which simulation parameters have the greatest impact on sweep efficiency and their associated uncertainty.

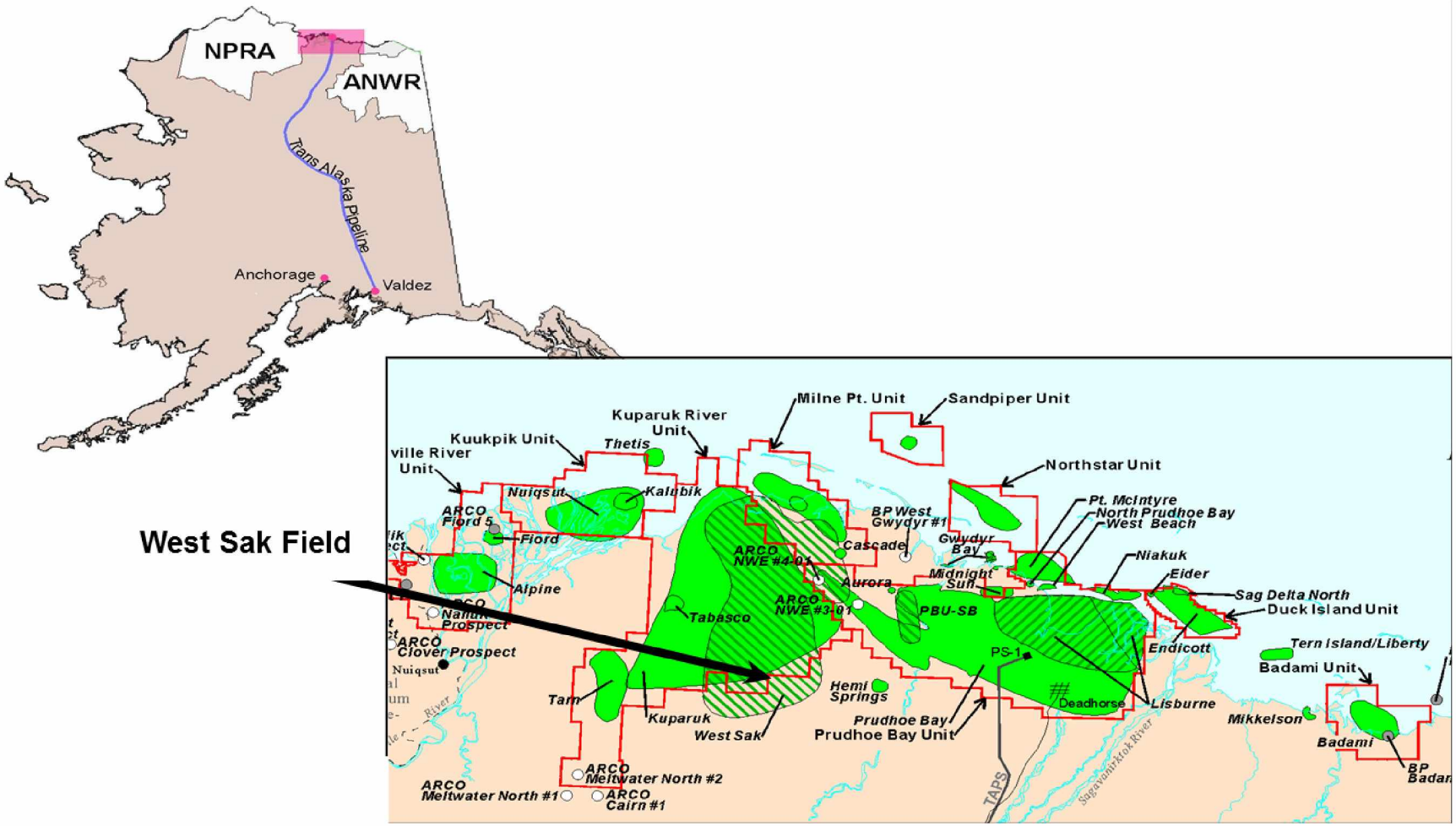

Figure 1-1: Alaska North Slope Location Indicator (after Burton et al. 2005; Davis et al. 2005; Peirce et al. 2014)

1.2 Objectives

The primary objectives for this study are listed below and discussed in further detail in the next section.

- Build a fine-grid reservoir model that accurately represents the West Sak pilot area
- Identify key uncertainties affecting sweep efficiency in the reservoir model
- Document insights into reservoir sweep efficiency gained through the workflow
- Document the study workflow for use in future studies

1.3 Methodology

The first step of this project was to conduct a literature survey of industry articles to determine best practices for an integrated approach to conducting a simulation study. Next, a simulation model was built. This began by incorporating a static grid model into the reservoir simulation environment. All needed production and surveillance data was also gathered and imported into the simulation package. A conventional history match was used to validate the model to ensure it was an adequate representation of actual behavior. Once the model was built and validated, the most significant factors affecting sweep efficiency were identified.

A diagram of the study workflow is illustrated in Figure 1-2. Each step of the workflow is discussed in more detail in Section 3 of this document.

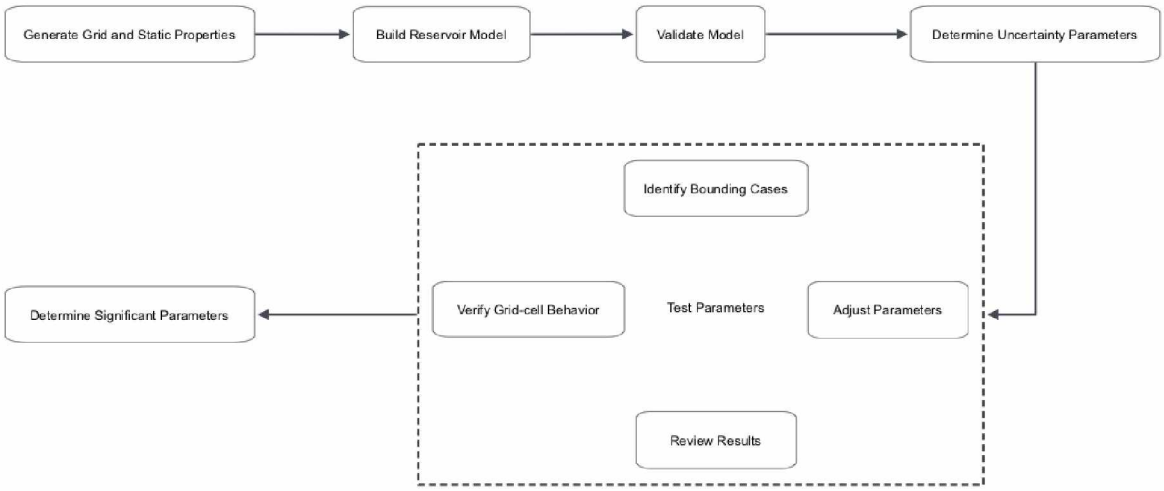

Figure 1-2: Simulation Study Workflow

1.4 Summary of Results

A simulation model of the West Sak Pilot area was successfully built and validated. A history match was obtained and compared to similar modeling efforts conducted during a

heritage post-audit of the pilot. Learnings from the last 30 years of commercial developments guided the history matching efforts. Knowledge of reservoir behavior was crucial to choosing which simulator parameters were the key drivers to match observed data.

Once the model was validated, uncertainty parameters were identified with their ranges of uncertainty. These ranges were tested and adjusted to capture bounding cases. Once the parameters and ranges were established, a Latin Hypercube simulation run matrix was developed and the simulation runs completed. Results of the simulation runs were used to calculate contributions to variance. From the results the most significant uncertainty parameters affecting match quality were identified. They are listed here in order of significance.

1. Initial water saturation
2. Relative permeability relationships between oil and water
3. Permeability multiplier in the high permeability layers of the B sand
4. Permeability multiplier in the high permeability layers of the D sand
5. Net-to-gross in the high permeability layers of the D sand
6. Permeability multiplier in the A2 sand
7. Net-to-gross in the high permeability layers of the A2 sand

Conclusions about the sweep efficiency of the waterflood were then made from the overall project workflow. The project's primary conclusion indicated observed displacement efficiency was better than premised in existing simulation models. This was observed in the top two uncertainty parameters and confirmed by log data. Essentially, the high permeability D sands were swept to high water saturations during the West Sak Pilot waterflood. To recreate this behavior in the model, the relative permeability curves were adjusted. Shifts in the relative permeability curves allowed average water saturations behind the waterflood front to increase thereby bringing the model saturations much closer to observed values.

The other significant conclusion regarding sweep efficiency focused on the permeability adjustments in the high permeability layers of the model. Permeability multipliers in these layers were three of the most significant uncertainty parameters from the contribution to variance analysis. These results suggested areal and vertical sweep were relatively high in the high permeability layers and remained low or nonexistent in the lower permeability layers.

CHAPTER 2.0
LITERATURE SURVEY

A literature survey was conducted to determine what approaches of this study type were conducted by other industry professionals. Much has been published in recent past regarding simulation-study design. The focus of many studies was statistical methods for employing experimental design as a method to adequately and efficiently evaluate a multitude of viable scenarios.

The nature of reservoir simulation makes it a natural proving ground for experimental design methodologies. Several industry studies document the usefulness of experimental design as an efficient approach to simulation studies and the quantification of uncertainties within experimental design. Kalla and White (2005) reviewed the elements of experimental design and response surface modeling. They then applied the methods of experimental design to a gas coning problem. Lee et al. (2006) provided a workflow approach to uncertainty analysis for reservoir performance. Experimental design was a key part of their workflow. White and Royer (2003) showed the usefulness of designed reservoir simulation using response surfaces to efficiently simulate, analyze, and optimize a potential deep-water development.

The more common use of experimental design in reservoir simulation studies has been to quantify uncertainties for optimizing development plans. Esmaiel (2005) used experimental design methods to optimize a smart-well water-alternating-gas flood. He showed the efficiency of response surface modeling in determining the uncertainty associated with various factors affecting ultimate hydrocarbon recovery. Manceau et al. (2002) used experimental design to perform a technical risk analysis on a case study field. They showed the benefits of applying experimental design techniques to make better decisions in risk-prone environments. Nguyen et al. (2011) used experimental design to optimize a SAGD development in Alberta, Canada. They used a response surface methodology based on a central composite design to determine which development design maximized cumulative oil and net present value. Zhang et al. (2005) also showed the usefulness of experimental design in optimizing an improved oil recovery process. They used an integrated reservoir simulation system to distribute the computational load and show an appropriate workflow to develop the system. It included a response surface methodology, an optimization algorithm, and integration of a cash flow economic model. They successfully identified the significant factors to maximize value of the improved recovery process.

History matching is one area of reservoir simulation where experimental design provides a framework for investigation. The outcome of history matching is often dependent on the skills of the reservoir engineer. Comparing calculated to actual field data and then applying relevant changes to the simulator based on a keen understanding of the reservoir is a difficult task. Experimental design and probabilistic approaches to history matching show benefit and provide a framework for consistency. den Boer at al. (2006) described a workflow to quantify and rank reservoir and geologic uncertainties. They showed how this workflow assists the reservoir engineer in honoring production data in the reservoir model. Sahni et al. (2010) clearly document an assisted history match process using experimental design to assess the quality of match and perform uncertainty analysis. They demonstrated this using a sector model. Sonde et al. (2013) describe another workflow to identify key uncertainty parameters and match criteria, determine parameters with the most impact, and develop an adequate response surface model. The model was then used to generate a range of adequate history matches for the non-unique history-matching solution. Uldrich et al. (2002) developed a novel approach to determine a quality of match parameter which includes the inherent uncertainties of field measurement and simulator calculations. They used the quality of match parameter as a guide to determine the best history-match scenario.

CHAPTER 3.0
PROJECT BACKGROUND

3.1 Geological Review

The West Sak viscous oil reservoir is late Cretaceous consisting of very fine to fine-grained sandstone and silty sandstone with interbedded siltstone and mudstone. West Sak is a monocline with northwest to southeast strike and corresponding one to two degree dip northeast to southwest (Werner 1987). The reservoir ranges in depth from approximately 2000 ft subsea in the southwest to approximately 4500 ft subsea in the northeast (Foerster et al. 1997) and has a gross thickness ranging from 200 ft to 450 ft (Panda et al. 1989). Additionally, continuity of the highly-stratified West Sak sands has been demonstrated at up to 80 acre well spacing (Davis et al. 2005).

The West Sak sands are unconsolidated and very friable with unconfined compressive strengths ranging from less than 100 psi to greater than 8000 psi (Burton et al. 2005). The unconsolidated nature of the sands has been the source of many challenges. Fundamental changes to the overall field development plan were implemented to meet these challenges including a shift from sand exclusion to sand management practices. (Targac et al. 2005). Additionally, sand production is believed to have created short-circuits between injectors and producers thereby damaging pattern sweep (Peirce et al. 2014).

The West Sak sands consist of an upper and lower member. The upper member includes two main sand packages called the D and B sands. The average thickness of the D and B sands are 30 ft and 20 ft respectively. The lower member consists of many thin bedded layers ranging from less than 1 ft to 10 ft thick with a net sand thickness of 80 ft to 90 ft (Burton et al. 2005, Davis et al. 2005; Werner 1987). Figure 3-1 is a general type log of West Sak sands illustrating the above mentioned stratigraphy.

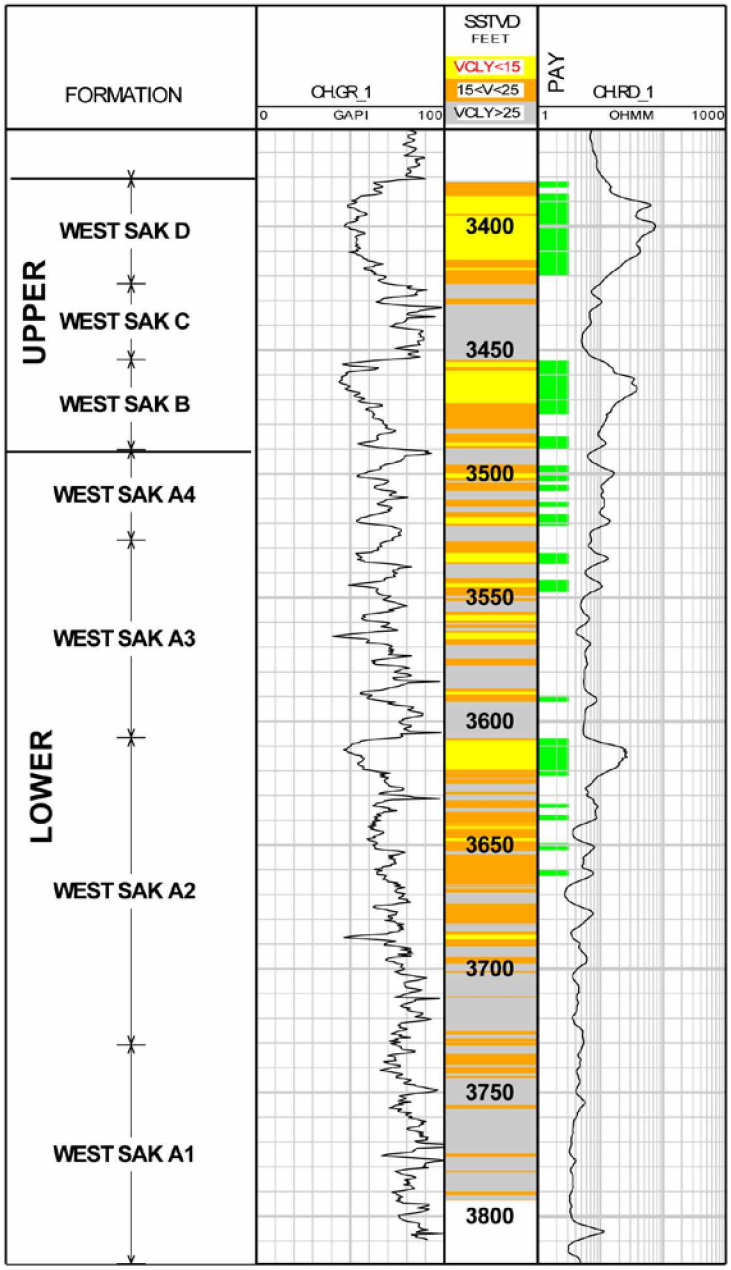

Figure 3-1: West Sak Type Log

(after Burton et al. 2005; Davis et al. 2005; Peirce et al. 2014)

3.2 Reservoir Properties

In general, reservoir temperature, pressure, and API gravity increase with depth. This trend highlights the varying degree of oil quality associated with biodegradation and proximity to permafrost by depth (Werner 1987). Table 3-1 summarizes the general reservoir properties associated with the oil of the West Sak reservoir.

Table 3-1: Summary of West Sak Reservoir Properties
(Foerster et al. 1997; McGuire et al. 2005; Sharma et al. 1989; Werner 1987)

Reservoir Property	Average Value or Range
API Gravity	10° - 22°
Reservoir Temperature	45°F - 100°F
Reservoir Pressure	1000 psi - 1800 psi
Porosity	25% - 35%
Permeability	50 md - 400 md
Viscosity	<30 cp - >3000 cp

3.3 West Sak Commercial Pilot

Atlantic Richfield Company (ARCO) premised a two to three year pilot to determine the economic feasibility of a full-field development in West Sak. The primary objectives were to evaluate waterflood response, and drilling and completion technologies (Werner 1987). The two and a half year pilot, which began in 1983, produced a cumulative of almost 800 thousand barrels of oil for a total investment of approximately 135 million dollars (Bidinger and Dillon 1995). A total of 15 wells were drilled, consisting of vertical cased-hole gravel-pack and frac-pack producers, and vertical cased-hole and perforated injectors. All intervals, the A, B, and D sands, were targeted in each of the wells. They were drilled in an inverted nine-spot pattern on five acre spacing (Burton et al. 2005; Davis et al. 2005). The tight well spacing allowed for higher throughput and thus quicker response time to observe waterflood behavior. In terms of performance, the producers averaged 120 BOPD without stimulation and 250 BOPD with stimulation (Bidinger and Dillon 1995). Figure 3-2 is an illustration of the West Sak pilot area and depicts the bottomhole location of each well.

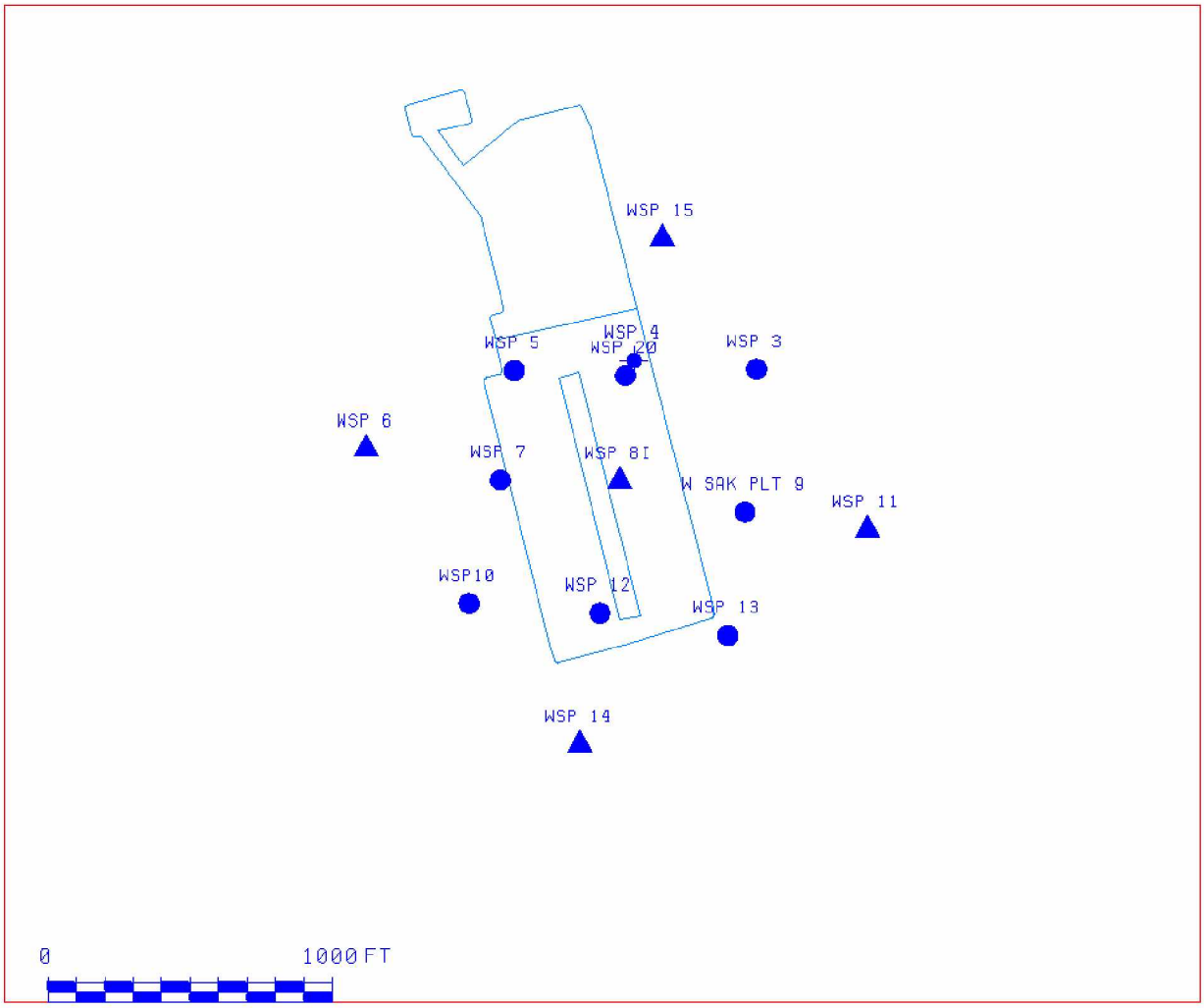

Figure 3-2: West Sak Pilot Area Bottomhole Locations (after Targac et al. 2005)

In short, the pilot successfully met its technical objectives. The reservoir did indeed exhibit a waterflood response and several types of drilling and completion designs were evaluated. The results of the pilot became the foundation for many decisions made during the commercial development phases of West Sak. The highly technical nature of the West Sak pilot necessitated the capturing of data for every decision and major event while in operation. Additionally, much effort was spent at the conclusion of the pilot to consolidate, organize, and analyze the data collected. The vast amount of data provides a rich backdrop for a fundamental study of the West Sak reservoir. This is the primary reason this dataset was used for this simulation study.

CHAPTER 4.0
SIMULATION STUDY

4.1 West Sak Pilot Area Simulation Model

The geostatistical model for this project was developed and validated by Mark H. Scheihing (Scheihing, 2014). The total area of influence is 3,050 ft. by 3,050 ft. with a grid block size of 50 ft. by 50 ft. in the x and y directions, respectively. This results in a 61 x 61 grid with 99 layers yielding a total cell count of 368,379. The thickness of each layer varies in an effort to more accurately capture the laminar nature of the West Sak sands. Figure 4-1 is a plan view of the geostatistical model.

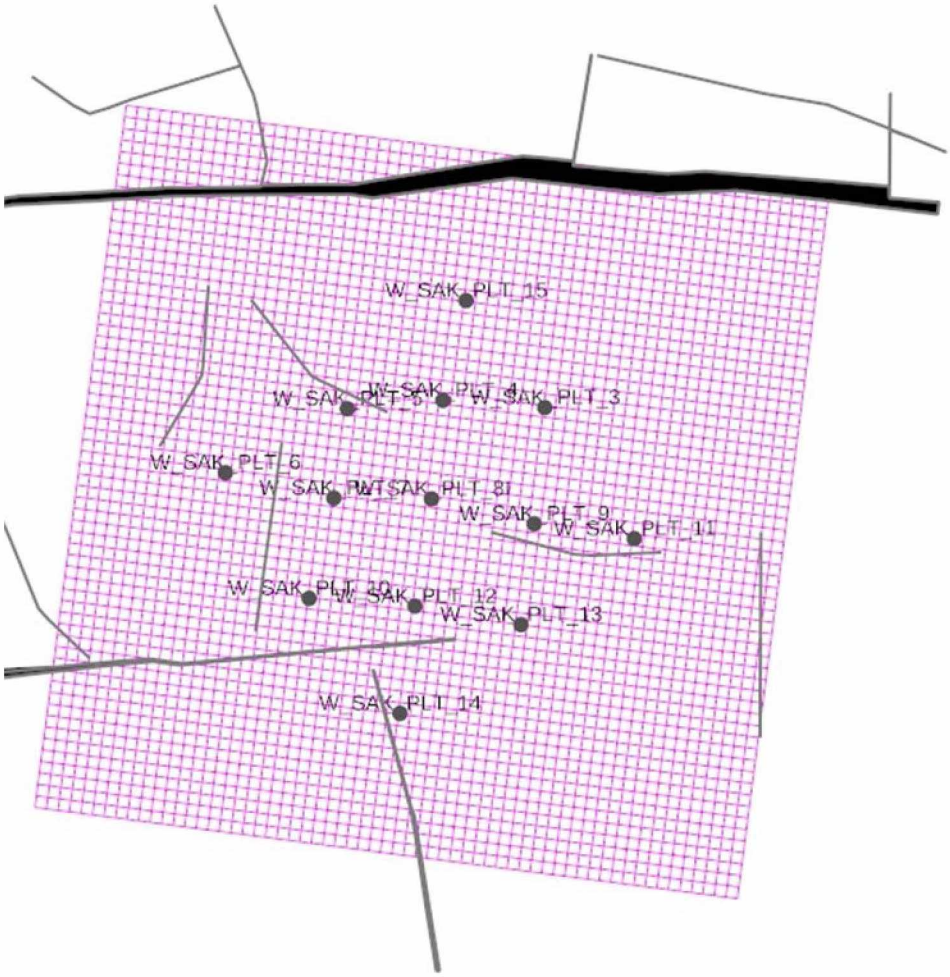

Figure 4-1: Plan View of Geostatistical Model

The fine-gridded layering enhances resolution to break out zonal flow and provides the ability to capture discrete and highly permeable layers as well as thin sands and shale barriers.

Also, the area of investigation is small enough to eliminate the need to uplayer the reservoir simulation model while retaining acceptable model speeds. The static properties of the grid blocks were generated through Kriging techniques using the porosity and permeability to water saturation of oil-based cores in the area.

The geostatistical gridding and static properties were imported to an in-house reservoir simulation package. Additionally, the dynamic and initialization properties from previously validated simulation models in the area were used as a starting point for the study. Table 4-1 lists the average properties for the central pilot injector, West Sak Pilot well 8i. They closely represent those properties used to populate the grid-cells of the simulation model.

Table 4-1: Average Properties for West Sak Pilot 8i (McGuire et al. 2005)

D Sand	
API gravity:	17.4 °API
Bubble point pressure:	1,486 psi
Solution gas/oil ratio:	173 SCF/STB
Initial oil viscosity:	68 cp
B Sand	
API gravity:	18.4 °API
Bubble point pressure:	1,526 psi
Solution gas/oil ratio:	190 SCF/STB
Initial oil viscosity:	42 cp
A2 Sand	
API gravity:	20.5 °API
Bubble point pressure:	1,593 psi
Solution gas/oil ratio:	218 SCF/STB
Initial oil viscosity:	27 cp

Figure 4-2 is a 3D visualization of the simulation model. Individual well trajectories may be observed as the pink cylinders penetrating the model. The two offset horizontal wells were drilled approximately 20 years after the pilot.

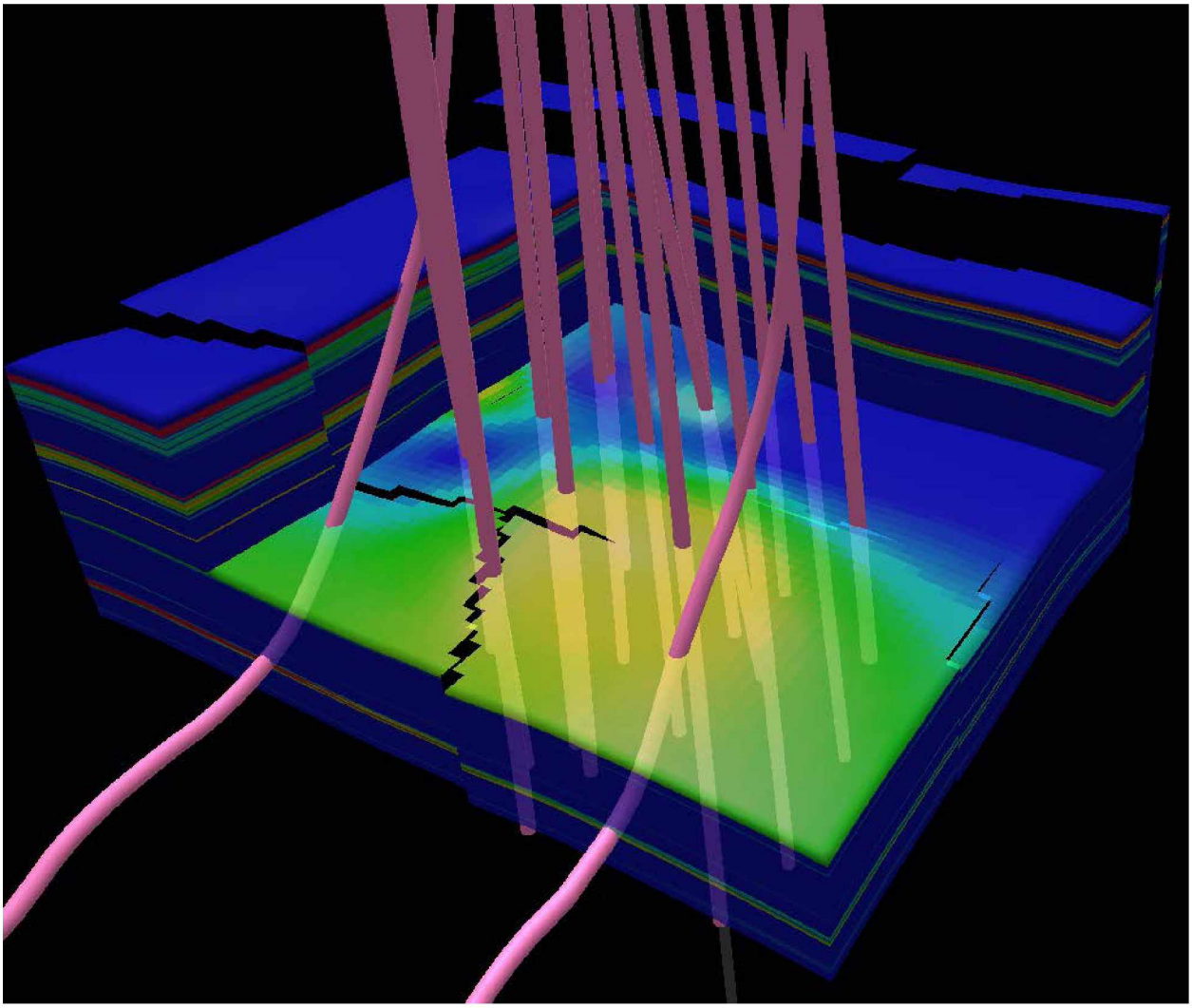

Figure 4-2: 3D Simulation View of West Sak Pilot

4.2 Model Validation

Model validation is an essential step before progressing any simulation study. Ensuring the model yields acceptable and intuitive results will lend credibility to the conclusions reached at the end of the study.

An initial history match of observed production data was used to validate the West Sak Pilot model. Observed production data incorporated into the model included oil production rates, water production rates, gas production rates, water injection rates, and bottomhole pressures

(Alaska Oil and Gas Conservation Commission, 2014). Deterministic iterations were used to achieve calculated values which closely matched observed data for production rates and bottomhole pressures.

Layer permeability multipliers were the main variable used to match both production rates and bottomhole pressures. Figures 4-3 through 4-5 are grid snapshots from the model illustrating the permeability variation within the most productive layers in the D, B and A sands respectively. Production performance in these layers dominated overall field and well-level rates and pressures.

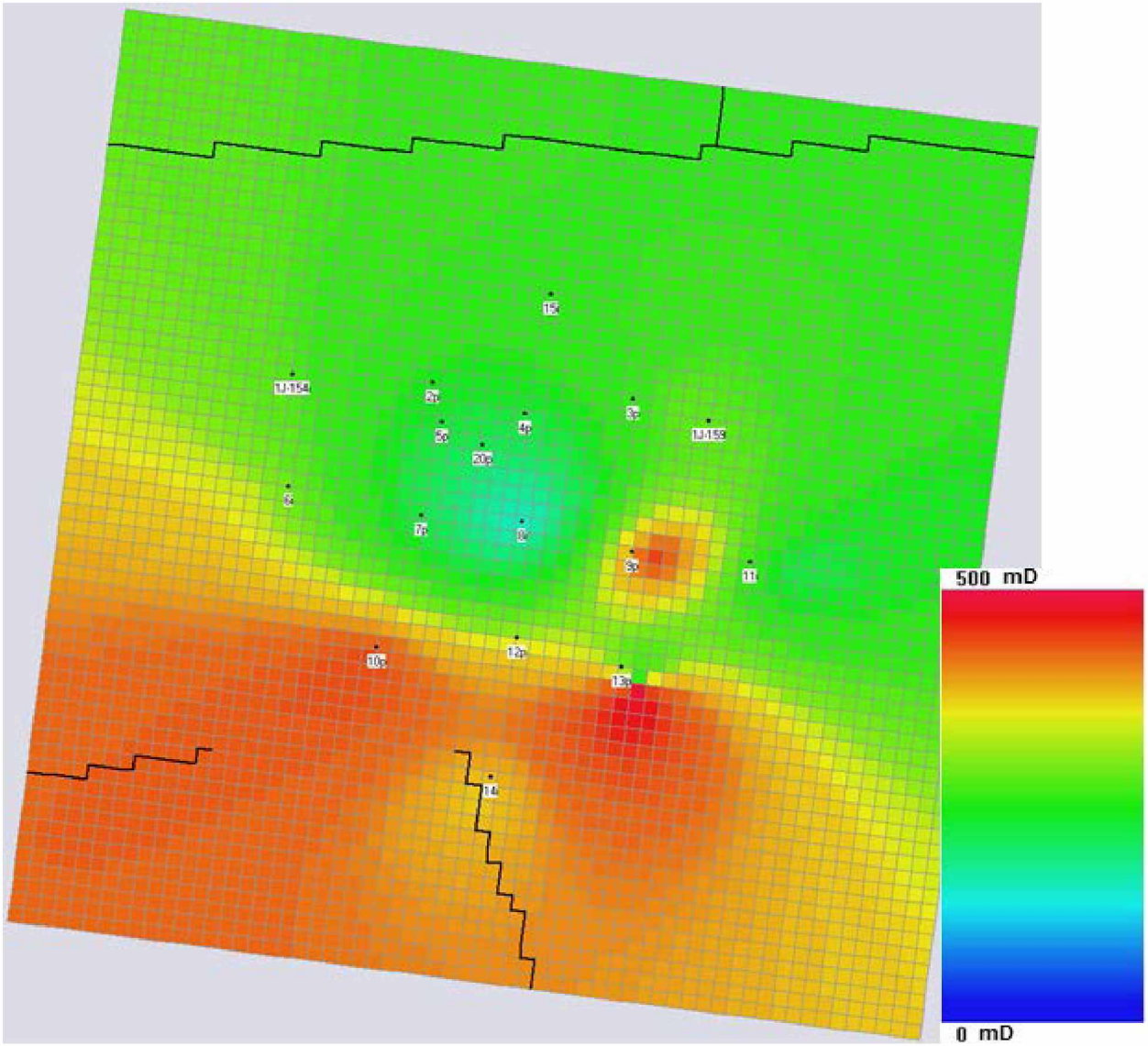

Figure 4-3: D Sand Permeability Distribution, Model Layer 4

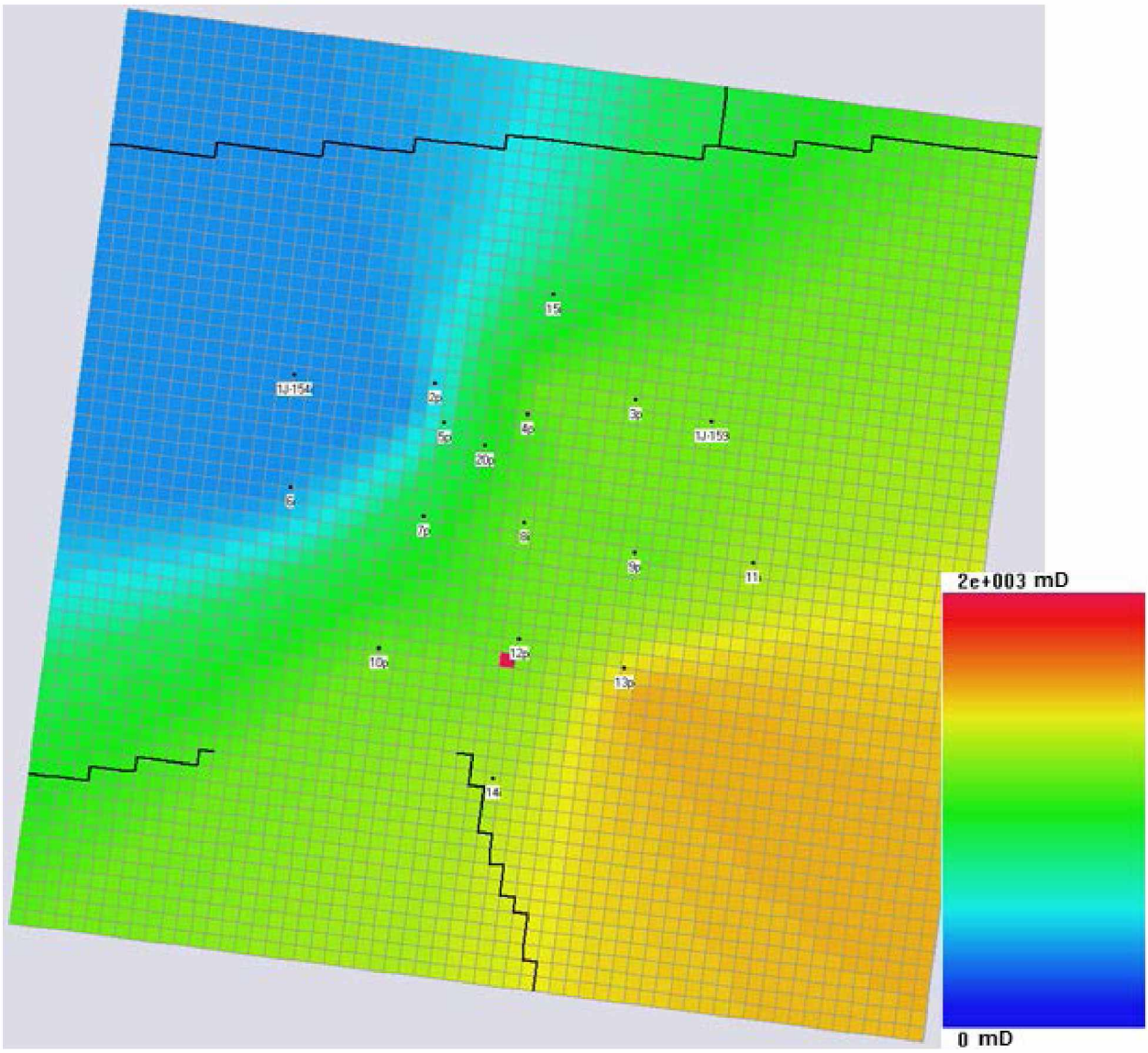

Figure 4-4: B Sand Permeability Distribution, Model Layer 24

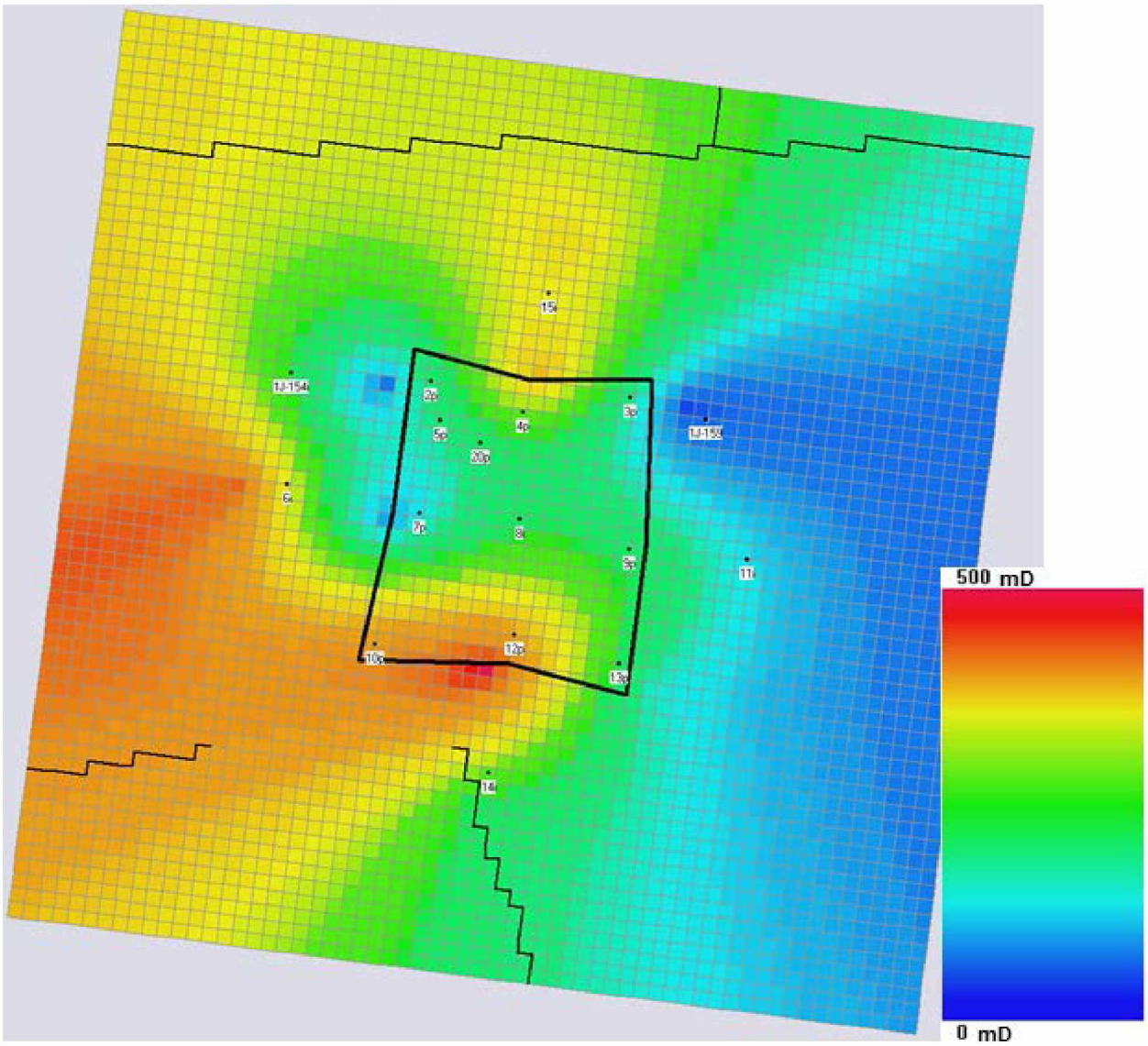

Figure 4-5: A Sand Permeability Distribution, Model Layer 77

A knowledge of field production and injection logging results, geochemistry, and well behavior helped guide model adjustments. Not unexpectedly, injection profiles acquired during the life of the field indicate high permeability layers within each sand took the largest injection volumes. These layers are also those with conduit-like failures observed during later developments (Peirce et al. 2014). Additionally, a vertical permeability modifier was added to reduce fluid "slumping" between layers. Field data suggests matrix fluids did not readily move in the vertical direction. This is related to the highly laminar nature of the sands.

Also, additional pore volume was added to the edge cells of the model to allow pressure leak-off. This captures the behavior expected in reality because the natural extent of the

reservoir is relatively large compared to the model area. Table 4-2 summarizes the adjustments to the model used to achieve an acceptable deterministic match.

Table 4-2: Summary of History Matched Model Adjustments

Grid Property	Adjustment
Pore Volume	100 multiplier
Vertical Permeability	0.1 multiplier
Horizontal Permeability:	
Layers 4 through 6	1.125 multiplier
Layer 24	1.25 multiplier
Layers greater than 75	0.25 multiplier
Remaining layers	0.5 multiplier

Figures 4-6 through 4-9 are field-level plots showing the quality of history match. Red lines are observed data while green lines show model or calculated data. Well-level plots are also provided in Appendix A.

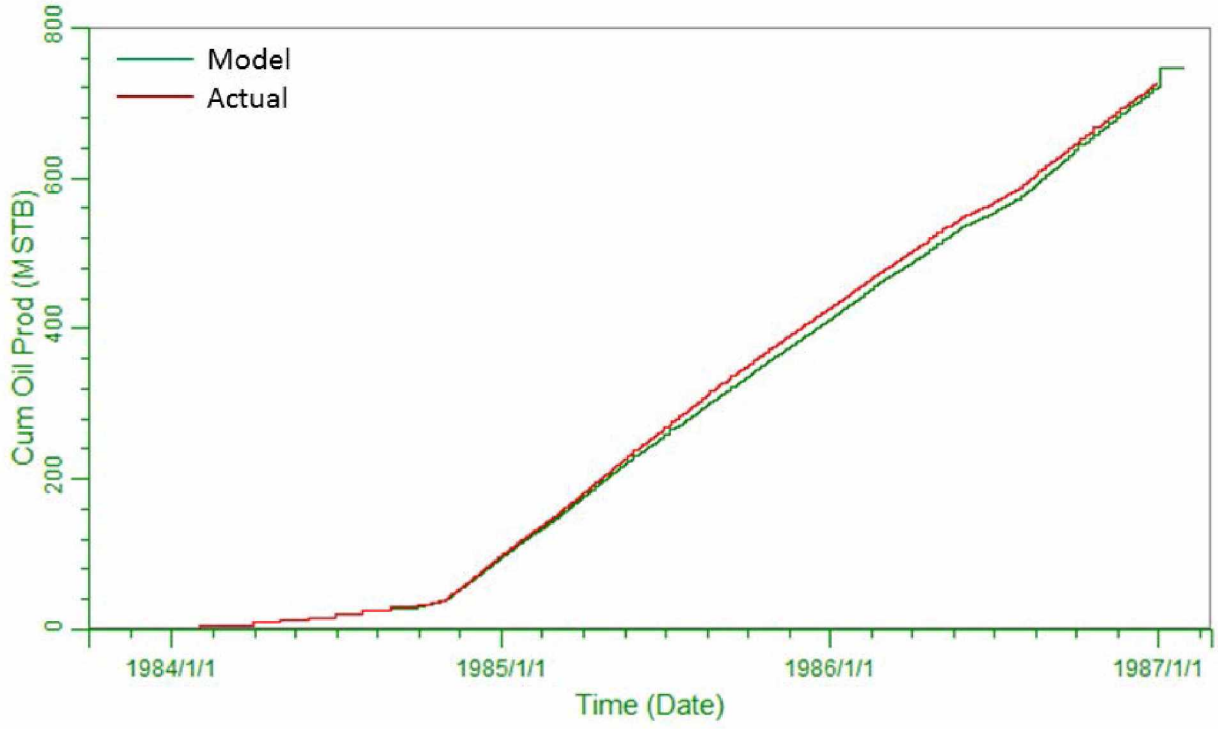

Figure 4-6: Comparison of Actual and Calculated Model Cumulative Oil Volumes

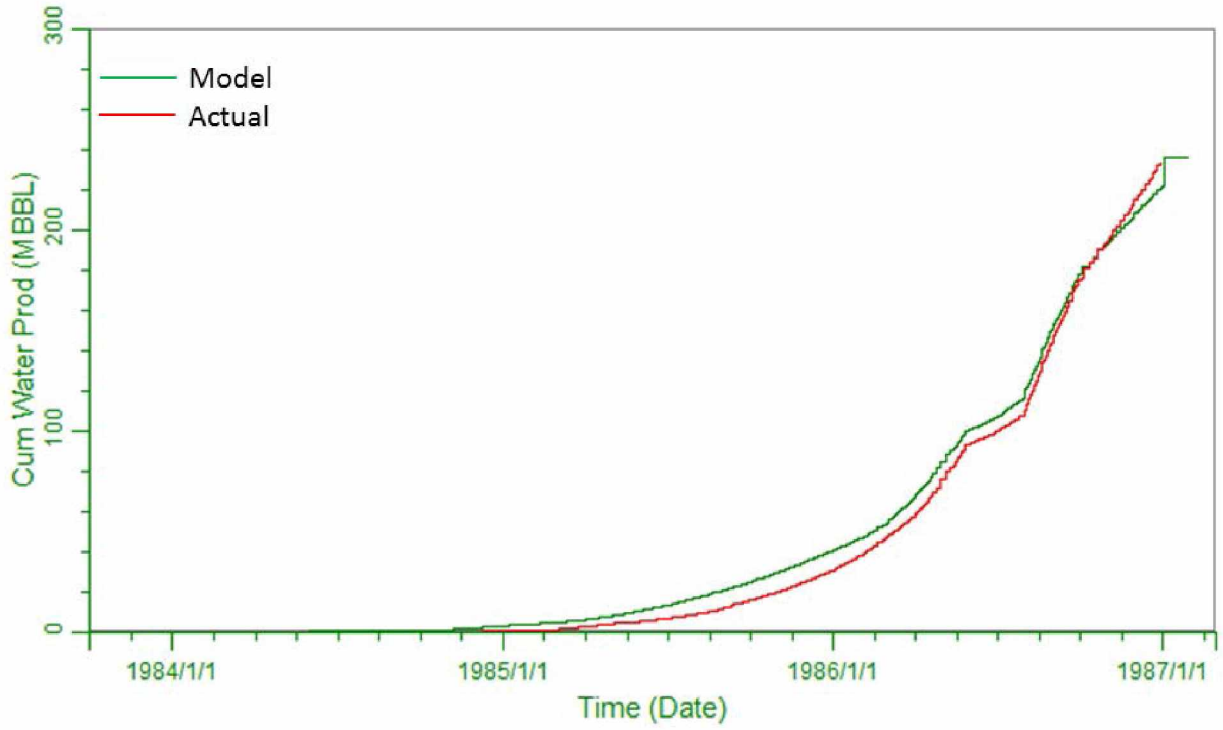

Figure 4-7: Comparison of Actual and Calculated Model Cumulative Produced Water Volumes

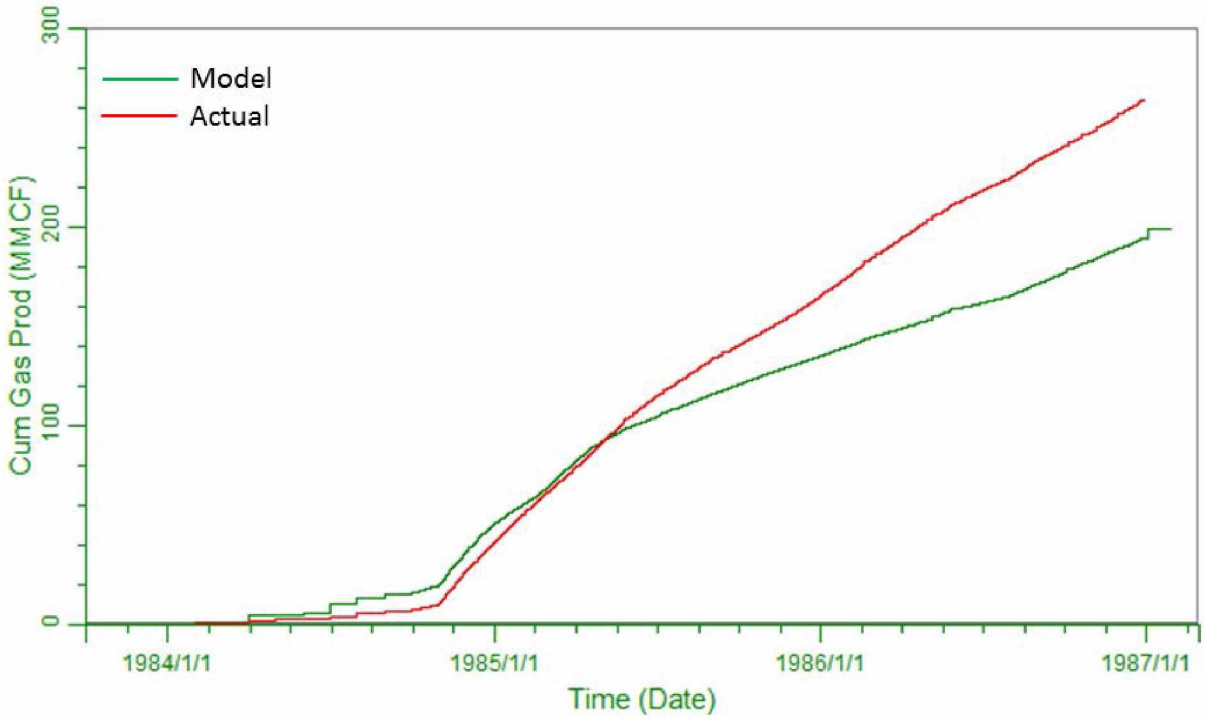

Figure 4-8: Comparison of Actual and Calculated Model Cumulative Gas Volumes

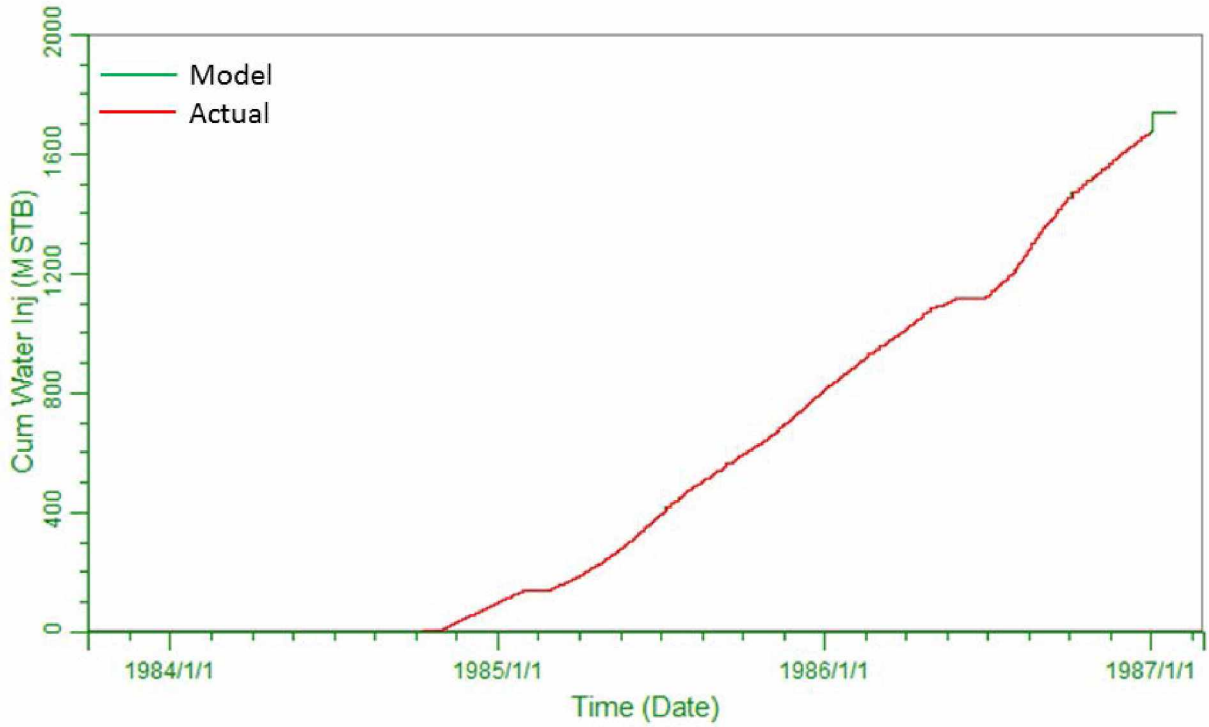

Figure 4-9: Comparison of Actual and Calculated Model Injection Water Volumes

The perfect match in Figure 4-9 was a result of the injectors being controlled on injection rate. The producers in the model were controlled on total liquid rate to assist with matching at the well level. Calculated cumulative oil and water volumes were within 5% of actual. Bottomhole pressures were honored at the well level as much as possible, see Appendix A for appropriate plots. The largest discrepancy in match quality is found with the gas behavior in the model. Gas production rates were difficult to match. This is a result of a local gas zone which affected the three western producers West Sak pilot producers, 3, 9, and 13. The gas zone was confirmed through petrophysical logs in the southwestern producer West Sak Pilot well 13.

An anomalous water breakthrough event occurred late in the pilot between West Sak Pilot producer 12 and injector 14. Well-level model adjustments were made to capture this behavior. Similar anomalous water breakthrough events occurred in the subsequent commercial development of West Sak. The events were primarily found in the highly permeable zones within the B sand (Peirce et al. 2014). This experience was incorporated into the pilot model by creating a highly permeable conduit between the injector and producer in the highest permeability layer of the B sand. To create this conduit, pore volume between the injector and producer was decreased by a factor of 16, the y-transmissibility was increased by a factor of 1000, the x-transmissibility was decreased by a factor of 100, and the horizontal permeability

near the producer was increased by a factor of 16. Essentially, a highly permeable “pipe” was simulated between the two wells. These changes accurately captured the anomalous water behavior. Figure 4-10 is a snapshot showing saturation change at the end of history and illustrates the location of this highly permeable conduit in layer 24 of the model.

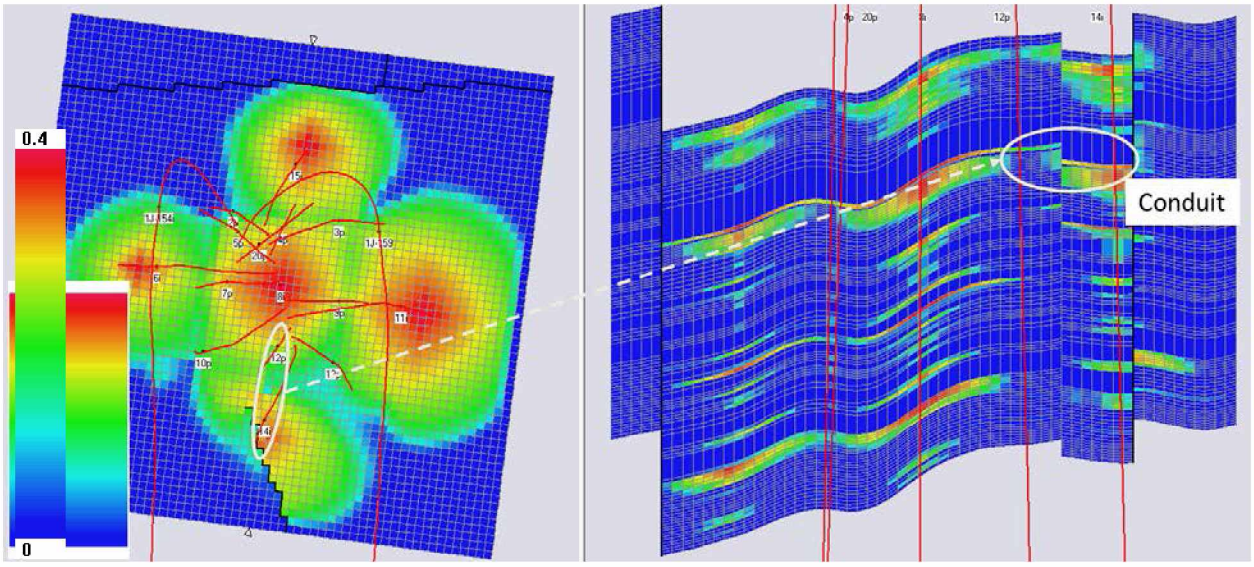

Figure 4-10: Saturation Change Snapshot and Location of Conduit

Figures 4-11 and 4-12 illustrate the model successfully captures this anomalous water breakthrough event with the adjustments described above.

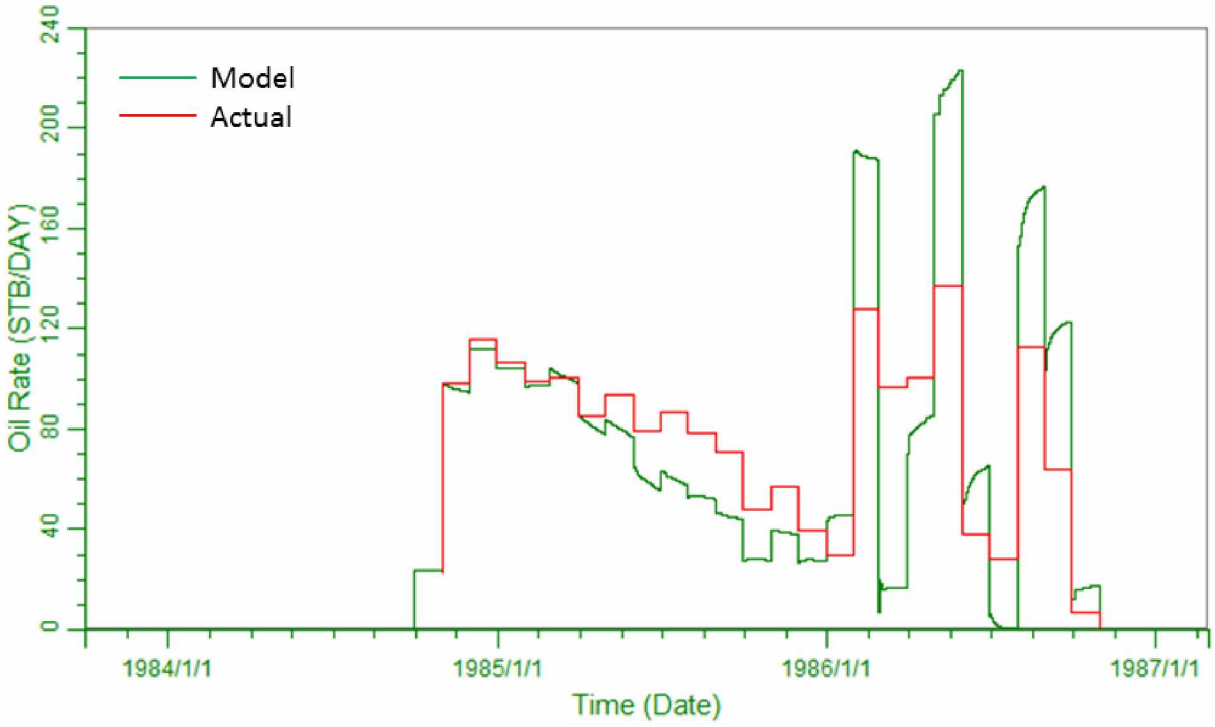

Figure 4-11: Comparison of Actual and Calculated Model Oil Rates for West Sak Pilot Producer 12

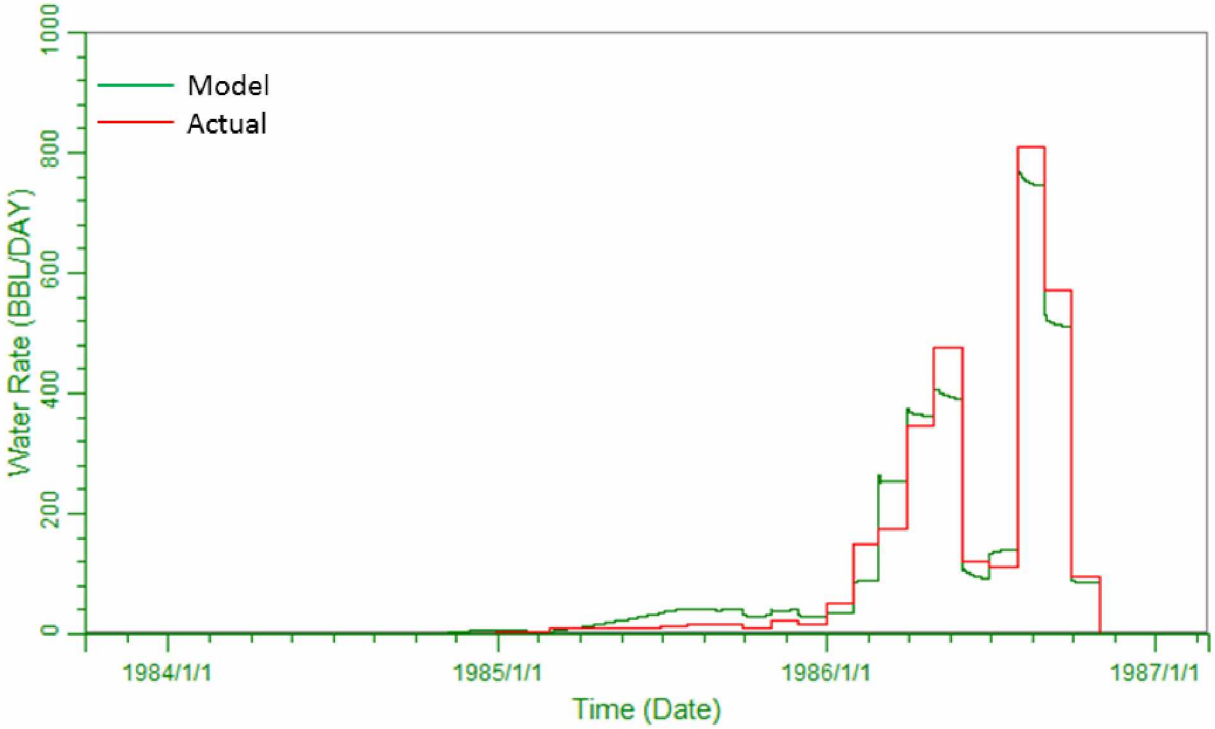

Figure 4-12: Comparison of Actual and Calculated Model Water Rates for West Sak Pilot Producer 12

Saturation profiles from two offset horizontal wells offer another unique constraint considered during model validation. Figure 4-10 shows well trajectories for all pilot wells and two horizontal wells. The horizontal wells are illustrated in Figure 4-10 as "J" shapes in plan view. The horizontal well trajectories begin heading north and then turn in the z-direction to land heading south in the target sands. The horizontal wells effectively bracket the West Sak pilot waterflood on the East and West. These two wells were drilled during the 1J development program in late 2005 and early 2006. Full log suites were run in the wells during drilling. Figure 4-13 illustrates the resistivity values for a West to East cross-section of the field starting with horizontal well 1J-154 progressing through the lower row of West Sak pilot producers. The logs from West Sak pilot producers 10, 12, and 13 were acquired at the beginning of the pilot project in 1983. Their resistivities, shown in Figure 4-13, illustrate a baseline of values prior to waterflood. The logs from horizontal well 1J-154 were acquired 20 years later. Figure 4-13 shows a suppressed D sand resistivity in well 1J-154 relative to the pilot wells. The suppressed resistivity suggests reduced water saturations in that interval. Additionally, the suppressed resistivity signature was only observed in the high permeability D sands, and nowhere else in the oil-bearing column. Two key conclusions may be drawn from these data. The first is the reservoir demonstrates good waterflood sweep in the high permeability zone of the D sand. Also, after 20 years there appears to be no significant gravity drainage of water into the lower permeability layers suggesting low vertical permeability. For the purpose of the simulation study, the observed water saturation values in the offset horizontal wells provide a unique constraint to match with calculated data.

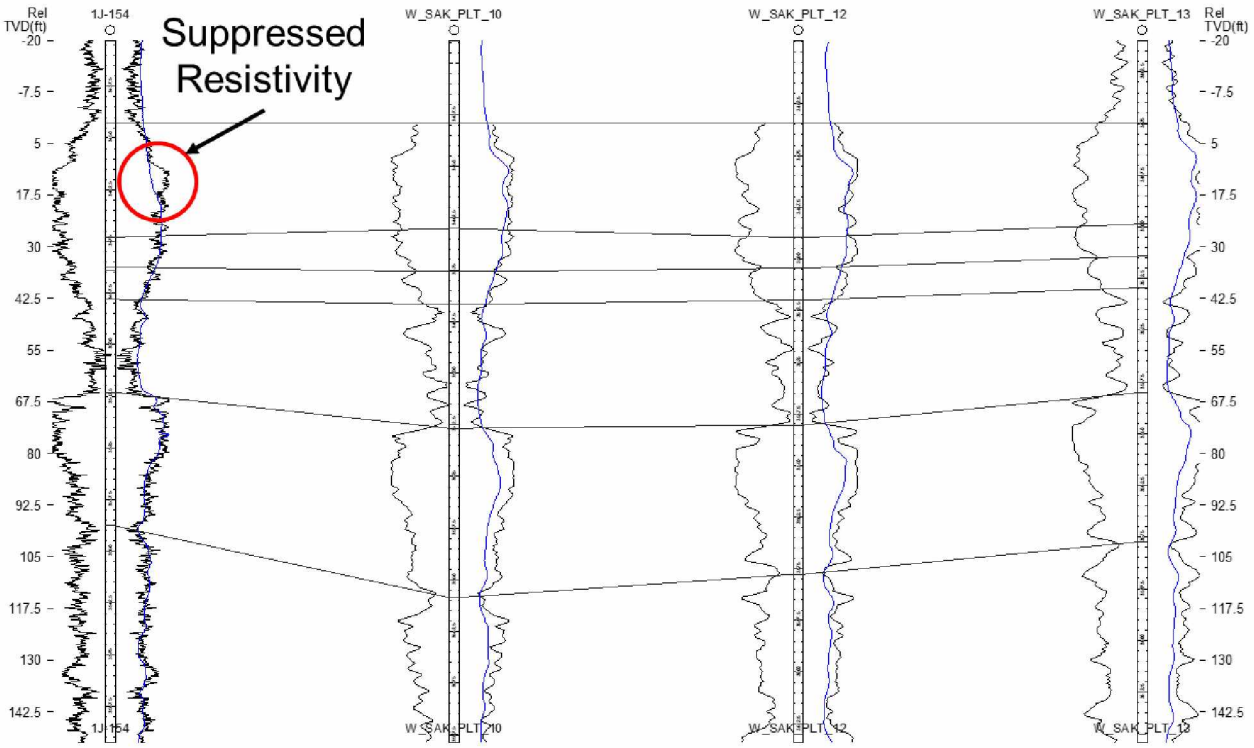

Figure 4-13: D Sand Suppressed Resistivity in Offset Well Log

General water saturation trends were honored at this stage in the project, but were not considered critical to validating the model. However, the use of this constraint is addressed in more detail in Section 4.3.

Following the West Sak pilot conclusion in 1986, a reservoir model was built and history matched using the pilot data. The results of this heritage, post-audit West Sak Pilot simulation model were recorded in sufficient detail to use as a benchmark in validating the model created for this project. The primary objective of the heritage modeling study was to provide a method to estimate recovery from the West Sak sands under waterflood. The model was built in ARCO's proprietary simulation software and history matched using conventional deterministic methods. Results from the simulation model built for this project were compared with the results from the heritage model. The models were compared for the time period associated with forecasting to a combined-sand water-oil-ratio (WOR) of 15. A comparison of forecasted results between the heritage model and the model for this project is summarized in Table 4-3. Table 4-3 shows the percent hydrocarbon pore volume injected (HCPVi), percent recovery factor (RF), and the WOR for each sand in the respective two models.

Table 4-3: Comparison of Heritage and Project Model Results

	HCPVi		%RF		%RF/HCPVi		WOR, dimensionless	
	Heritage	This Work	Heritage	This Work	Heritage	This Work	Heritage	This Work
D Sand	0.55	0.50	16.3	14.3	29.6	28.6	5.8	14.2
B Sand	3.54	1.72	33.7	21.9	9.5	12.7	39.4	30.7
A Sand	0.46	0.42	17.9	15.5	38.9	36.9	6.5	8.5
Total	1.21	0.72	21.1	16.2	17.4	22.5	15	15

Figure 4-14 also illustrates the comparison of the two models by plotting HCPVi on the horizontal axis and RF on the vertical axis.

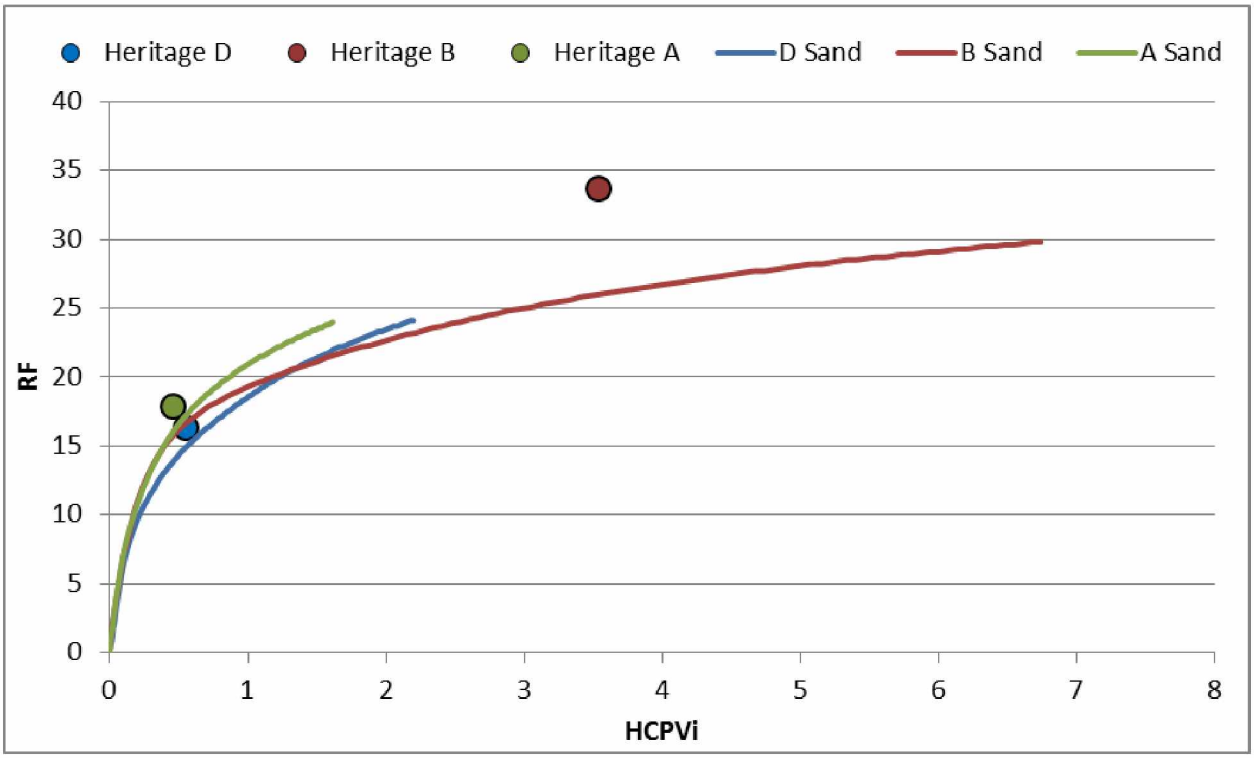

Figure 4-14: Comparison of Heritage and Project Model Results

The general intra-sand trends are similar. The B sand has the greatest throughput and highest recovery. Additionally, the A sand has the lowest throughput, but the D sand has the lowest recovery factor.

The higher HCPVi of the heritage model indicates it is more optimistic in terms of injection throughput, particularly in the B sand. This is also what leads to the higher RF in the B sand. The difference is a result of incorporating the known split behaviors observed in injection logging, and geochemical allocations into the project model. This highlights the value of including additional operational data for more realistic model behaviors.

In summary, the model was successfully validated by achieving an acceptable history match. Field experience gained through reservoir surveillance was a critical component to knowing which simulation parameters should be adjusted. Additionally, other unique constraints such as anomalous water breakthrough and saturation trends were honored.

4.3 Determine Uncertainty Parameters and Ranges

The validated model provided the basis for the uncertainty study. The next stage of the project focused on determining the key uncertainty parameters and ranges for those parameters. This was accomplished in two ways: data review and interviews with subject matter experts.

Knowing the dataset is crucial to understanding data quality and therefore the range of uncertainty associated with the parameters under investigation. A comprehensive look at the West Sak pilot data and operational history showed that the heterogeneity of the reservoir was a key uncertainty. This is observed in the horizontal and vertical permeabilities of the model.

Tapping into existing institutional knowledge is often the most efficient way to determine which parameters to investigate. Those who have worked pieces of the problem before can provide insight into key parameters that were important in other projects. In this case, the lead reservoir engineer for the West Sak field was interviewed to determine key uncertainty parameters and ranges for investigation.

Table 4-4 summarizes the uncertainty parameters and their corresponding ranges which were identified during the project. The uncertainty parameters can be organized into two categories: reservoir heterogeneity and fluid properties.

Table 4-4: Summary of Uncertainty Parameters

Reservoir Heterogeneity

Permeability Multipliers

Parameter	Abbreviated Keyword	Affected Layers	Range
Vertical perm	_%MOD_KZ%_	All	$1x10^{-4}$ - 1
D sand – high perm	_%DT_KX%_	4 - 6	0.625 - 1.875
D sand – remaining	_%DR_KX%_	7 - 23	0.5 -1.5
B sand – high perm	_%BT_KX%_	24	0.75 - 2.25
B sand – remaining	_%BR_KX4%_	25 - 42	0.5 - 1.5
A4 sand – high perm	_%A4T_KX%_	43	0.5 - 1.5
A4 sand – remaining	_%A4R_KX%_	44 - 54	0.5 - 1.5
A3 sand – high perm	_%A3T_KX%_	55	0.5 - 1.5
A3 sand – remaining	_%A3R_KX%_	56 - 75	0.5 - 1.5
A2 sand – high perm	_%A2T_KX%_	76 - 80	0.25 - 0.75
A2 sand – remaining	_%A2R_KX%_	81 - 99	0.25 - 0.75

Net to Gross Multipliers

Parameter	Abbreviated Keyword	Affected Layers	Range
D sand – high perm	_%DT_NTG%_	4 - 6	0 - 1
D sand – remaining	_%DR_NTG%_	7 - 23	0 - 1
B sand – high perm	_%BT_NTG%_	24	0 - 1
B sand – remaining	_%BR_NTG4%_	25 - 42	0 - 1
A4 sand – high perm	_%A4T_NTG%_	43	0 - 1
A4 sand – remaining	_%A4R_NTG%_	44 - 54	0 - 1
A3 sand – high perm	_%A3T_NTG%_	55	0 - 1
A3 sand – remaining	_%A3R_NTG%_	56 - 75	0 - 1
A2 sand – high perm	_%A2T_NTG%_	76 - 80	0 - 1
A2 sand – remaining	_%A2R_NTG%_	81 - 99	0 - 1

Fluid Properties

Parameter	Abbreviated Keyword	Affected Layers	Range
Viscosity	_%PVTIndex%_	All	Low - High
Initial Water Saturation	_%GLOBAL_Swinit%_	All	0.8 - 1.2

4.4 Test Uncertainty Range

A number of model runs were completed to test the uncertainty ranges identified through data review and expert interviews. The objective of the test was to obtain bounding cases to ensure known constraints were met within the given ranges. This emerged as a significant step in achieving a model that adequately honored all the constraints from the dataset.

Although a good history match was achieved during the model validation phase of the project, a method was needed to observe zonal injection and production, and saturation profiles from a database of 500-800 simulation runs. An in-house software script was used which efficiently processes and calculates the quality of match between observed and calculated values. Additionally, it streamlines the process of creating, submitting, and visualizing large matrices of simulation runs.

This script enabled the efficient testing of the bounding cases for the uncertainty ranges listed in Table 4-4. One such bounding case included achieving an adequate field level match while honoring the reduced D sand water saturations observed in the offset horizontal wells. Multiple runs were made to achieve this bounding case. The results of these runs indicated the existing uncertainty parameters and ranges were insufficient to honor the saturation profiles. There was no way to achieve the log-derived water saturation values in the D sand under the injection constraints of the observable data. The calculated water saturation behind the flood front with the existing model settings was insufficient to achieve an adequate match. To capture this bounding case, a relative permeability parameter was added to the list of uncertainty variables. Figure 4-15 is a fractional flow curve from the base relative permeability curve. It shows the need to shift the curve in order to achieve a higher saturation behind the flood front.

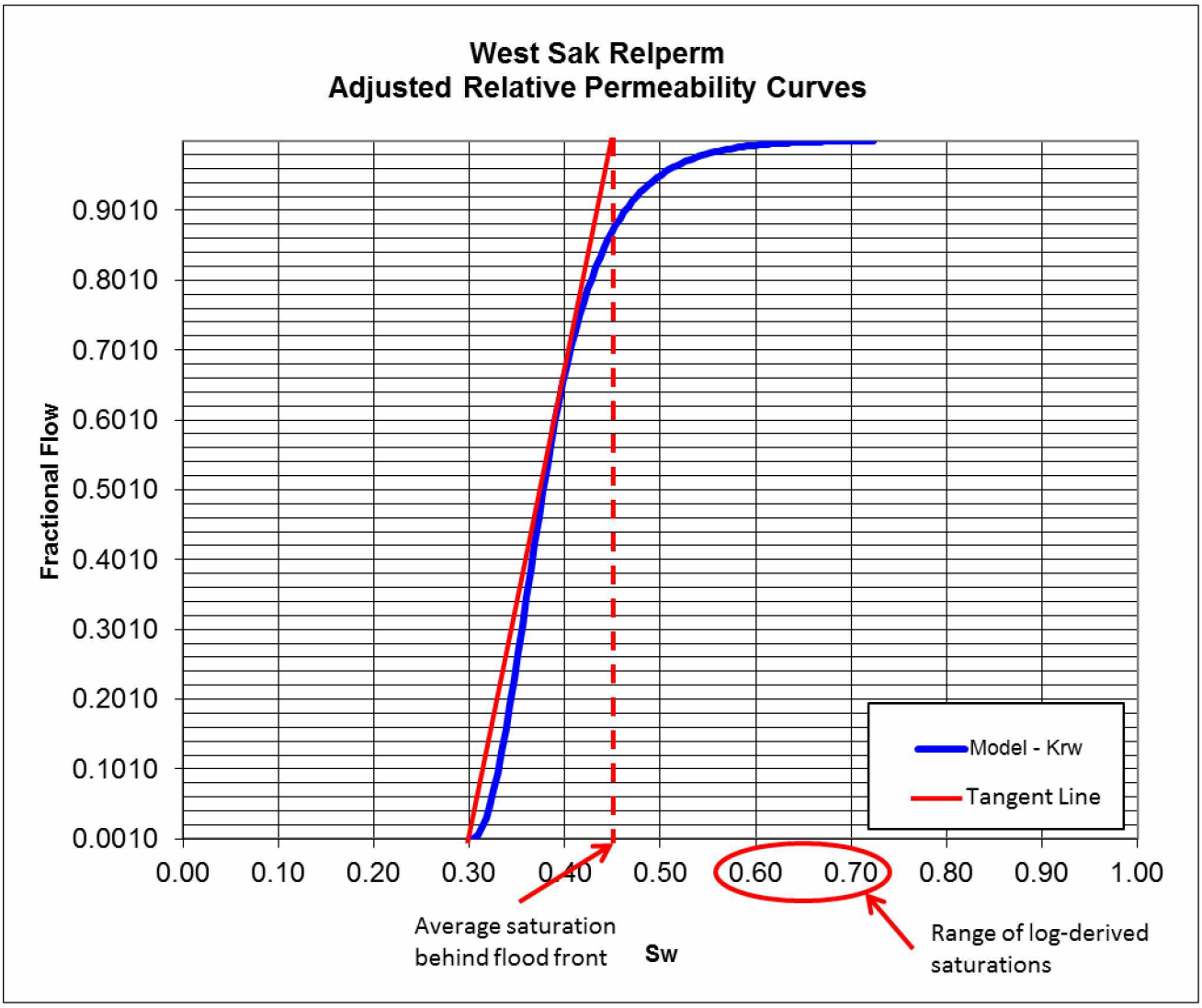

Figure 4-15: Base Case Fractional Flow Curve

Corey's equations, included below, were used to develop relative permeability relationships favorable to achieving high water saturation behind the flood front (Corey 1954; Brooks and Corey 1964).

$$K_{row} = \left(1 - \frac{S_w - S_{wi}}{1 - S_{wi} - S_{orw}}\right)^{N_o}$$

$$K_{rw} = K_{rw}^0 \left(\frac{S_w - S_{wi}}{1 - S_{wi} - S_{orw}}\right)^{N_w}$$

Where:

K_{row} is the relative permeability to oil;

K_{rw} is the relative permeability to water;

K_{rw}^{0} is the endpoint of the relative permeability to water curve;

S_w is the water saturation at the point of investigation;

S_{wi} is the initial water saturation;

S_{orw} is the residual oil saturation achievable through waterflood;

N_o is the empirically derived oil exponent;

and, N_w is the empirically derived water exponent.

Figure 4-16 illustrates the fractional flow curve developed by adjusting the Corey exponents. For this bounding case, the oil exponent was reduced to 1 and the water exponent was increased to 6 where the original values were 2.3 and 2.0 for the oil and water exponents, respectively. This adjustment increased the average water saturation behind the flood front by approximately 150%.

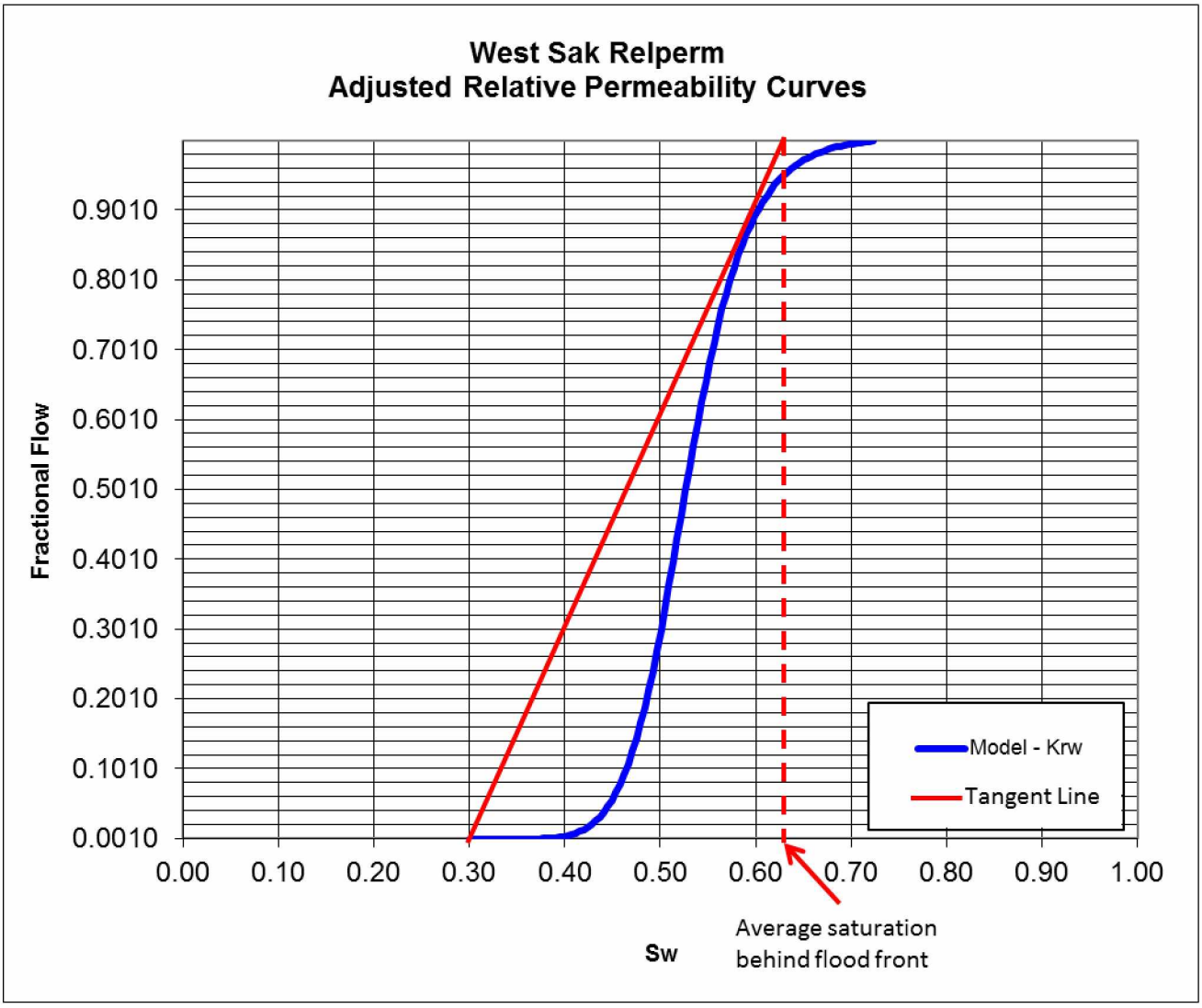

Figure 4-16: Modified Fractional Flow Curve

In addition to adding relative permeability to the list of uncertainty parameters, the uncertainty ranges were increased. Again, the multiple runs made to achieve the bounding cases indicated a need to widen the ranges in order to fully capture observed behavior. Table 4-5 lists the final parameter list and ranges following this step in the workflow.

Table 4-5: Updated Summary of Uncertainty Parameters

Reservoir Heterogeneity

Permeability Multipliers

Parameter	Abbreviated Keyword	Affected Layers	Range
Vertical perm	_%MOD_KZ%_	All	$1x10^{-6}$ - 1
D sand – high perm	_%DT_KX%_	4 - 6	1 - 20
D sand – remaining	_%DR_KX%_	7 - 23	$1x10^{-4}$ - 2
B sand – high perm	_%BT_KX%_	24	1 - 15
B sand – remaining	_%BR_KX4%_	25 - 42	$1x10^{-4}$ - 2
A4 sand – high perm	_%A4T_KX%_	43	0.5 - 2
A4 sand – remaining	_%A4R_KX%_	44 - 54	0.5 - 2
A3 sand – high perm	_%A3T_KX%_	55	0.5 - 2
A3 sand – remaining	_%A3R_KX%_	56 - 75	0.5 - 2
A2 sand – high perm	_%A2T_KX%_	76 - 80	0.25 - 2
A2 sand – remaining	_%A2R_KX%_	81 - 99	0.25 - 2

Net to Gross Multipliers

Parameter	Abbreviated Keyword	Affected Layers	Range
D sand – high perm	_%DT_NTG%_	4 - 6	0 - 1
D sand – remaining	_%DR_NTG%_	7 - 23	0 - 1
B sand – high perm	_%BT_NTG%_	24	0 - 1
B sand – remaining	_%BR_NTG4%_	25 - 42	0 - 1
A4 sand – high perm	_%A4T_NTG%_	43	0 - 1
A4 sand – remaining	_%A4R_NTG%_	44 - 54	0 - 1
A3 sand – high perm	_%A3T_NTG%_	55	0 - 1
A3 sand – remaining	_%A3R_NTG%_	56 - 75	0 - 1
A2 sand – high perm	_%A2T_NTG%_	76 - 80	0 - 1
A2 sand – remaining	_%A2R_NTG%_	81 - 99	0 - 1

Fluid Properties

Parameter	Abbreviated Keyword	Affected Layers	Range
Viscosity	_%PVTIndex%_	All	Low - High
Initial Water Saturation	_%GLOBAL_Swinit%_	All	0.8 - 1.2
Relative Permeability	_%MOD_Rock%_	All	Low - High

A post-processing visualization package assisted in understanding fluid behavior in the model. The multi-run visualization tool provided the means to quickly run models and visualize outputs in relation to one another, but it lacked the resolution to observe gridcell-to-gridcell changes. The post-processing visualization package was an important part of the workflow. It allowed troubleshooting of unexpected pressure and fluid movement within the model that would have otherwise been impossible to observe.

In summary, testing the uncertainty ranges to meet bounding cases is an important part of characterizing the uncertainty. In this case, it led to additional parameters to include in the analysis. Also, including a post-processing package to visualize grid-cell properties is an important part of understanding fluid movement in the simulation grid system.

4.5 Determine Significant Parameters

The next phase of the project identified the parameters with the highest uncertainty through the means of experimental design. Again, the in-house multi-run visualization script was a crucial part of the workflow by enabling efficient sampling of the uncertainty space. The script employs a Latin Hypercube algorithm to generate a run matrix for the investigation. The parameters and ranges listed in Table 4-5 were used to generate the run matrix. A probability distribution was assigned to each parameter and used by the algorithm in generating the parameter settings for each run. For the number of parameters listed, the number of runs required to sample the solution space was 720.

The multi-run visualization script also provides an efficient platform to evaluate run results. The script allows for the user to output a quality of match parameter. The user specifies match points in the actual data which is then compared to the calculated data. The greater the difference between the two points, the greater the value of the quality parameter. For this project, the cumulative water production at end of history, cumulative oil production at end of history, and water saturation values in four layers of the offset horizontal wells were used to generate the quality of match parameter.

The parameter settings generated using the Latin Hypercube algorithm are the factor settings or independent variables used in experimental design. The quality of match parameter is the response variable or dependent variable. The value for the quality of match parameter was obtained for each run as it was completed. A matrix of factor settings and response variable values was then available for statistical analysis. A contribution to variance statistical analysis was completed for this project through the aid of the multi-run visualization tool.

Contribution to variance is a means to quantify the impact on response when one parameter is varied in the presence of other changing parameters. A parameter with the highest contribution to variance has the greatest impact on the response variable relative to other parameters. In other words, contribution to variance points to the parameters with greatest uncertainty and provides a guide for further investigation. By focusing investigation efforts on the factors with greatest uncertainty, the user can better define, quantify, and narrow the uncertainty range. Repeating the study with the more accurate parameter ranges will show the contribution to variance has been reduced.

One method to visualize the contribution to variance associated with each parameter is through a tornado diagram. The contribution to variance associated with each parameter is normalized and sorted highest to lowest for comparison.

The tornado diagram in Figure 4-17 was developed from the contribution to variance analysis using the results of the simulation runs. It illustrates the most significant uncertainty parameters with their percentage contributions to the variance. The vertical axis lists the parameters with their corresponding percent contribution to variance along the horizontal axis. The color variation in Figure 4-17 indicates a positive correlation (blue) or a negative correlation (orange). For example an increase in initial water saturation leads to a decrease in the quality of match.

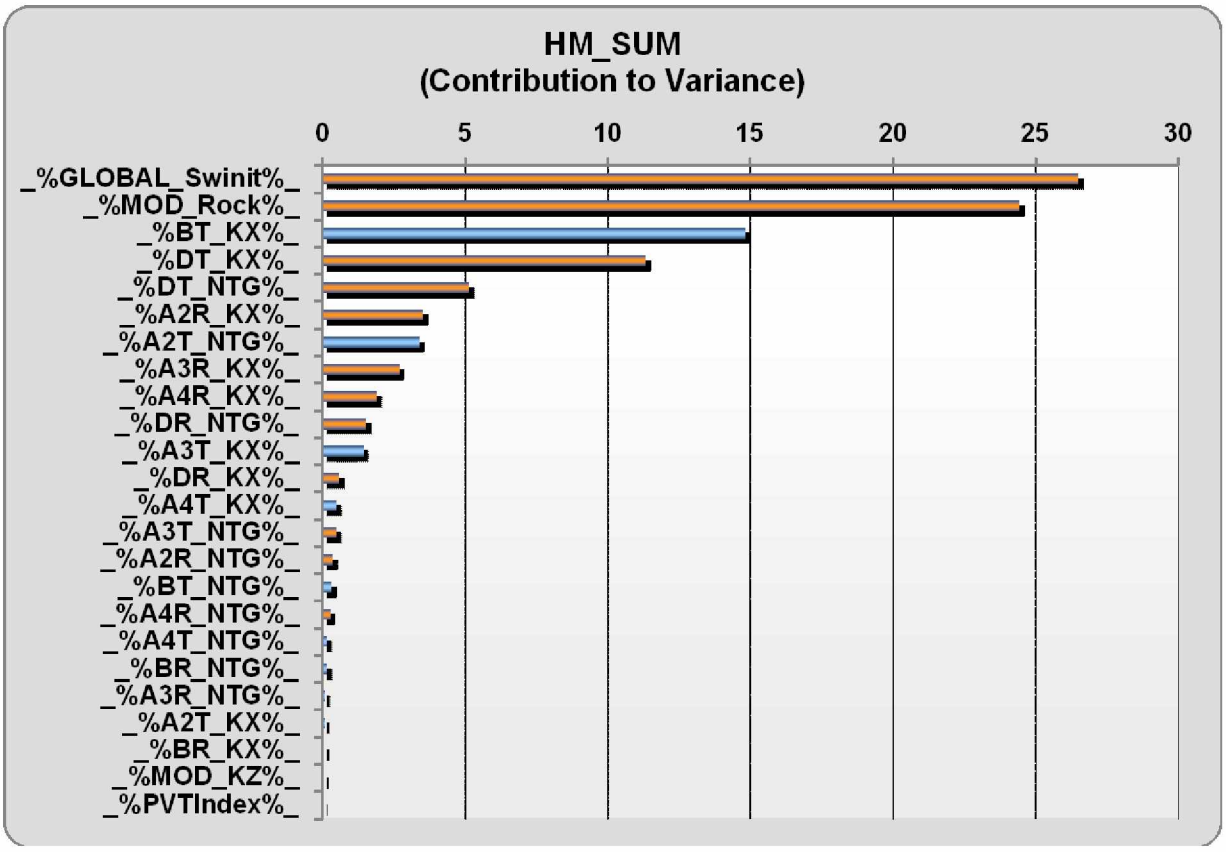

Figure 4-17: Contribution to Variance Tornado Diagram

The most significant parameters affecting the quality of match were found to be initial water saturation; relative permeability relative to oil and water; permeability multipliers in the high permeability layers of the D, B, and A2 sands; and the net-to-gross in the high permeability layers of the D and A2 sands. These seven parameters account for greater than 90% of the variance of the model results making them the most significant.

The top two most significant parameters are related to displacement efficiency. Initial water saturation affects the amount of oil available in the pore space for displacement by water. Relative permeability describes the resistance to flow or displacement due to multiphase flow in the pore throats.

Three other significant parameters were permeability multipliers which were applied to the associated layers. The layer permeabilities control fluid movement in the respective layers of the model and directly impact areal and vertical sweep efficiency.

The remaining significant parameters are associated with the net-to-gross or volumetrics of the model. This suggests there may be additional iterations required to change the geomodel volumes.

Five of the top seven parameters are directly related to the sweep efficiency of the West Sak waterflood. The contribution to variance analysis points to these parameters as the parameters that have the greatest uncertainty. This suggests these parameters are the least understood in current models of the waterflood. Further work to define and narrow the uncertainty in these parameters will yield models which better describe actual waterflood behavior.

CHAPTER 5.0
RESULTS AND DISCUSSION

Results from the completed workflow described in the previous sections give insight into the displacement, areal, and vertical sweep efficiency associated with the West Sak waterflood.

5.1 Displacement Sweep Efficiency Insights

Potential changes to the handling of displacement efficiency in current reservoir models were suggested by the results. The first indication of this came from including the later-time log-derived water saturations as a model constraint. To meet this constraint, the Corey equations were used to adjust the relative permeability relationships within the model. These adjustments allowed the model to achieve higher water saturations behind the flood front. The higher water saturations more accurately matched the observed behavior.

The other indication that displacement efficiency may not be handled correctly in current modeling techniques was shown in the contribution to variance analysis. The top two parameters with the greatest impact on variance, initial water saturation and relative permeability, are directly associated with displacement efficiency. This suggests these two parameters are in the most need of better definition. Further work is required to narrow their associated ranges of uncertainty. In doing this, a more realistic model describing the displacement efficiency of the West Sak waterflood may be implemented.

5.2 Areal and Vertical Sweep Efficiency Insights

The results of this study also suggest potential changes to the current understanding of fluid movement within the West Sak reservoir. This was demonstrated in the permeability multipliers required to achieve a valid history match and in the contribution to variance analysis. Three of the most significant parameters affecting match quality were permeability multipliers. The permeability multipliers with the greatest impact were all in the highest permeability layers of the model. In terms of production behavior, these results imply the sands with highest permeability are the predominant sources of oil production and receive the bulk of injection fluids. Smaller, less prolific sand layers may be bypassed and remain targets for future development.

Additionally, this behavior suggests potential changes to the ideal development design to achieve the highest ultimate recovery. Horizontal wells drilled in a single zone may have lower ultimate recoveries because they contact smaller vertical portions of the sand package thereby

bypassing some oil bearing layers. Whereas, well designs that contact a larger portion of the sands in the vertical direction will have higher ultimate recoveries. Vertical wells or fractured horizontal wells may be better suited to recover oil because they contact more oil bearing sand layers.

5.3 Additional Discussion

The most significant parameter illustrated in Figure 4-17 was initial water saturation and accounted for 25% of the contribution to variance. This is most likely a function of the uncertainty range assigned to this variable. The rich dataset available for West Sak includes a number of core studies by several different parties. A review of these data suggests the need to reduce the uncertainty range in future studies. This finding is reflected in the second recommendation made by this study. Also, uncertainty with respect to initial water saturation brings into question the certainty of the end-points to the relative permeability curves used in this project. A study in the early 1990's related the waterflood residual oil saturation to initial water saturations. The empirical correlations developed during this study were incorporated into the simulation such that the relative permeability curves reflect this relationship. Figures 4-15 and 4-16 represent a single visualization of fractional flow curves based on relative permeability curves with an initial water saturation of 30%.

CHAPTER 6.0
CONCLUSION

The primary objectives of this project were met. Required adjustments to the model in order to honor production data and field experience coupled with uncertainty analysis yielded an improved understanding of sweep efficiency of the West Sak waterflood. Additionally, an adequate simulation model was built, validated and the most significant parameters contributing to uncertainty in the model were identified. From the contribution to variance study, the most significant uncertainty parameters affecting match quality in the reservoir model were identified. They are listed here in order of significance.

1. Initial water saturation
2. Relative permeability relationships between oil and water
3. Permeability multiplier in the high permeability layers of the B sand
4. Permeability multiplier in the high permeability layers of the D sand
5. Net-to-gross in the high permeability layers of the D sand
6. Permeability multiplier in the A2 sand
7. Net-to-gross in the high permeability layers of the A2 sand

The workflow was also documented and may be used in future studies addressing similar issues.

These results provided two key learnings regarding sweep efficiency of the West Sak waterflood. The first key learning addressed displacement efficiency. The displacement efficiency in current West Sak models is conservative. The second key learning addressed areal and vertical sweep efficiency. High permeability layers within the West Sak reservoir experience high waterflood sweep potentially bypassing oil in lower permeability zones.

In conclusion, this project highlights the continuing challenges associated with developing the West Sak reservoir. New and innovative approaches are required to explain the reservoir behaviors observed in the field. This project represents one attempt to capture some of those observations in a format that assists future decision-making. The results of this project and their implications are still in their infancy. However, they suggest fundamental changes to existing reservoir modeling approaches. Continued studies are recommended to validate these results on a full-field basis, but they suggest changes could lead to additional recovery as development continues in the multi-billion barrel West Sak oilfield.

CHAPTER 7.0
RECOMMENDATIONS

The results and conclusions of this project lead to additional questions and further work. The following recommendations for additional work were given to the West Sak Development Team

1. Refine the geomodel to narrow the uncertainties associated with layer permeabilities and net-to-gross variation.
2. Revisit static property uncertainty ranges and narrow where possible.
3. Validate Corey equation derived relative permeability curves to reduce the uncertainty associated with relative permeability.
4. Perform sensitivities on vertical versus horizontal wells using the developed model to understand the ultimate recoveries associated with better displacement. This should include an economic analysis to understand the capital intensity of both options.
5. Incorporate relative permeability changes into the full-field development model.
6. Implement the documented workflow in a scaled-up model at a drillsite level.

CHAPTER 8.0
REFERENCES

Alaska Oil and Gas Conservation Commission (AOGCC). 2014. Well & Production Database, http://doa.alaska.gov/ogc/publicdb.html (accessed 1 September 2014).

Bidinger, C.R. and Dillon, J.F. 1995. Milne Point Schrader Bluff: Finding the Keys to Two Billion Barrels. Presented at the International Heavy Oil Symposium, Calgary, Alberta, Canada, 19-21 June. http://dx.doi.org/10.2118/30289-MS.

Brooks, R.H. and Corey, A.T. 1964. Hydraulic Properties of Porous Media. Hydrology Papers, No. 3, Colorado State U., Fort Collins, Colorado.

Burton, R.C., Chin, L.Y., Davis, E.R. Enderlin, M. Fuh, G., Hodge, R., Ramos, G.G., VanDeVerg, P., and Werner, M. 2005. North Slope Heavy-Oil Sand-Control Strategy: Detailed Case Study of Sand Production Predictions and Field Measurements for Alaskan Heavy-Oil Multilateral Field Developments. Paper SPE 97279 presented at the SPE Annual Technical Conference and Exhibition, Dallas, Texas, 9-12 October. http://dx.doi.org/10.2118/97279-MS.

Corey, A.T. 1954. The interrelation between gas and oil relative permeabilities. Producers Monthly 19 (November): 38–41.

Davis, E.R., Beardmore, D., Burton, R., Hedges, J., Hodge, R., Martens, H., and Svoboda, C. 2005. Laboratory Testing and Well Productivity Assessment of Drill-in-Fluid Systems in Order To Determine the Optimum Mud System for Alaskan Heavy-Oil Multilateral Field Developments. Paper SPE 96830 presented at the SPE Annual Technical Conference and Exhibition, Dallas, Texas, 9-12 October. http://dx.doi.org/10.2118/96830-MS.

den Boer, L., Poncet, J., Biver, P., Henriquel, P., and Marlot, V. 2006. A New Technique to Achieve History Match Using a Probabilistic Approach. Paper SPE 102871 presented at the 2006 SPE Annual Technical Conference and Exhibition, San Antonio, Texas, 24-27 September. http://dx.doi.org/10.2118/102871-MS.

Esmaiel, T. E. H. 2005. Applications of Experimental Design in Reservoir Management of Smart Wells. Paper SPE 94838 presented at the SPE Latin American and Caribbean Petroleum Engineering Conference, Rio de Janeiro, Brazil, 20-23 June. http://dx.doi.org/10.2118/94838-MS.

Foerster, C.P., Lynch, K.W., Stramp, R.L., Werner, M.R., and Thompson, R.R. 1997. West Sak Field Development: Analysis of a Marginal Project. Paper SPE 37946 presented at the SPE

Hydrocarbon Economics & Evaluation Symposium, Dallas, Texas, 16-18 March. http://dx.doi.org/10.2118/37946-MS.

Kalla, S. and White, C. D. 2005. Efficient Design of Reservoir Simulation Studies for Development and Optimization. Paper SPE 95456 presented at the 2005 SPE Annual Technical Conference and Exhibition, Dallas, 9-12 October. http://dx.doi.org/10.2118/95456-PA.

Lee, L. W., Krum, G. L., Yao, T., Wattenbarger, R. C. and Landis, L. H. 2006. Application of Model-Based Uncertainty Analysis. Paper SPE 101668 presented at the 2006 Abu Dhabi International Petroleum Exhibition and Conference, Abu Dhabi, U.A.E., 5-8 November . http://dx.doi.org/10.2118/101668-MS.

Manceau, E., Zabalza-Mezghani, I., and Roggero, F. 2002. Use of Experimental Design Methodology to Make Decisions in an Uncertain Reservoir Environment from Reservoir Uncertainties to Economic Risk Analysis. Paper WPC 32161 presented at the 17th World Petroleum Congress, Rio De Janeiro, Brazil, 1-5 September. http://dx.doi.org/10.2118/32161-WPC.

McGuire, P.L., Redman, R.S., Jhaveri, B.S., Yancey, K.E., and Ning, S.X. 2005. Viscosity Reduction WAG: An Effective EOR Process for North Slope Viscous Oils. Paper SPE 93914 presented at the SPE Western Regional Meeting, Irvine, California, 30 March-1 April. http://dx.doi.org/10.2118/93914-MS.

Nguyen, H. X., Bae, W., Tran, X. V., and Chung, T. 2011. Experimental Design to Optimize Operating Conditions for SAGD Process, Peace River Oilsands, Alberta. Paper SPE 145917 presented at the SPE Asia Pacific Oil and Gas Conference and Exhibition, Jakarta, Indonesia, 20-22 September. http://dx.doi.org/10.2118/145917-MS.

Panda, M.N., Zhang, M., Ogbe, D.O., Kamath, V.A., and Sharma, G.D. 1989. Reservoir Description of West Sak Sands Using Well Logs. Paper SPE 18759 presented at the SPE California Regional Meeting, Bakersfield, California, 5-7 April. http://dx.doi.org/10.2118/18759-MS.

Peirce, J.W., Hutcherson, M.R., Jensen, M.D., Brice, B., Vasquez, J.E., and Woods, A. 2014. An Overview of Conformance Control Efforts for the West Sak Field on the North Slope of Alaska. Paper SPE 169073 presented at the SPE Improved Oil Recovery Symposium, Tulsa, Oklahoma, 12-16 April. http://dx.doi.org/10.2118/169073-MS.

Sahni, I., David, S., Banfield, J., and Langenberg, M. 2010. History Match Case Study: Use of Assisted History Match Tools on Single-well Models in Conjunction with a Full-field History Match. Paper SPE 136432 presented at the 2010 SPE Russian Oil & Gas Technical

Conference and Exhibition, Moscow, Russia, 26-28 October. http://dx.doi.org/10.2118/136432-MS.

Scheihing, M.H., Personal Correspondence, January 2014.

Sharma, A.K., Patil, S.L., Kamath, V.A., and Sharma, G.D. 1989. Miscible Displacement of Heavy West Sak Crude by Solvents in Slim Tube. Presented at the SPE California Regional Meeting, Bakersfield, California, April 5-7. http://dx.doi.org/10.2118/18761-MS.

Sonde, A., Oyedeji-Olaniyan, O., and Ayeni, O. 2013. An Application of Experimental Design to Increase the Likelihood of Success in a Brown Field Re-Development. Paper SPE 167526 presented at the Nigeria Annual International Conference and Exhibition, Lagos, Nigeria, 30 July-1 August. http://dx.doi.org/10.2118/167526-MS.

Targac, G.W., Redman, R.S., Davis, E.R., Rennie, S.B., McKeever, S.O., and Chambers, B.C. 2005. Unlocking the Value in West Sak Heavy Oil. Paper SPE 97856 presented at the SPE International Thermal Operations and Heavy Oil Symposium, Calgary, Alberta, Canada, 1-3 November. http://dx.doi.org/10.2118/97856-MS.

Uldrich, D., Matar, S., and Miller, H. 2002. Using Statistics to Evaluate a History Match. Paper SPE 75223 presented at the SPE/DOE Improved Oil Recovery Symposium, Tulsa, Oklahoma, 13-17 April 2002. http://dx.doi.org/10.2118/75223-MS.

Werner, M., "West Sak and Ugnu Sands: Low Gravity Oil Zones of the Kuparuk River Area, Alaskan North Slope," Society of Economic Paleontologists and Mineralogists, Pacific Section, Vol. 1 pg. 109-118, Bakersfield, California, March 1987.

White, C. D. and Royer, S. A. 2003. Experimental Design as a Framework for Reservoir Studies. Paper SPE 79676 presented at the SPE Reservoir Simulation Symposium, Houston, Texas, 3-5 February. http://dx.doi.org/10.2118/79676-MS.

Zhang, J., Delshad, M., Sepehrnoori, K., and Pope, G. A. 2005. An Efficient Reservoir Simulation Approach to Design and Optimize Improved Oil Recovery Processes with Distributed Computing. Paper SPE 94733 presented at the SPE Latin American and Caribbean Petroleum Engineering Conference, Rio de Janeiro, Brazil, 20-23 June. http://dx.doi.org/10.2118/94733-MS.

CHAPTER 9.0

APPENDICES

Appendix A: Well-level Match Quality Plots

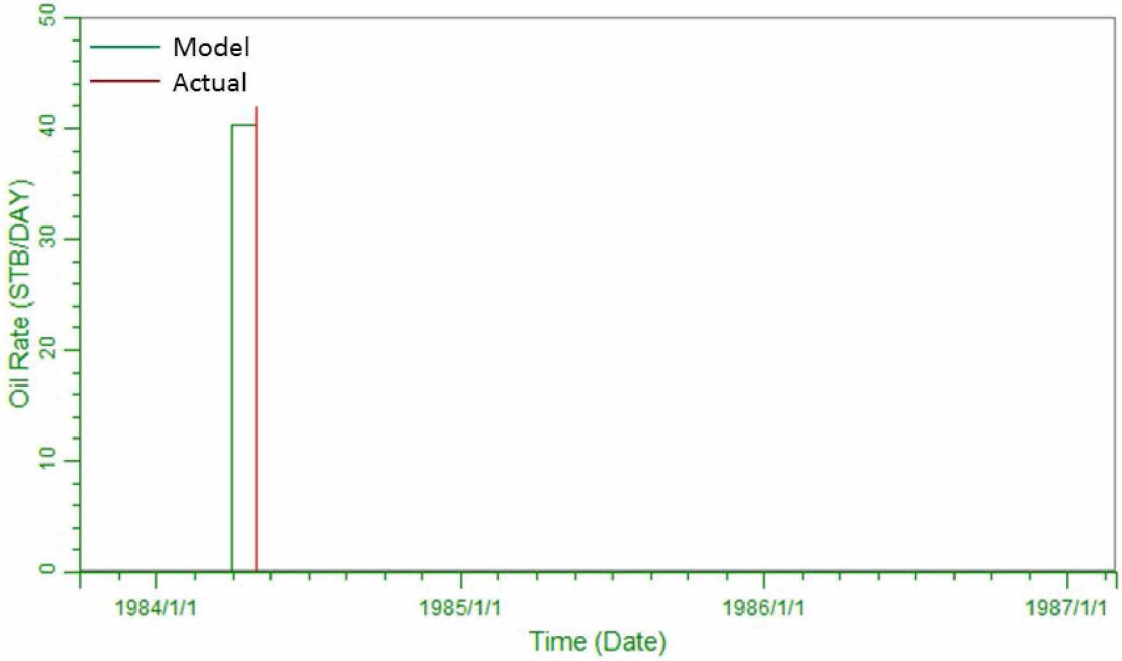

Figure A-1: Comparison of Actual and Calculated Model Oil Rates for West Sak Pilot Producer 2

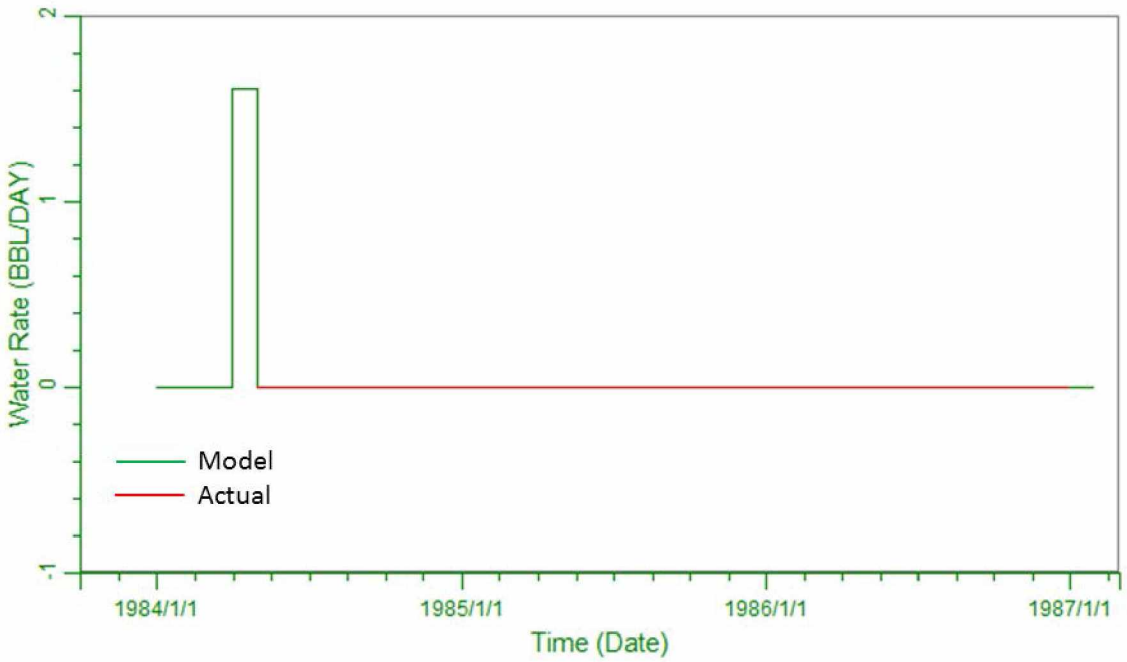

Figure A-2: Comparison of Actual and Calculated Model Water Rates for West Sak Pilot Producer 2

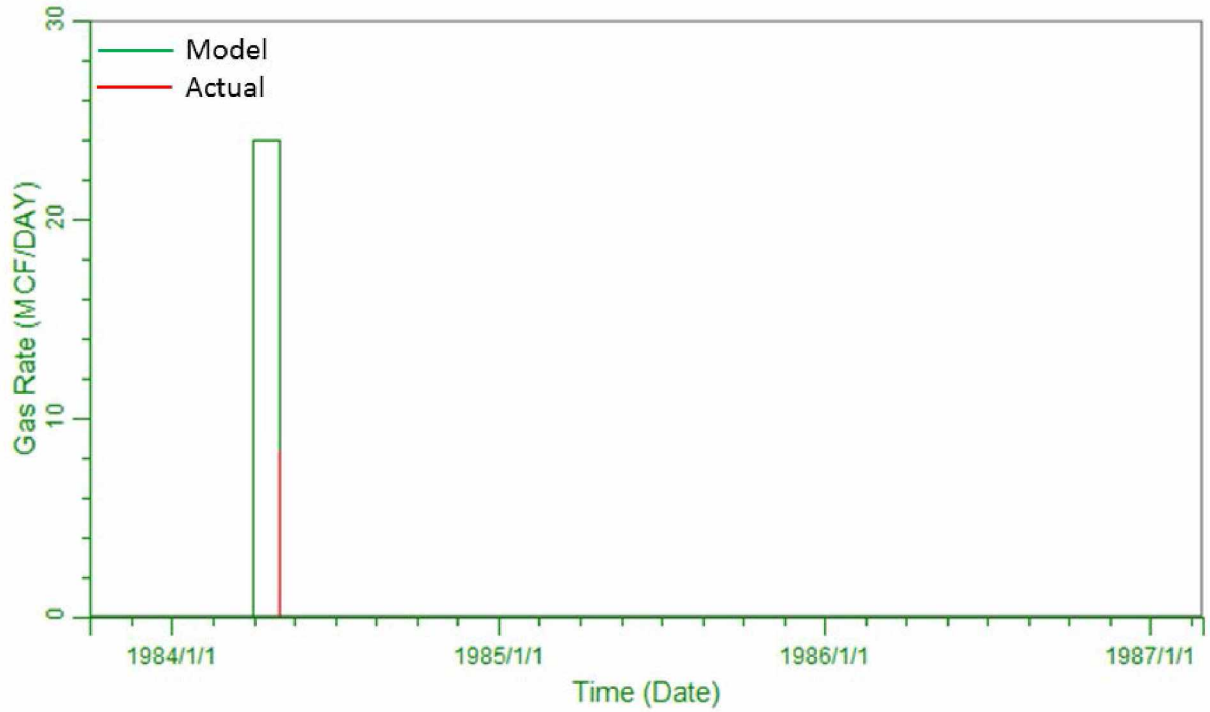

Figure A-3: Comparison of Actual and Calculated Model Gas Rates for West Sak Pilot Producer 2

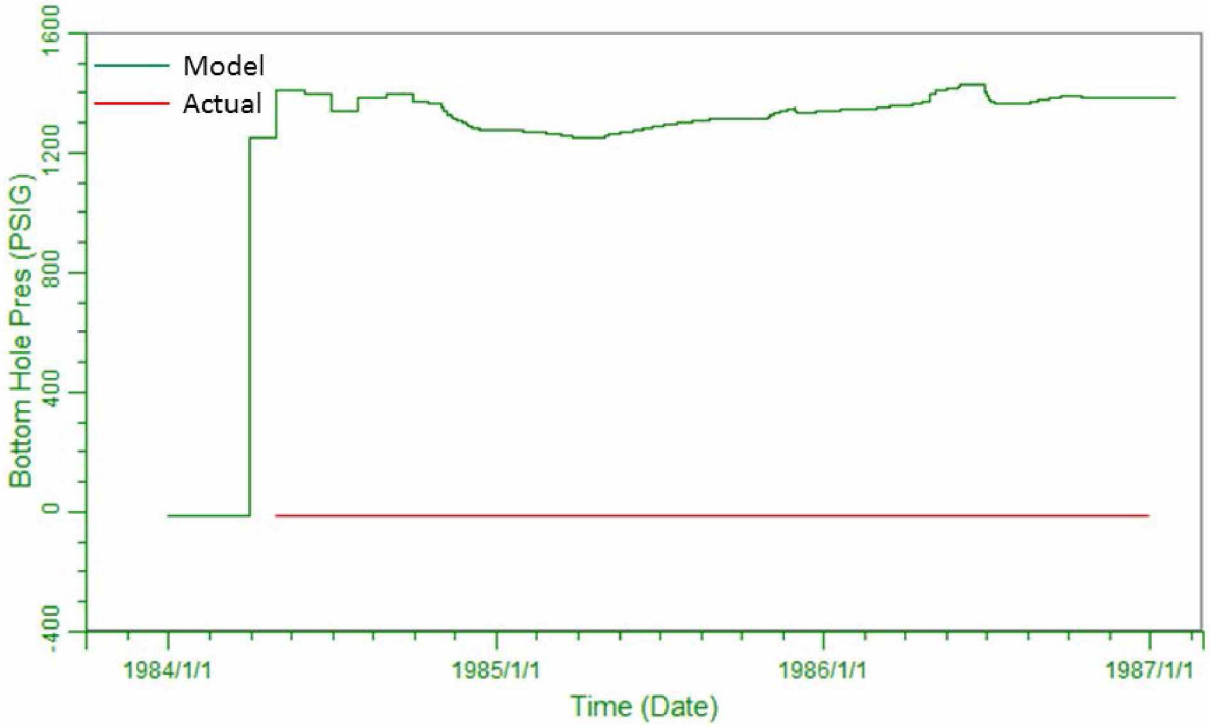

Figure A-4: Comparison of Actual and Calculated Model BHP for West Sak Pilot Producer 2

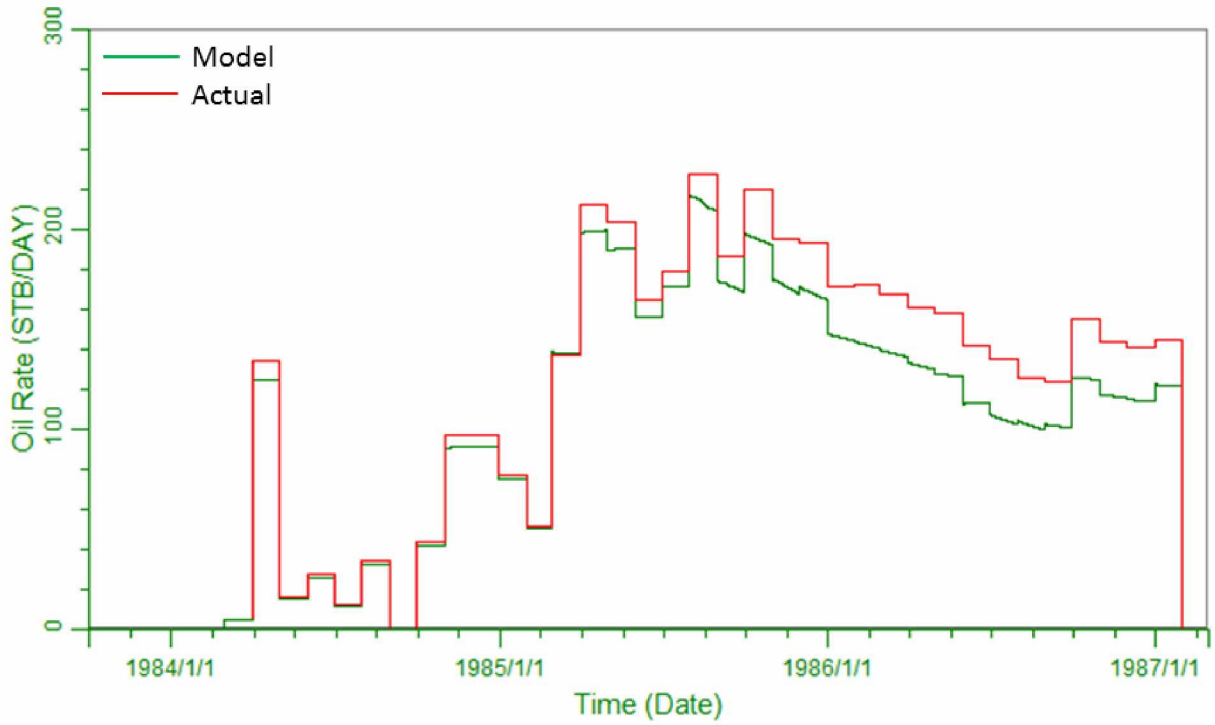

Figure A-5: Comparison of Actual and Calculated Model Oil Rates for West Sak Pilot Producer 3

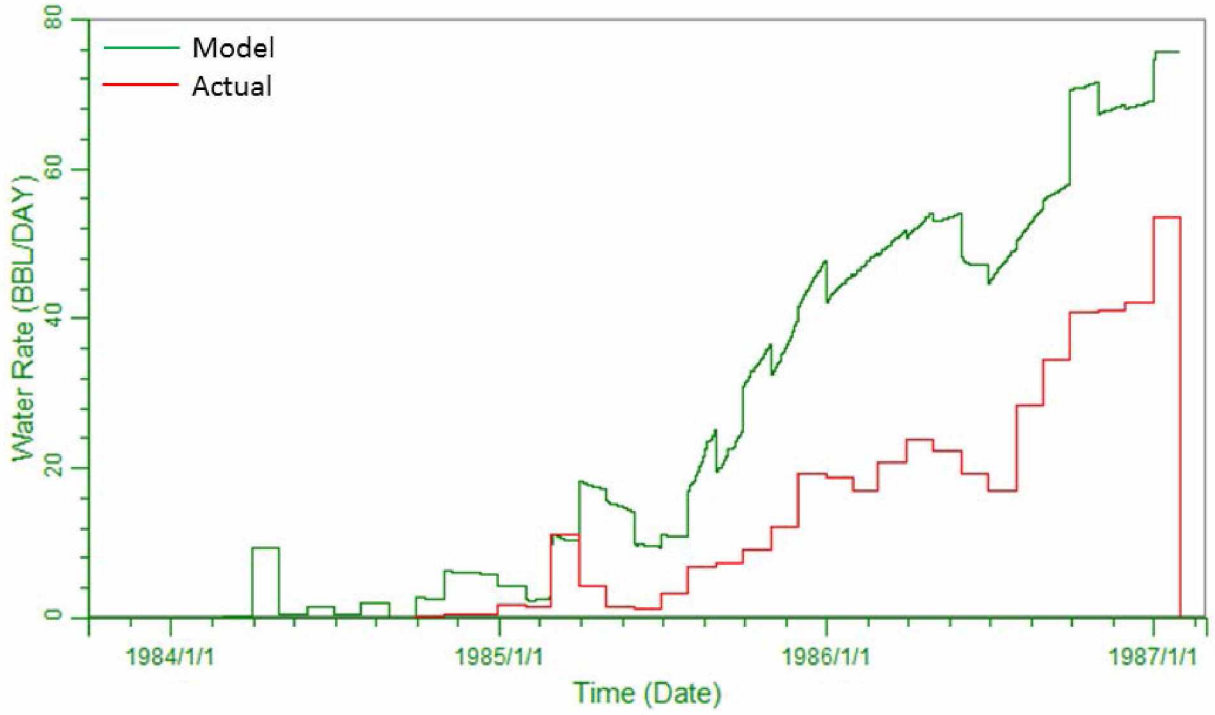

Figure A-6: Comparison of Actual and Calculated Model Water Rates for West Sak Pilot Producer 3

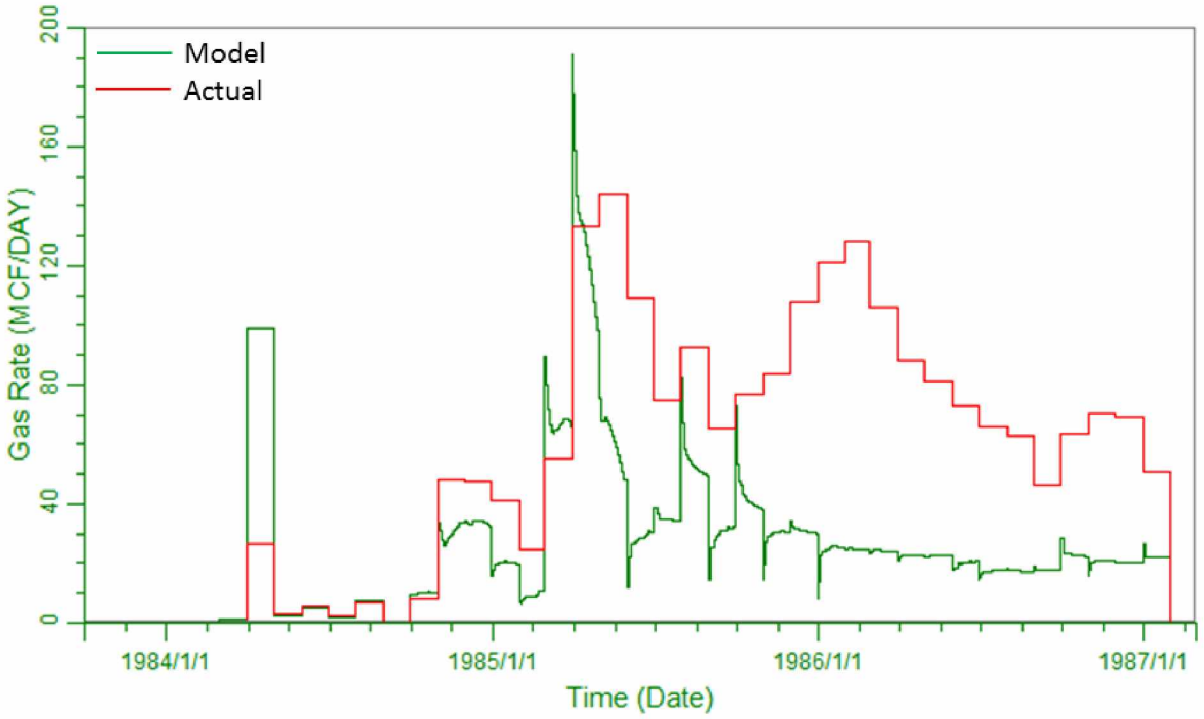

Figure A-7: Comparison of Actual and Calculated Model Gas Rates for West Sak Pilot Producer 3

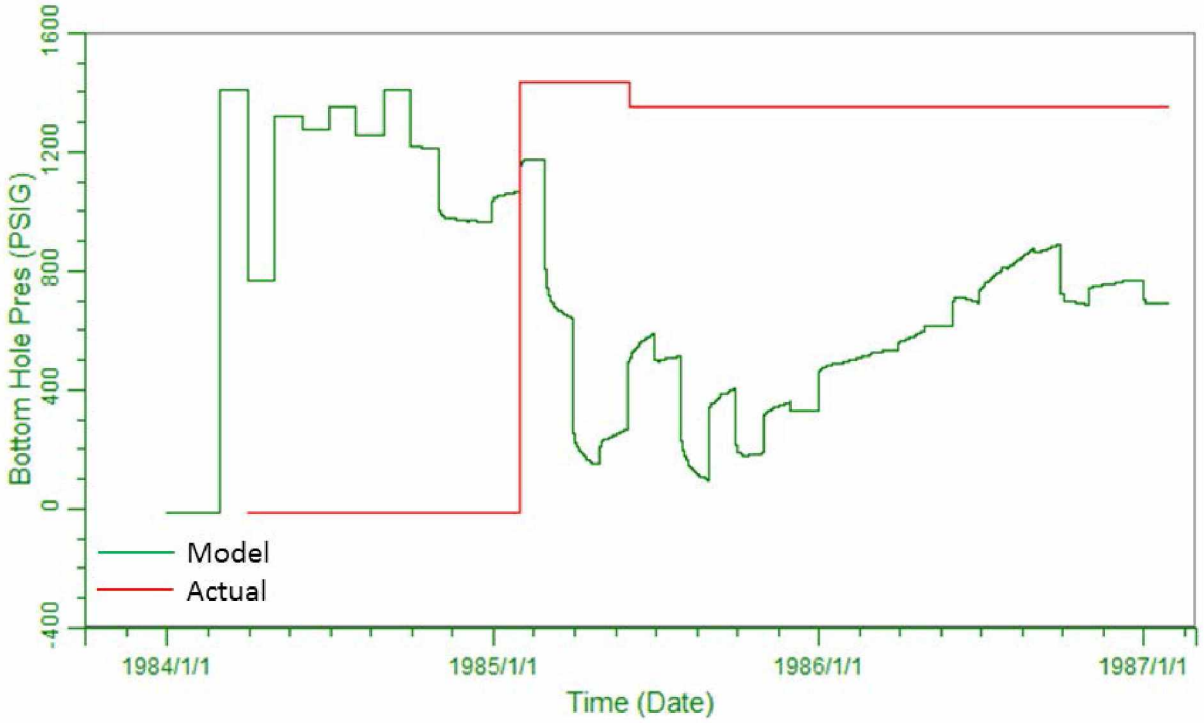

Figure A-8: Comparison of Actual and Calculated Model BHP for West Sak Pilot Producer 3

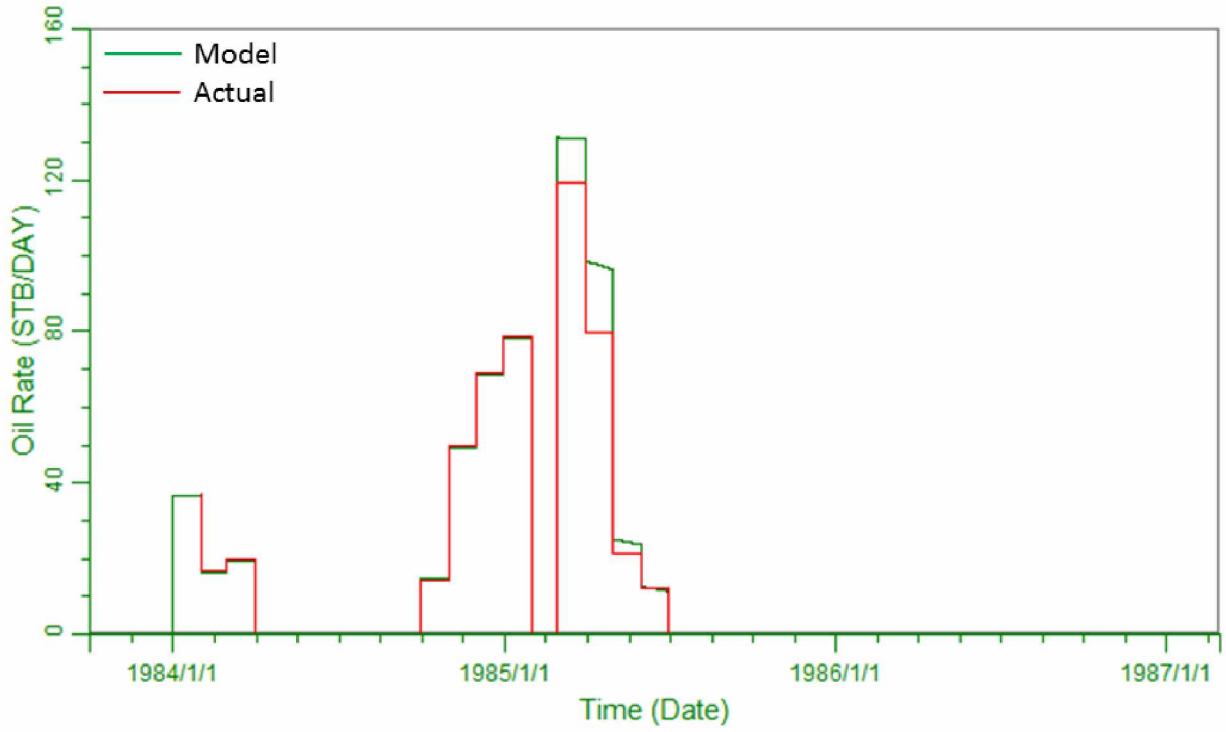

Figure A-9: Comparison of Actual and Calculated Model Oil Rates for West Sak Pilot Producer 4

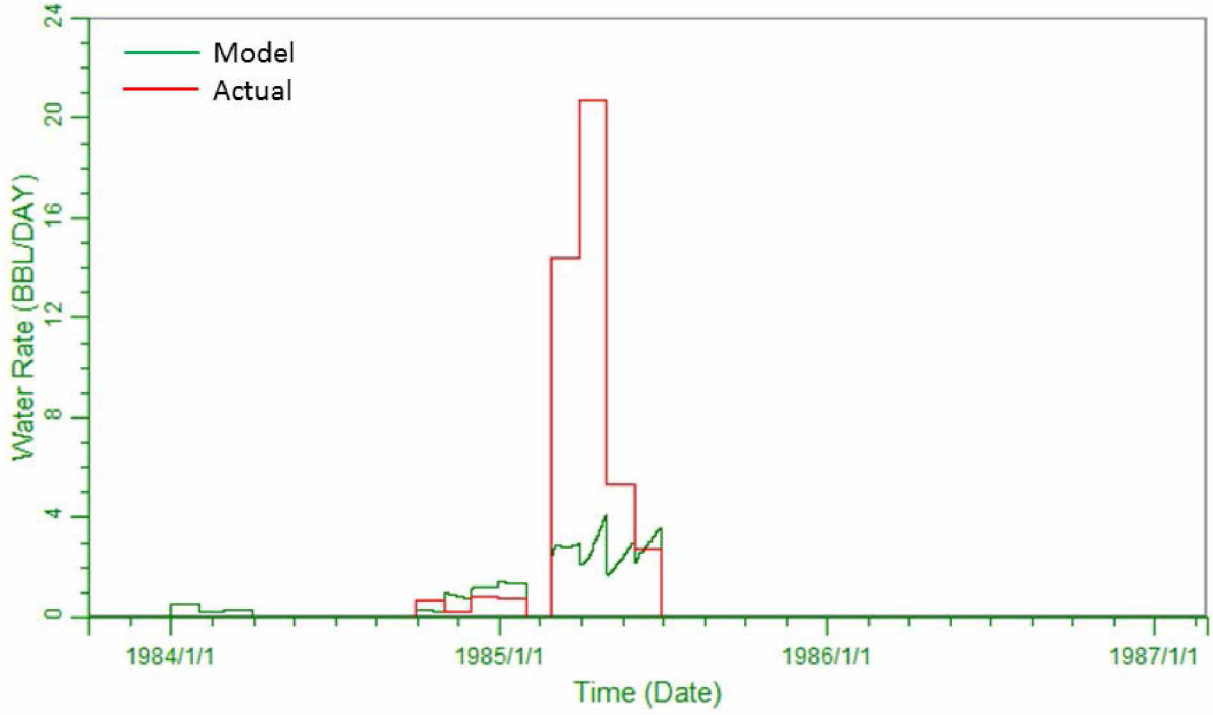

Figure A-10: Comparison of Actual and Calculated Model Water Rates for West Sak Pilot Producer 4

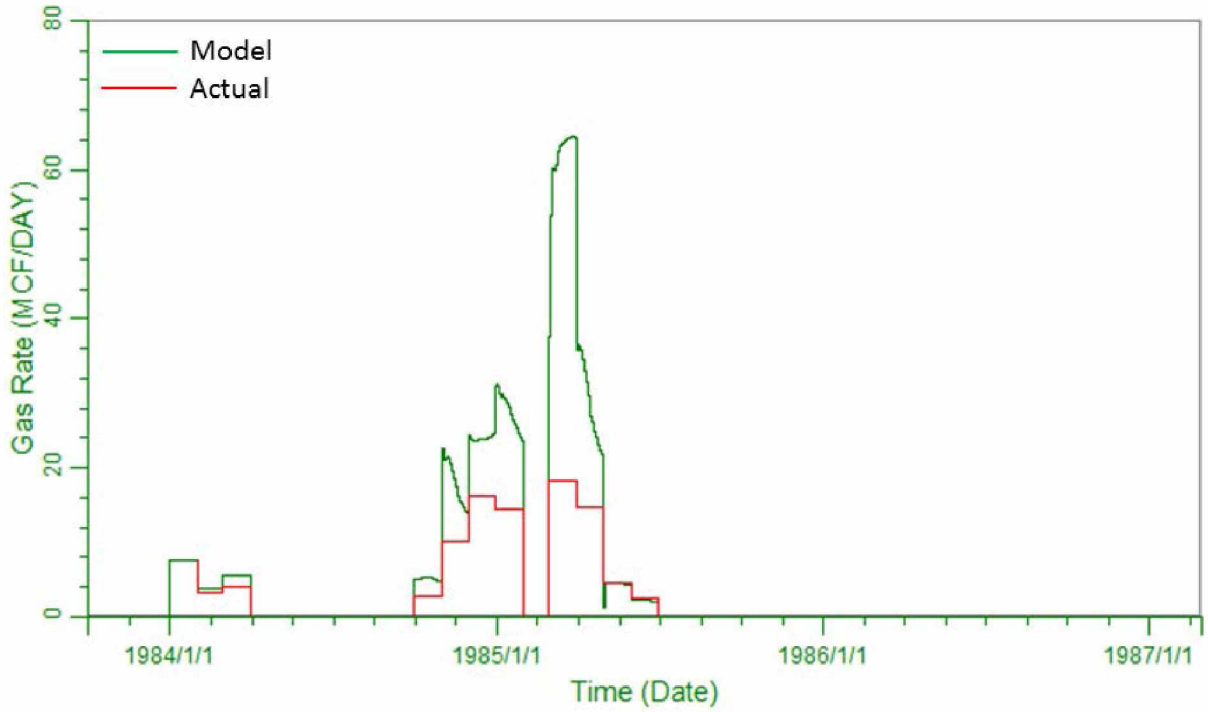

Figure A-11: Comparison of Actual and Calculated Model Gas Rates for West Sak Pilot Producer 4

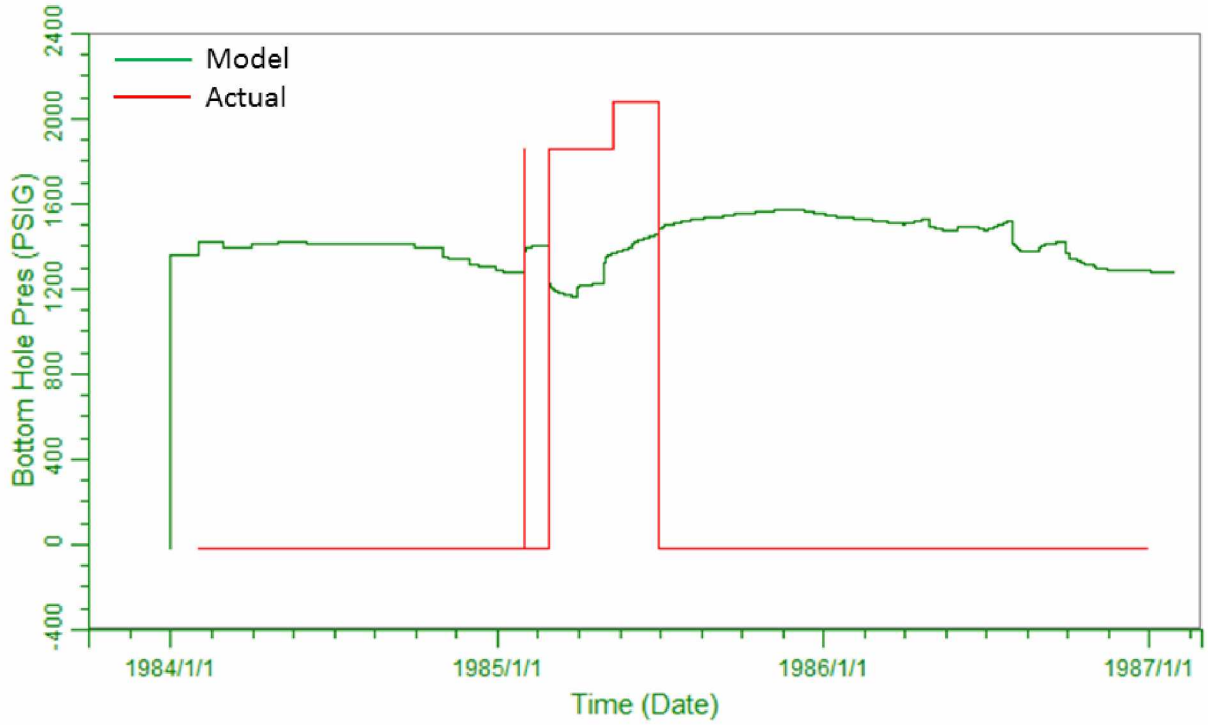

Figure A-12: Comparison of Actual and Calculated Model BHP for West Sak Pilot Producer 4

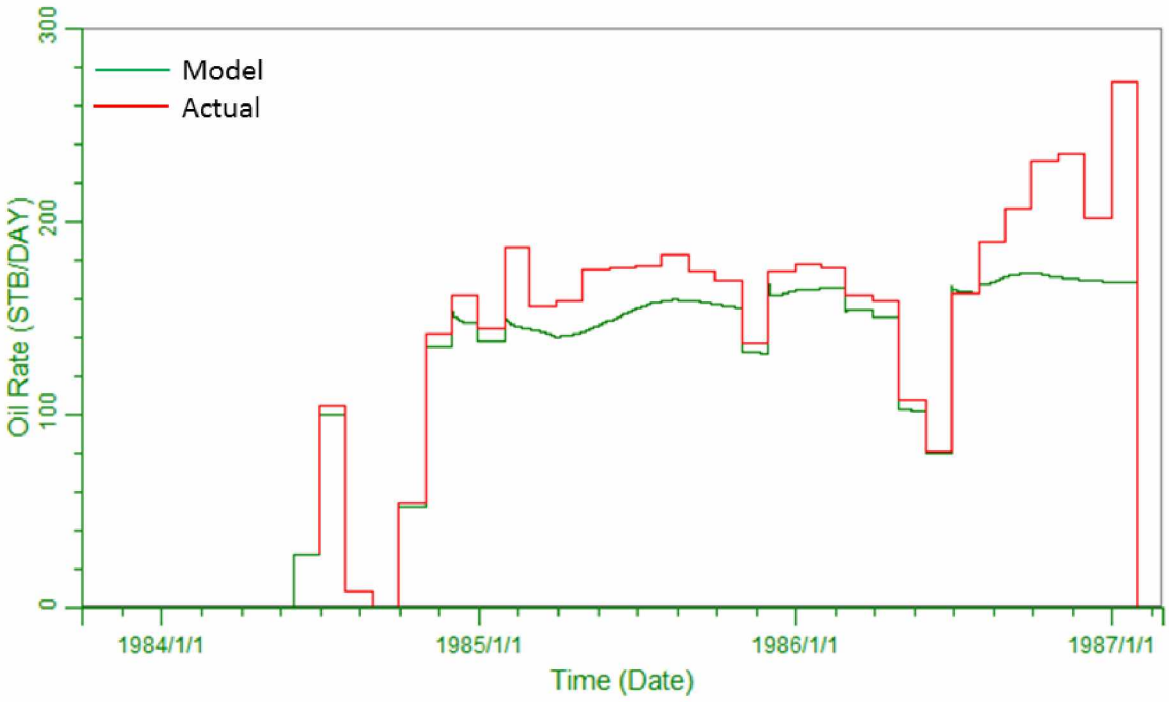

Figure A-13: Comparison of Actual and Calculated Model Oil Rates for West Sak Pilot Producer 5

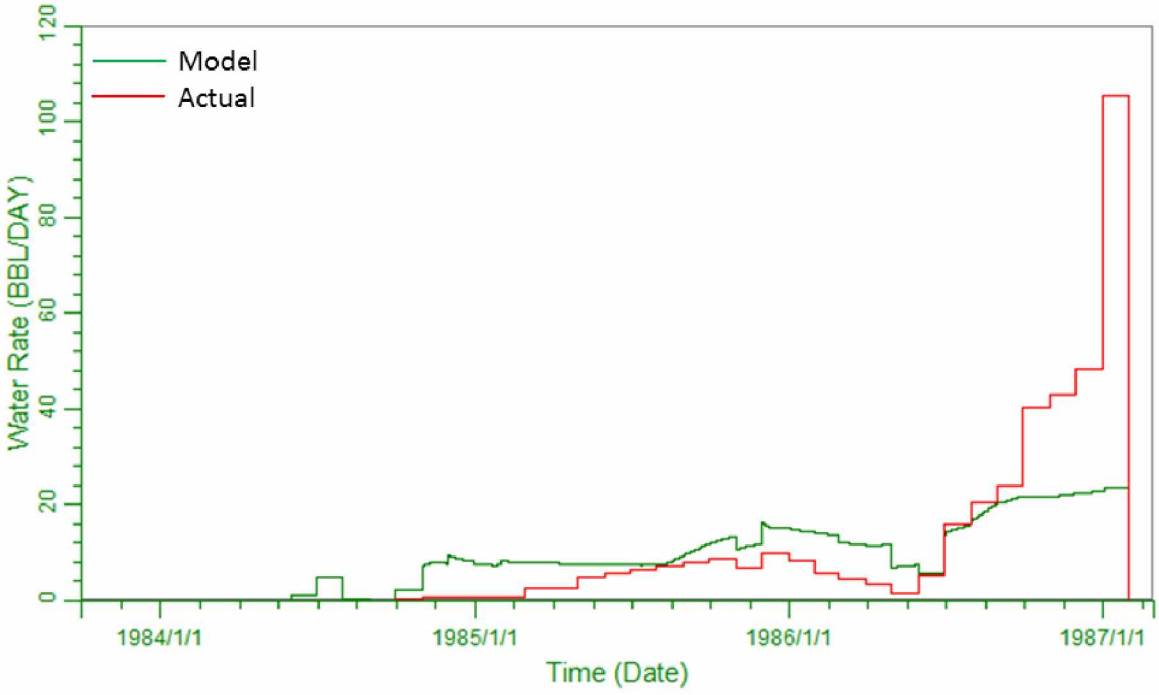

Figure A-14: Comparison of Actual and Calculated Model Water Rates for West Sak Pilot Producer 5

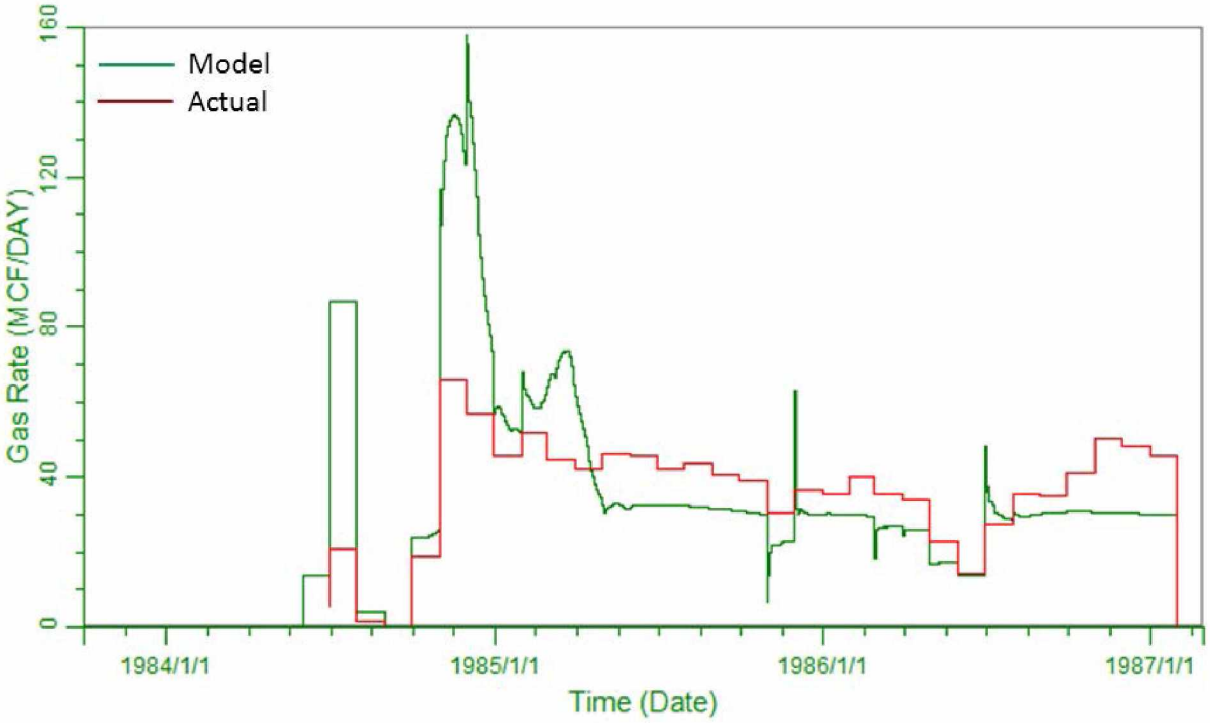

Figure A-15: Comparison of Actual and Calculated Model Gas Rates for West Sak Pilot Producer 5

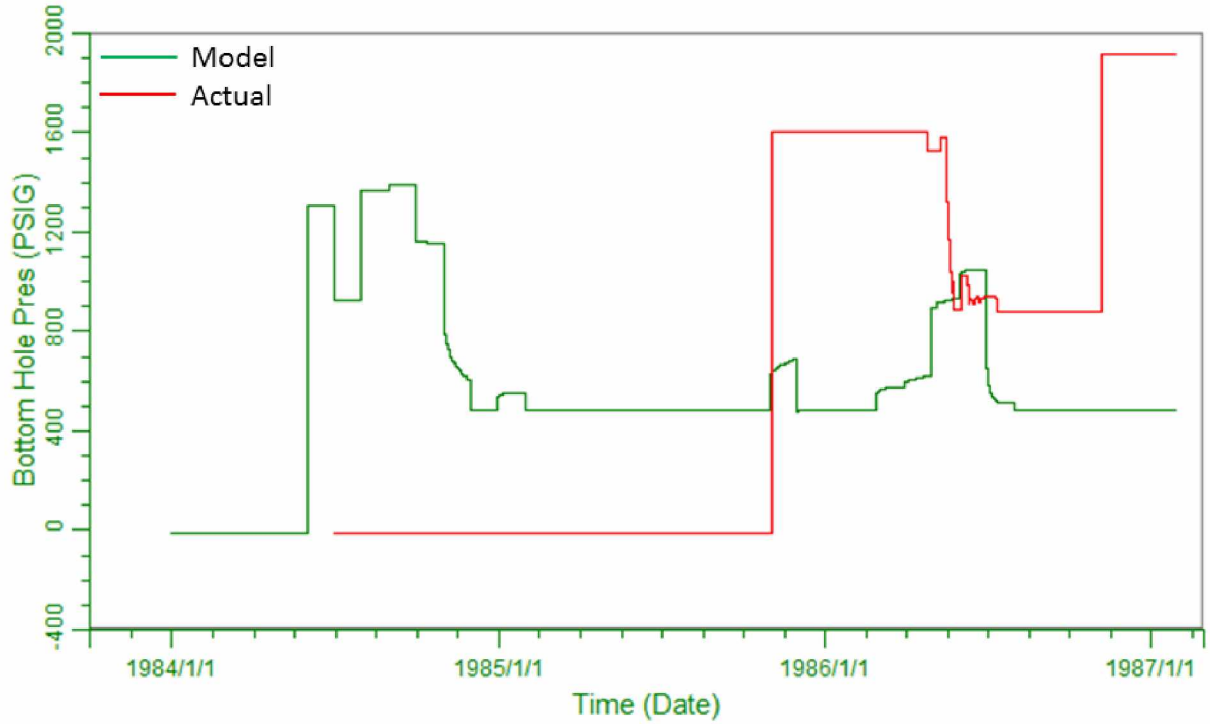

Figure A-16: Comparison of Actual and Calculated Model BHP for West Sak Pilot Producer 5

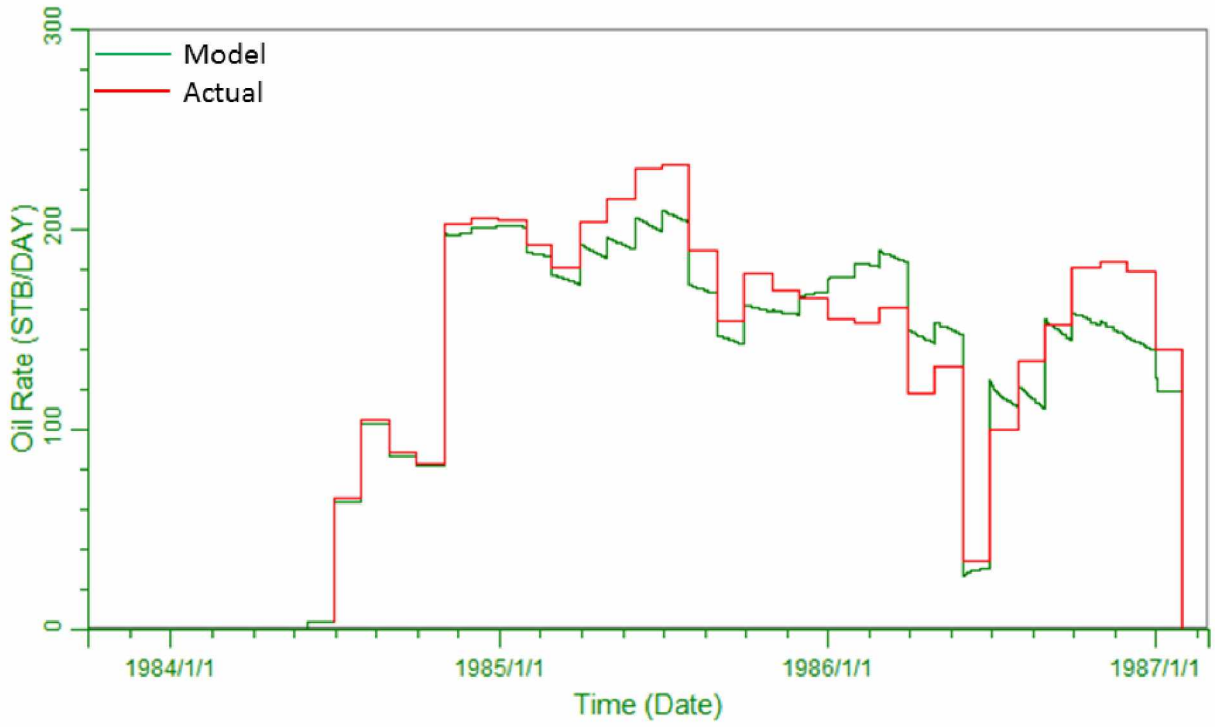

Figure A-17: Comparison of Actual and Calculated Model Oil Rates for West Sak Pilot Producer 7

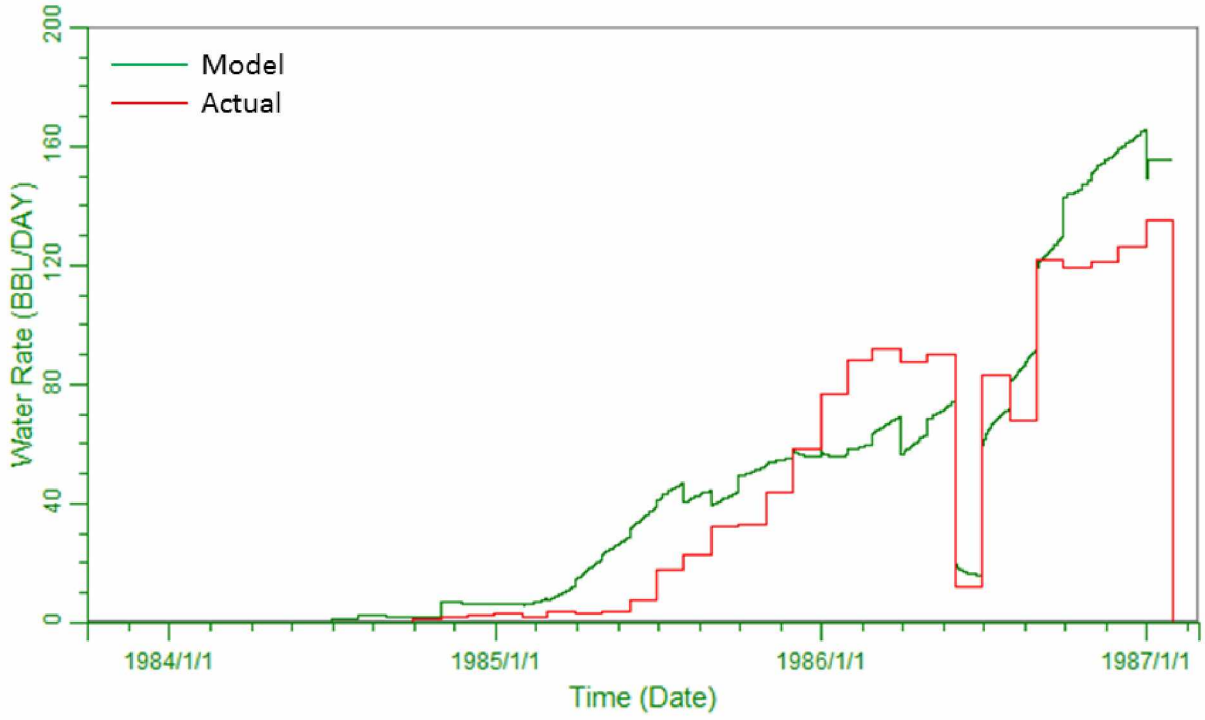

Figure A-18: Comparison of Actual and Calculated Model Water Rates for West Sak Pilot Producer 7

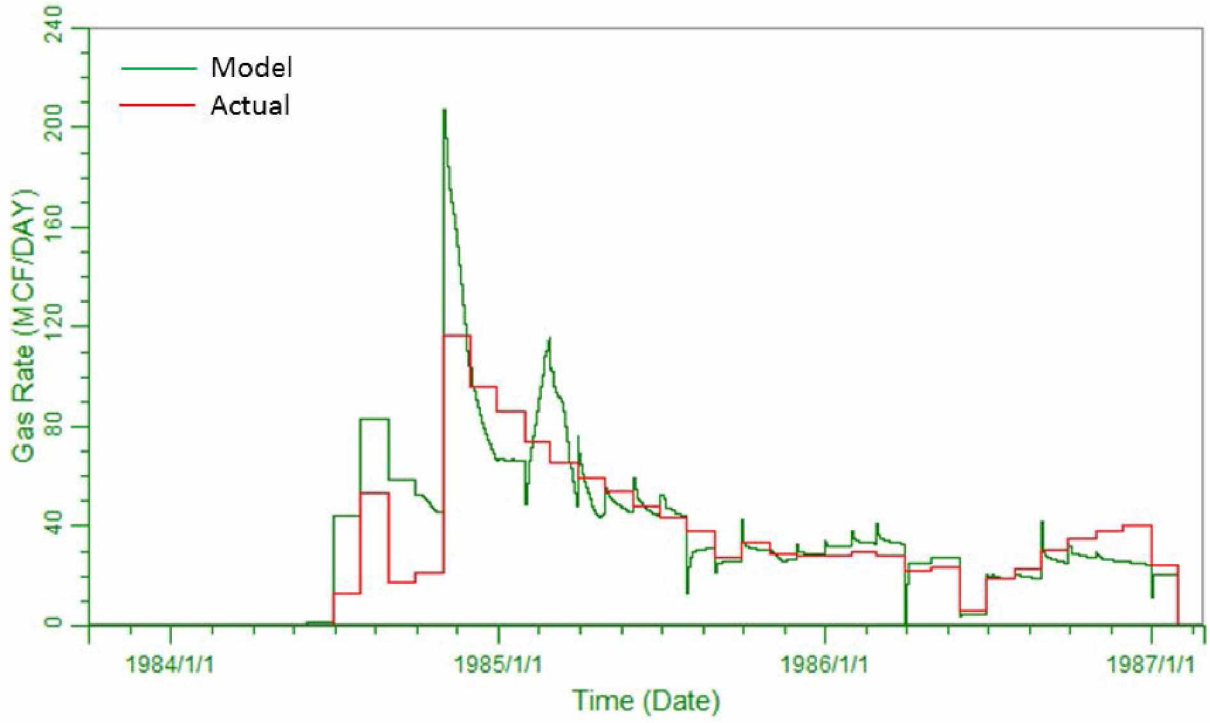

Figure A-19: Comparison of Actual and Calculated Model Gas Rates for West Sak Pilot Producer 7

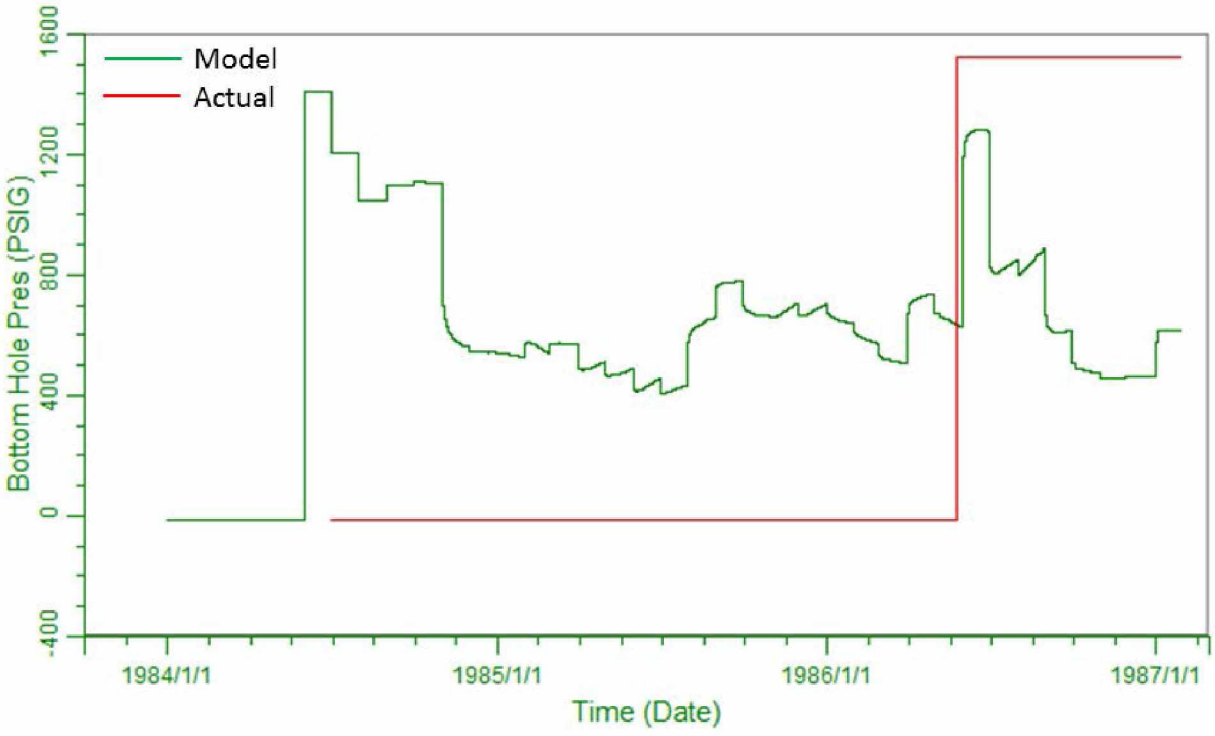

Figure A-20: Comparison of Actual and Calculated Model BHP for West Sak Pilot Producer 7

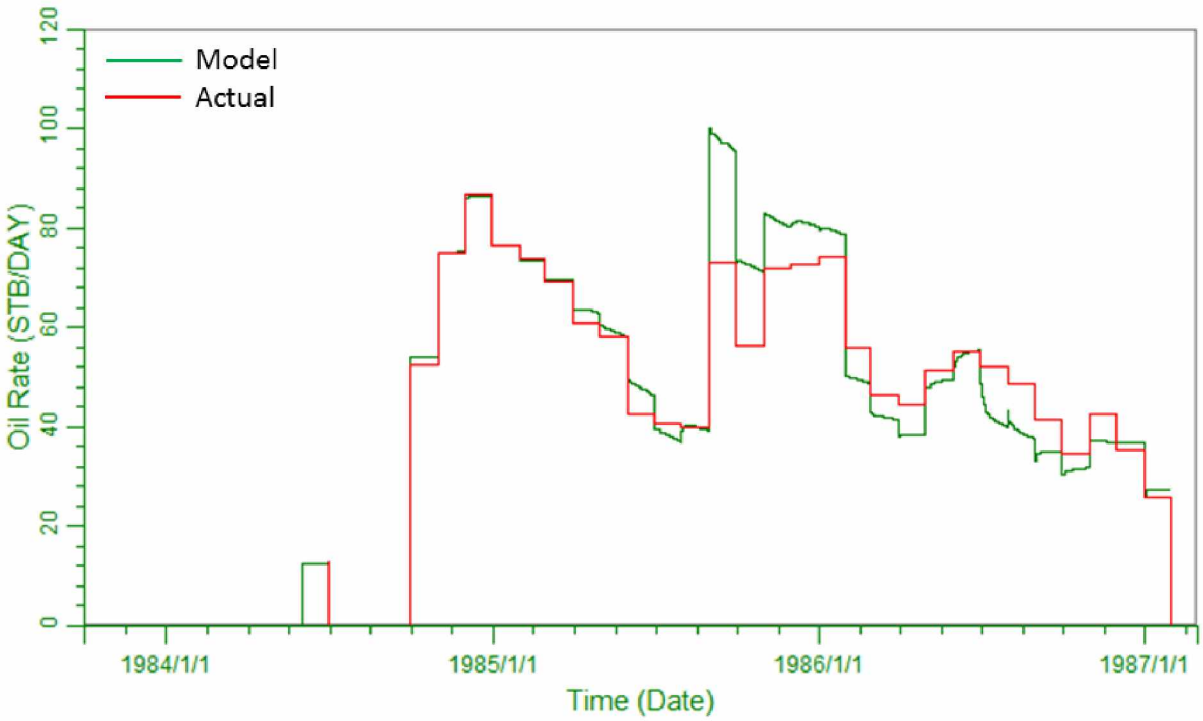

Figure A-21: Comparison of Actual and Calculated Model Oil Rates for West Sak Pilot Producer 9

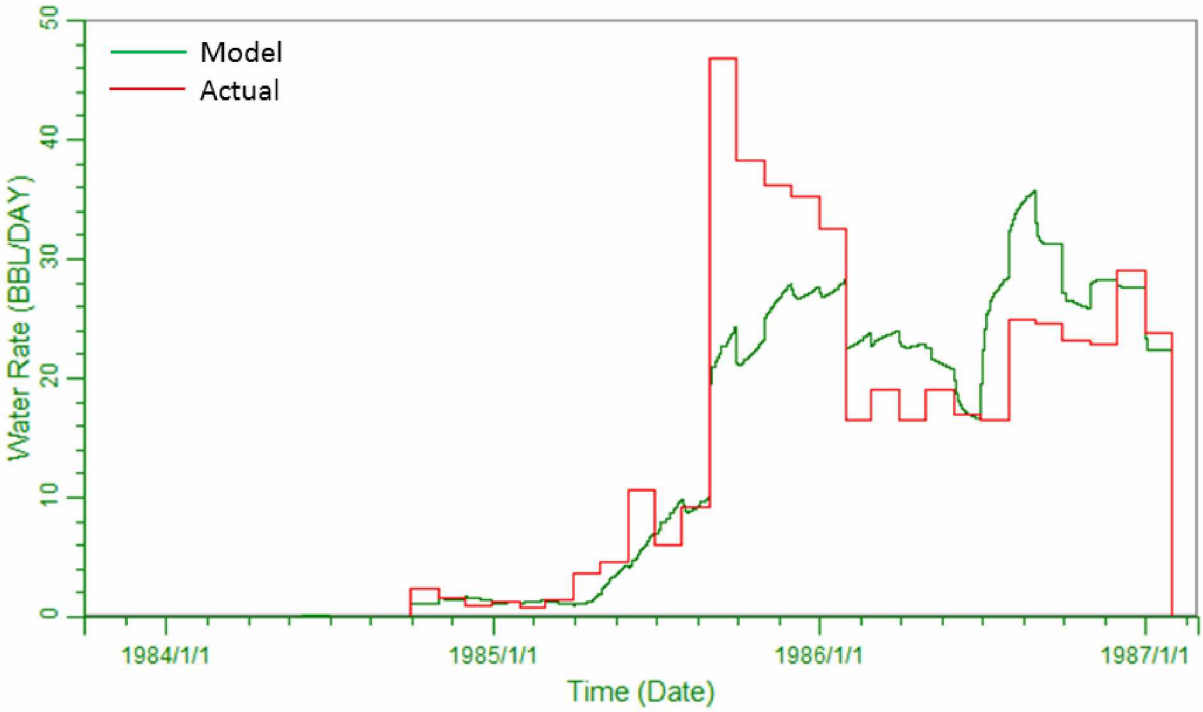

Figure A-22: Comparison of Actual and Calculated Model Water Rates for West Sak Pilot Producer 9

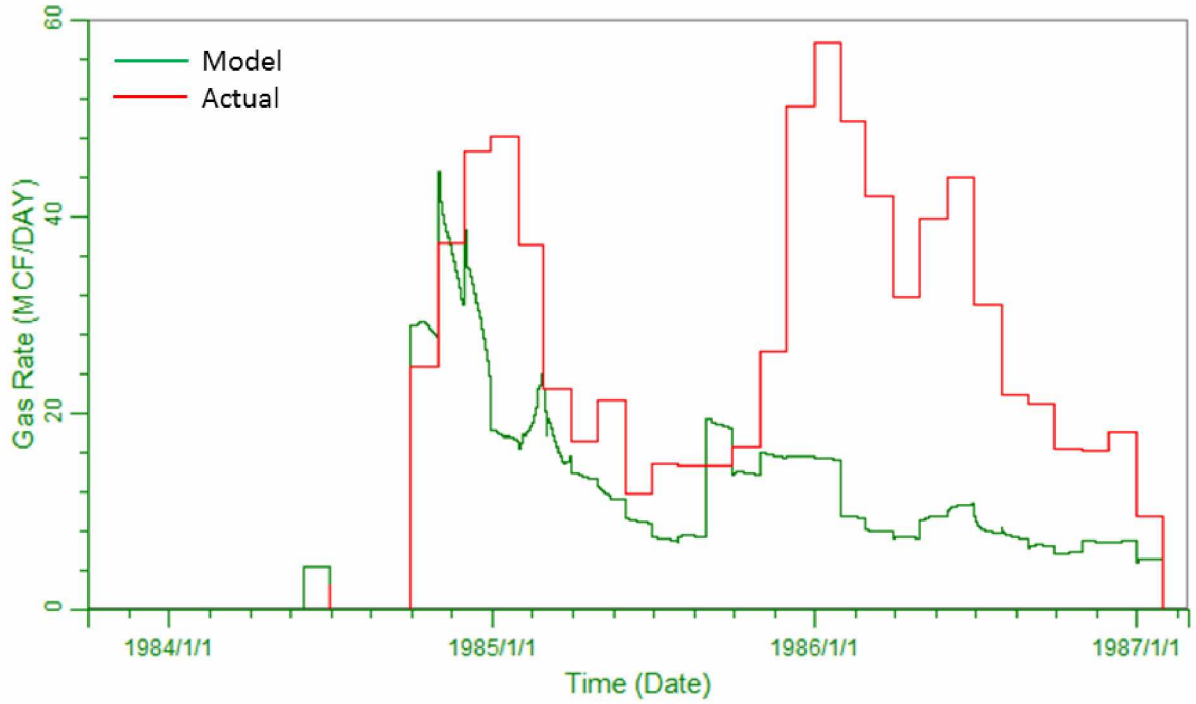

Figure A-23: Comparison of Actual and Calculated Model Gas Rates for West Sak Pilot Producer 9

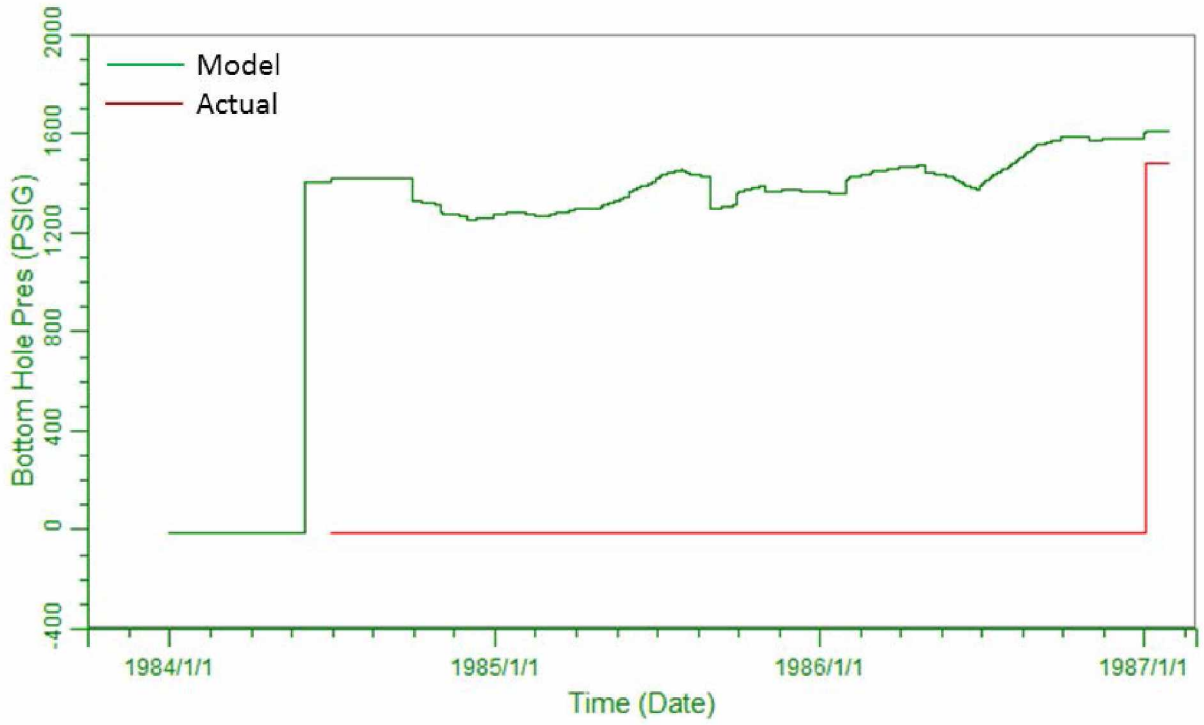

Figure A-24: Comparison of Actual and Calculated Model BHP for West Sak Pilot Producer 9

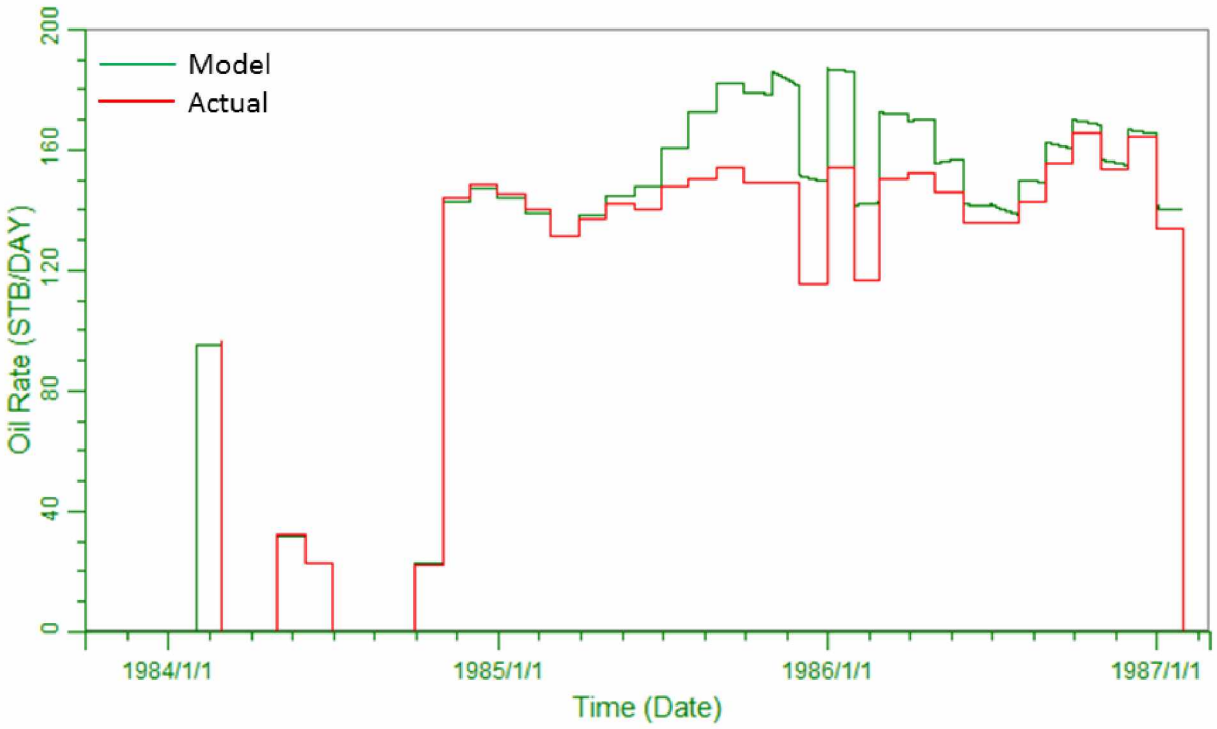

Figure A-25: Comparison of Actual and Calculated Model Oil Rates for West Sak Pilot Producer 10

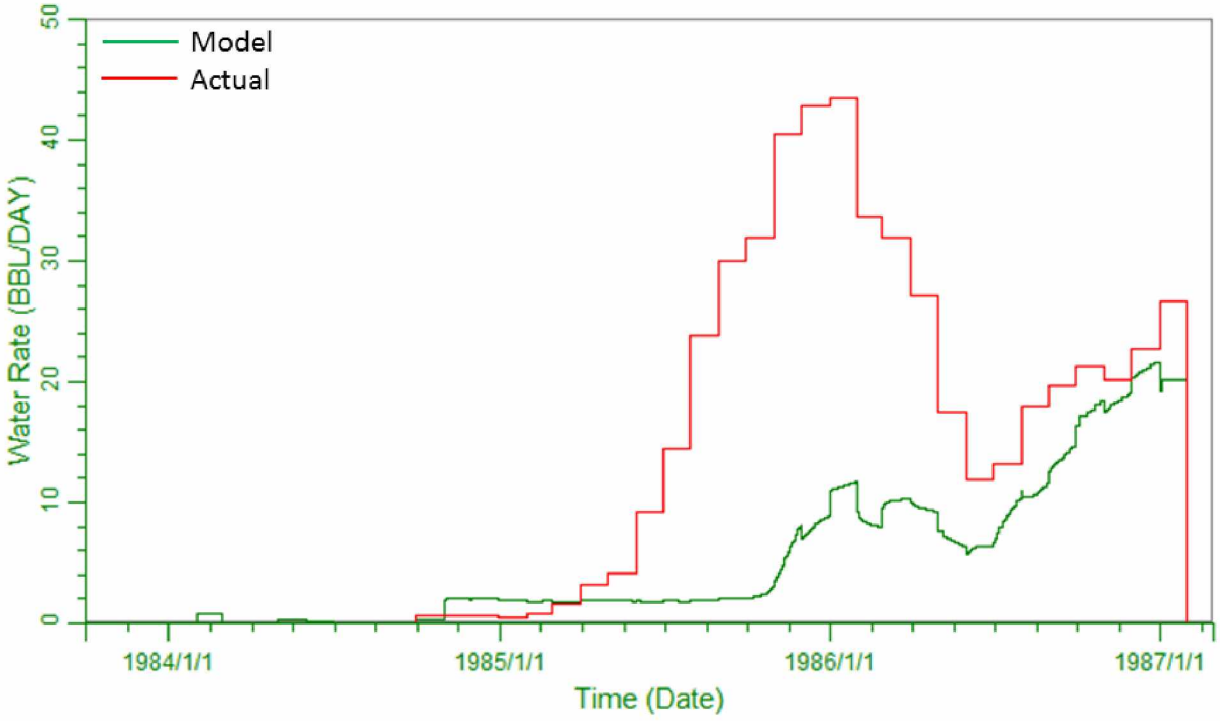

Figure A-26: Comparison of Actual and Calculated Model Water Rates for West Sak Pilot Producer 10

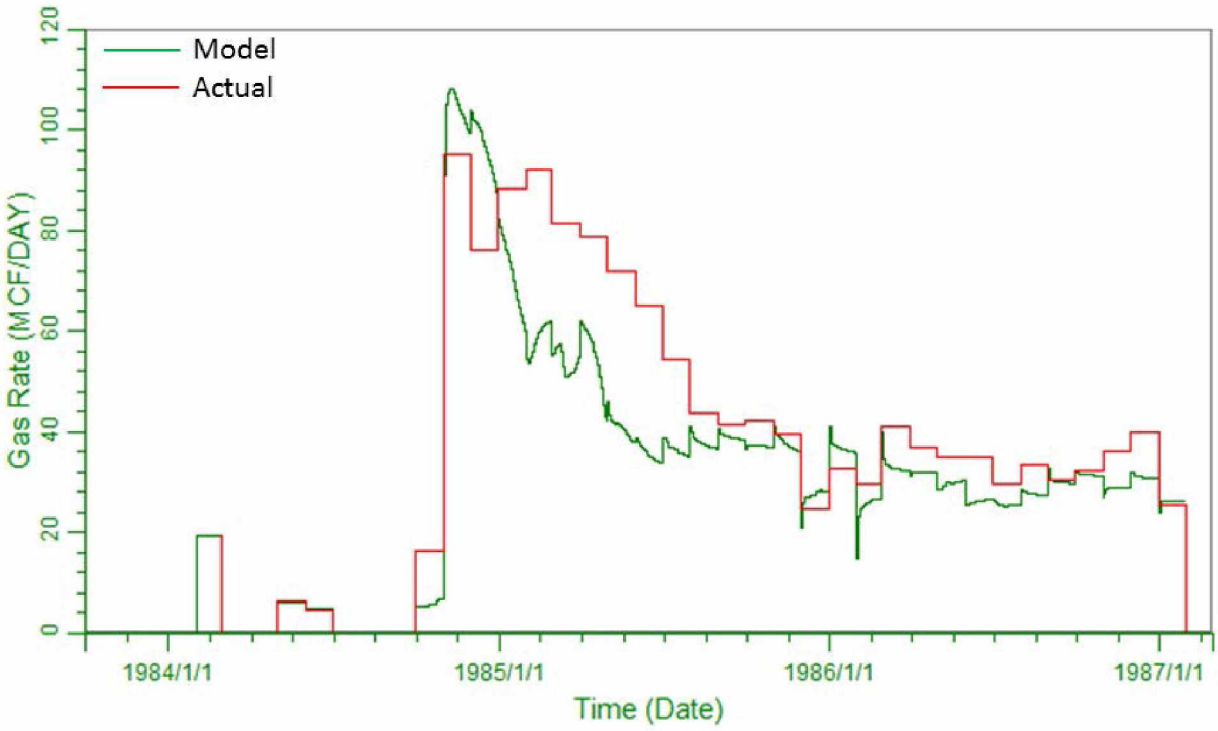

Figure A-27: Comparison of Actual and Calculated Model Gas Rates for West Sak Pilot Producer 10

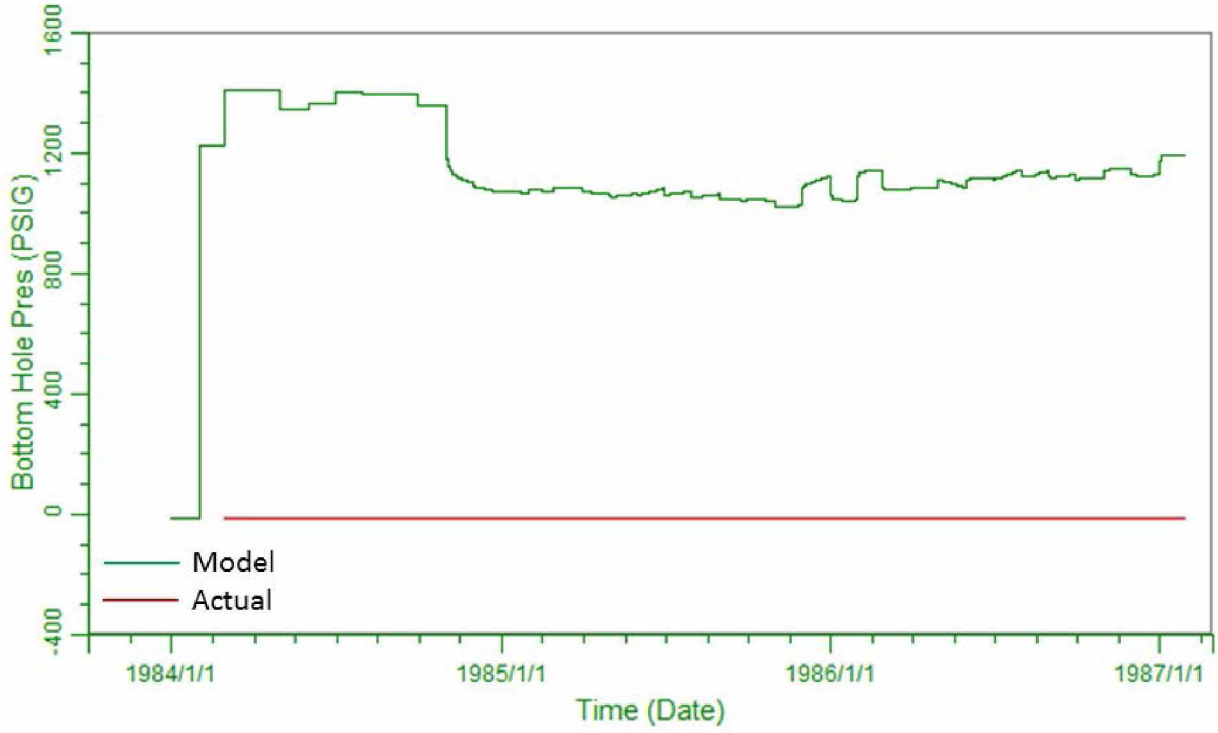

Figure A-28: Comparison of Actual and Calculated Model BHP for West Sak Pilot Producer 10

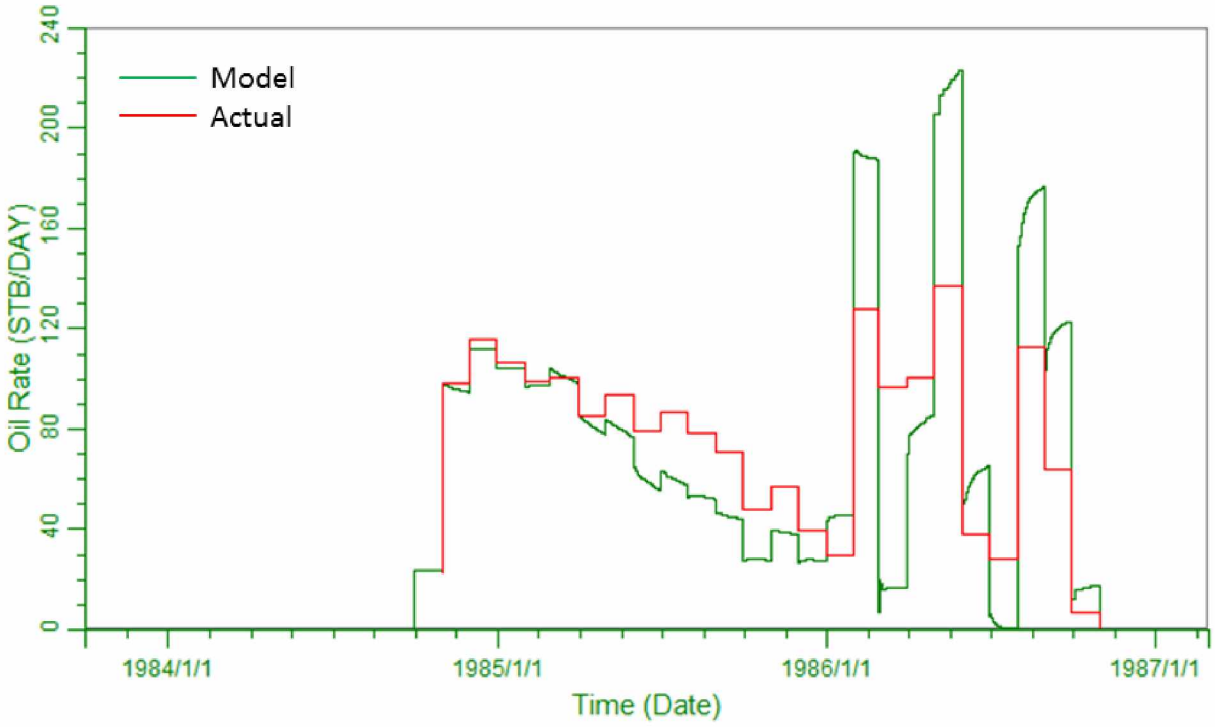

Figure A-29: Comparison of Actual and Calculated Model Oil Rates for West Sak Pilot Producer 12

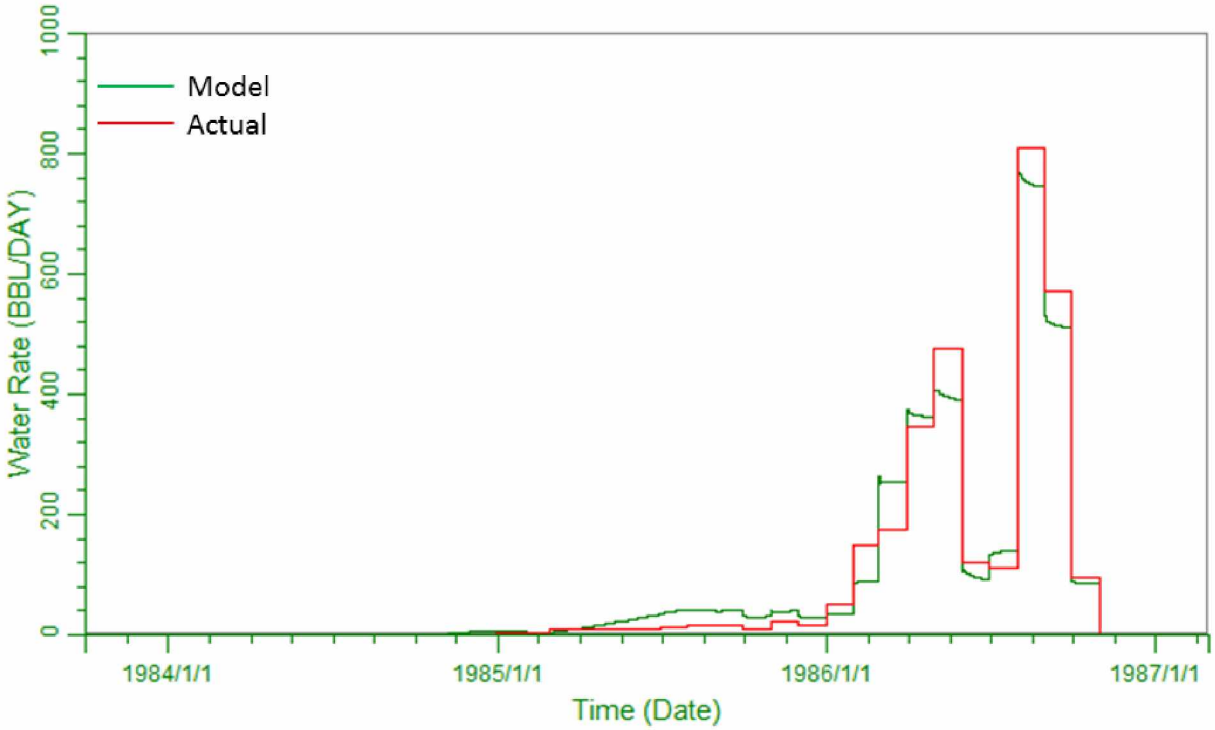

Figure A-30: Comparison of Actual and Calculated Model Water Rates for West Sak Pilot Producer 12

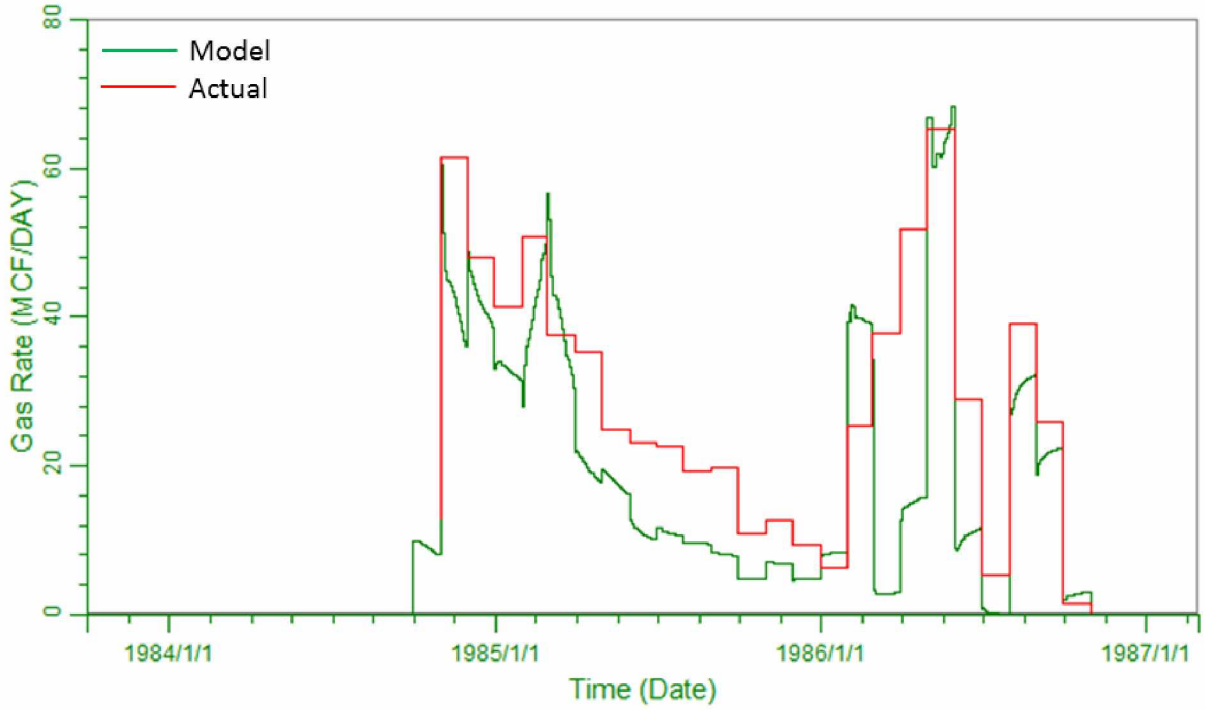

Figure A-31: Comparison of Actual and Calculated Model Gas Rates for West Sak Pilot Producer 12

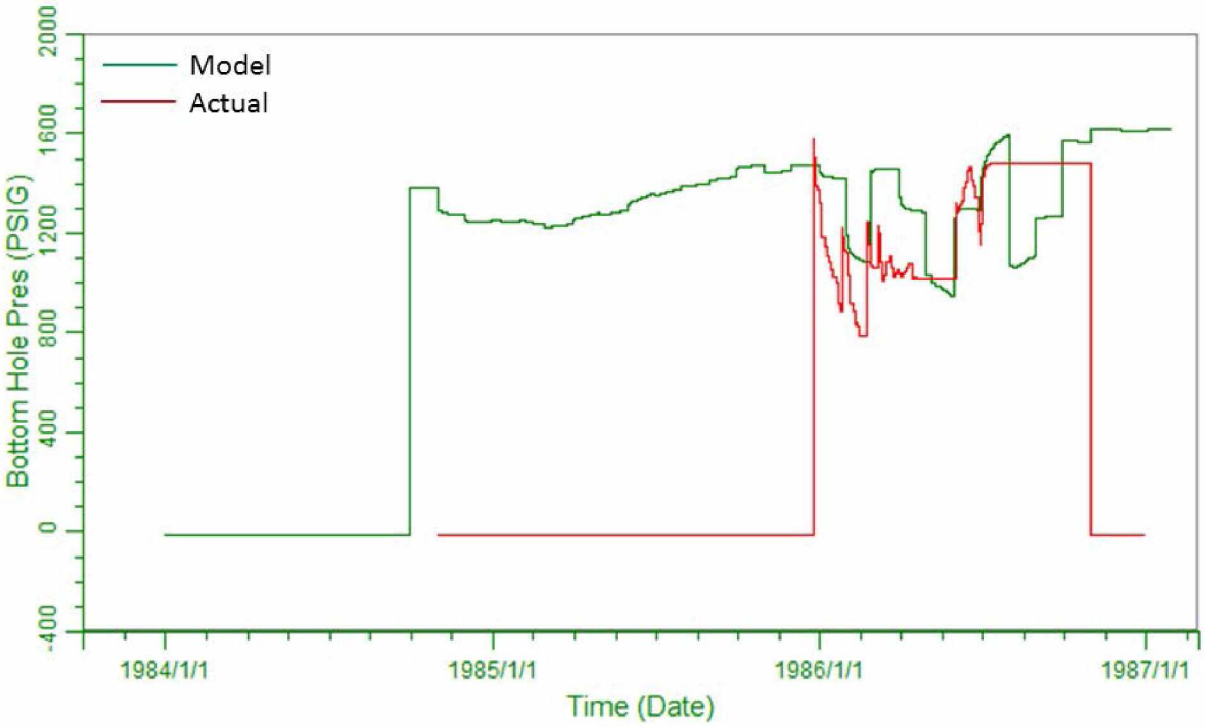

Figure A-32: Comparison of Actual and Calculated Model BHP for West Sak Pilot Producer 12

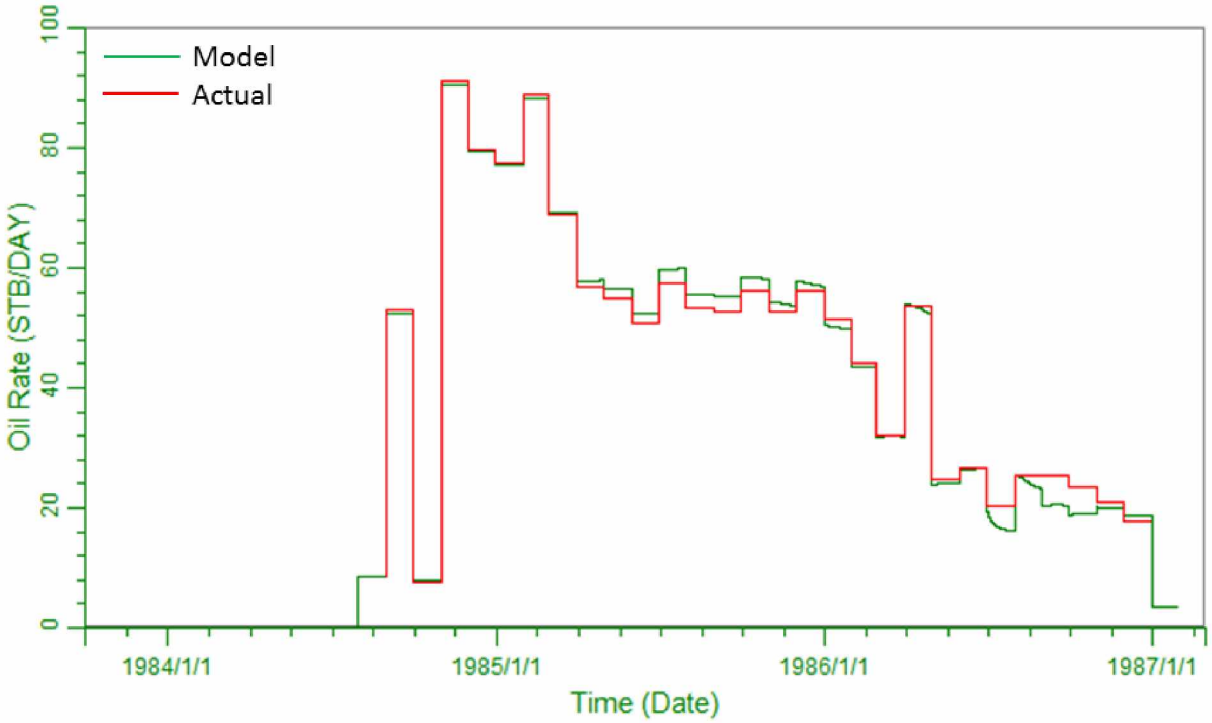

Figure A-33: Comparison of Actual and Calculated Model Oil Rates for West Sak Pilot Producer 13

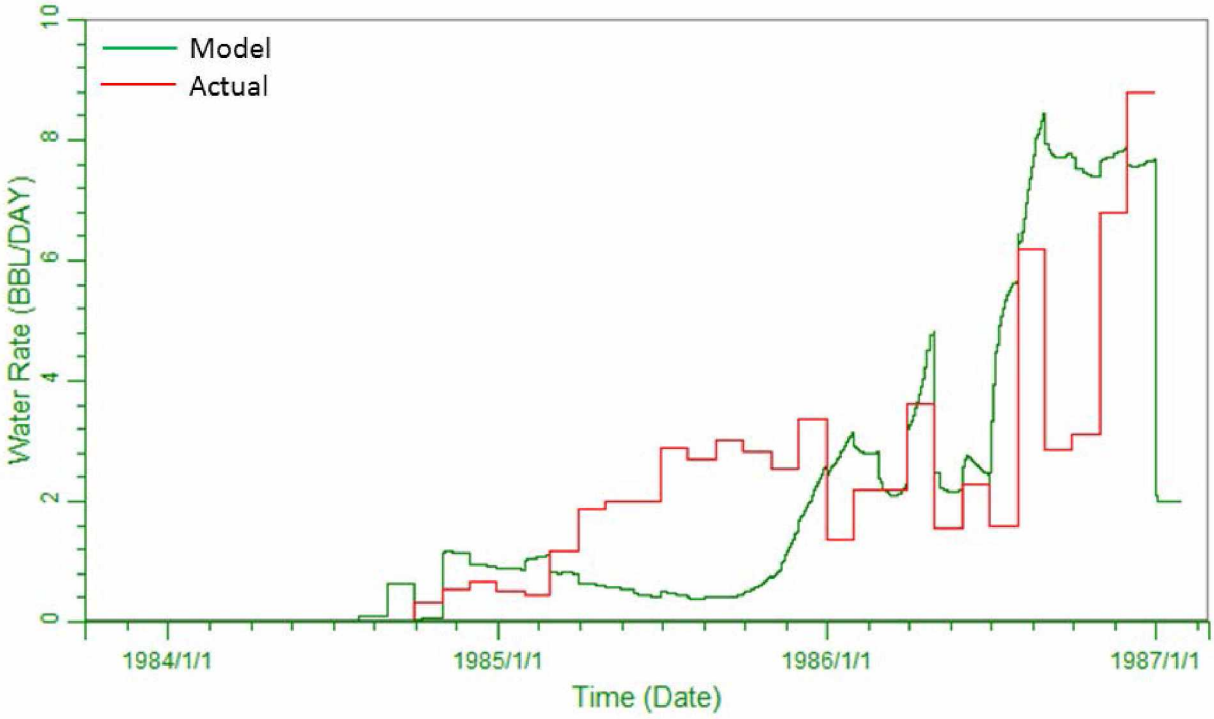

Figure A-34: Comparison of Actual and Calculated Model Water Rates for West Sak Pilot Producer 13

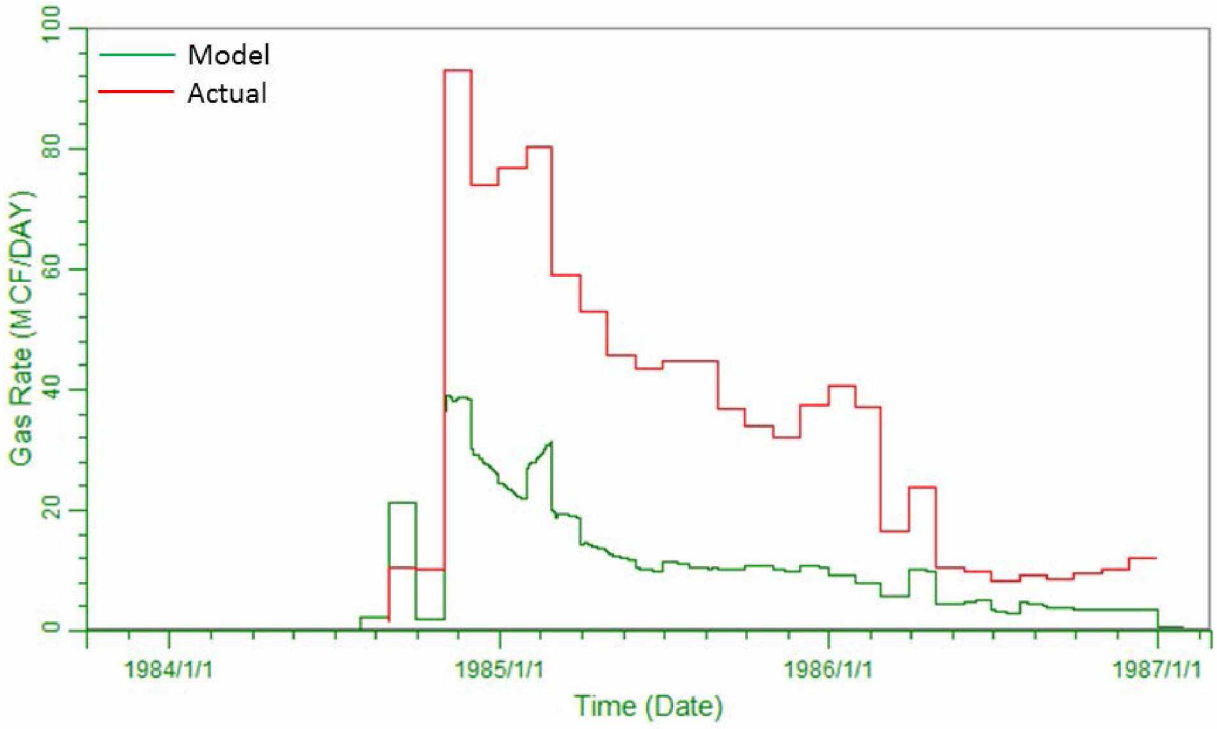

Figure A-35: Comparison of Actual and Calculated Model Gas Rates for West Sak Pilot Producer 13

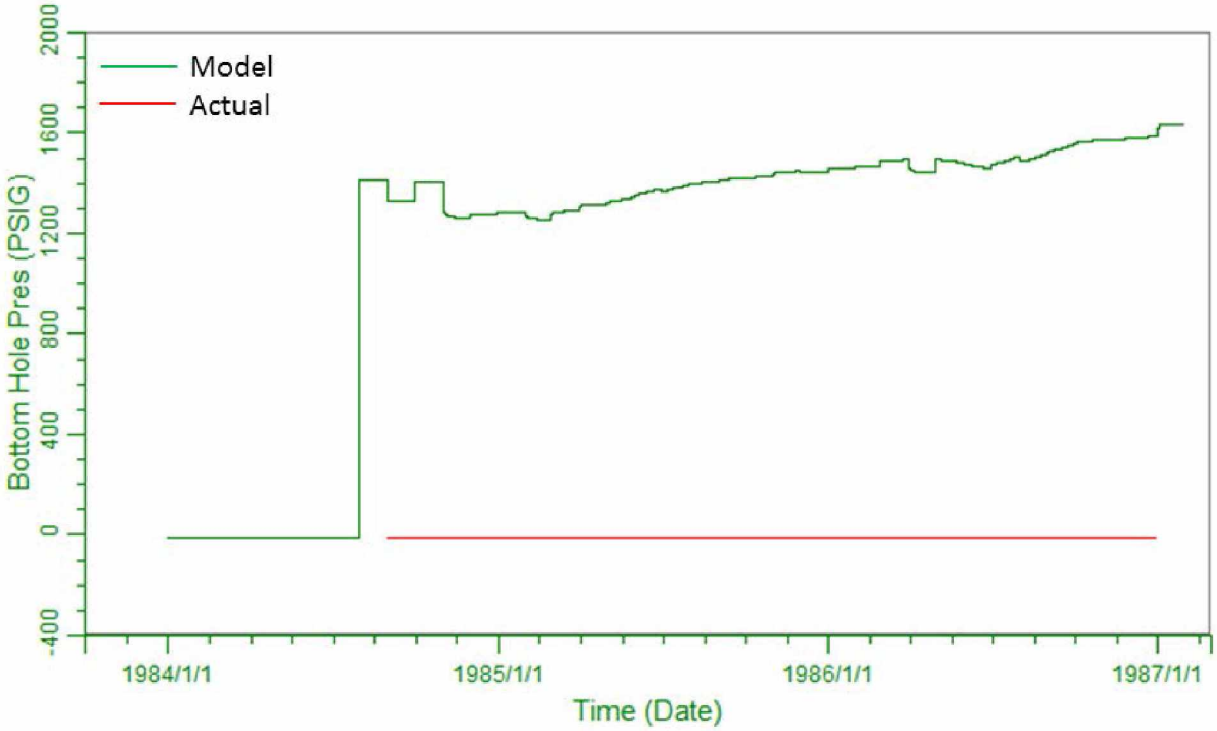

Figure A-36: Comparison of Actual and Calculated Model BHP for West Sak Pilot Producer 13

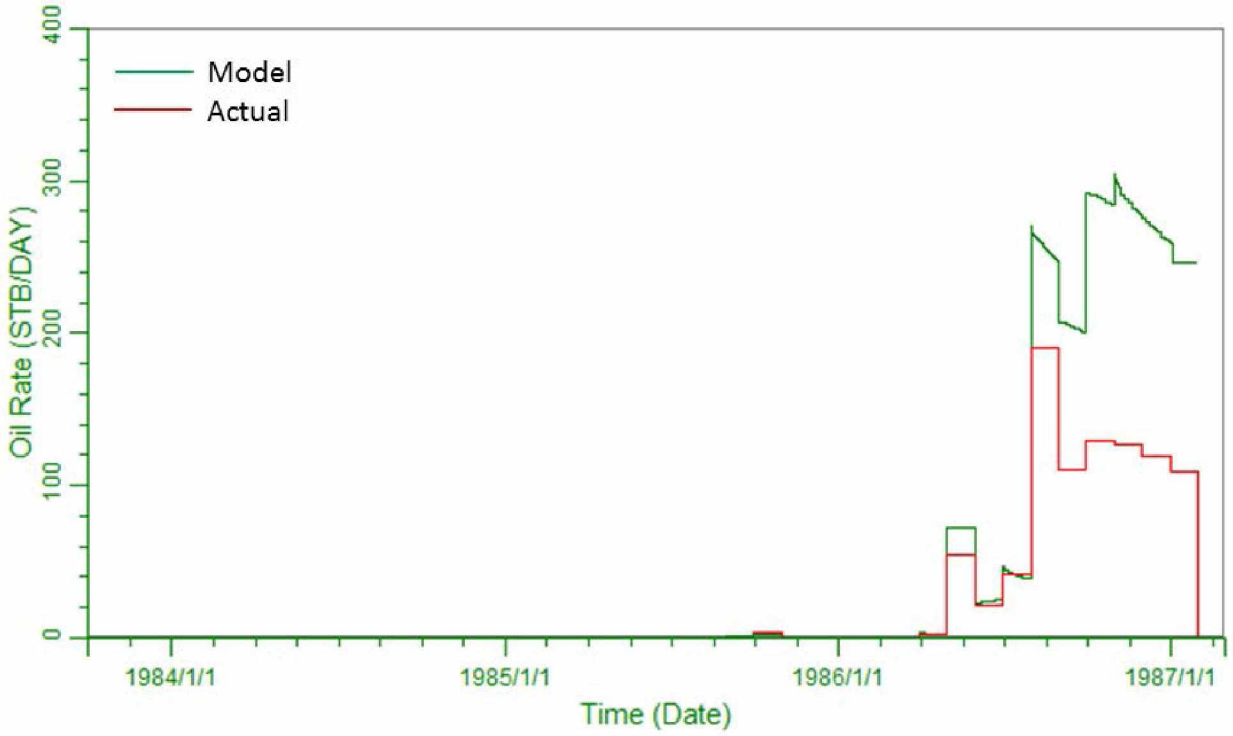

Figure A-37: Comparison of Actual and Calculated Model Oil Rates for West Sak Pilot Producer 20

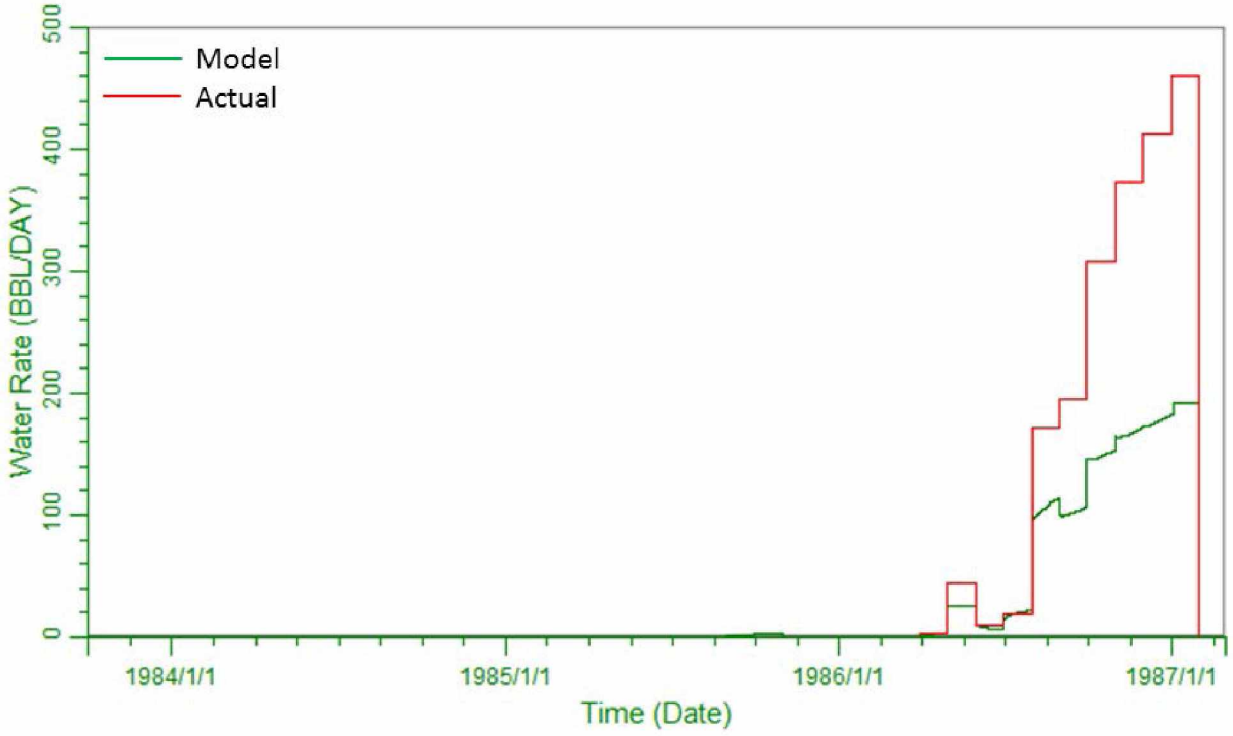

Figure A-38: Comparison of Actual and Calculated Model Water Rates for West Sak Pilot Producer 20

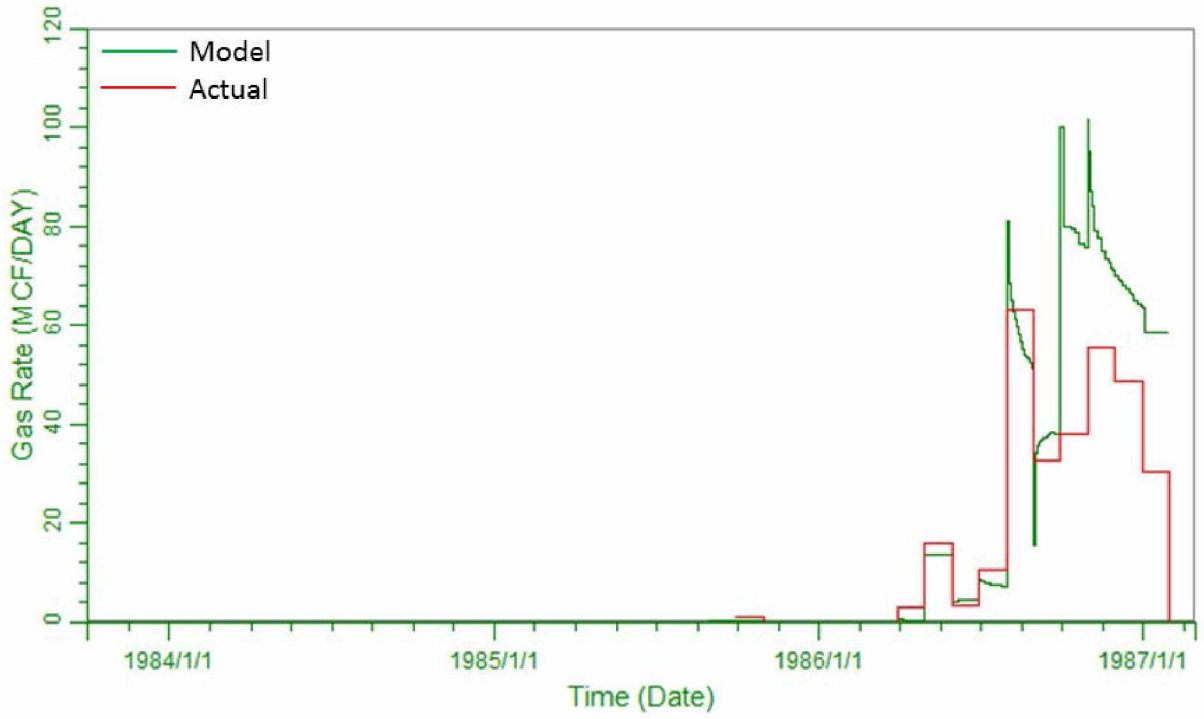

Figure A-39: Comparison of Actual and Calculated Model Gas Rates for West Sak Pilot Producer 20

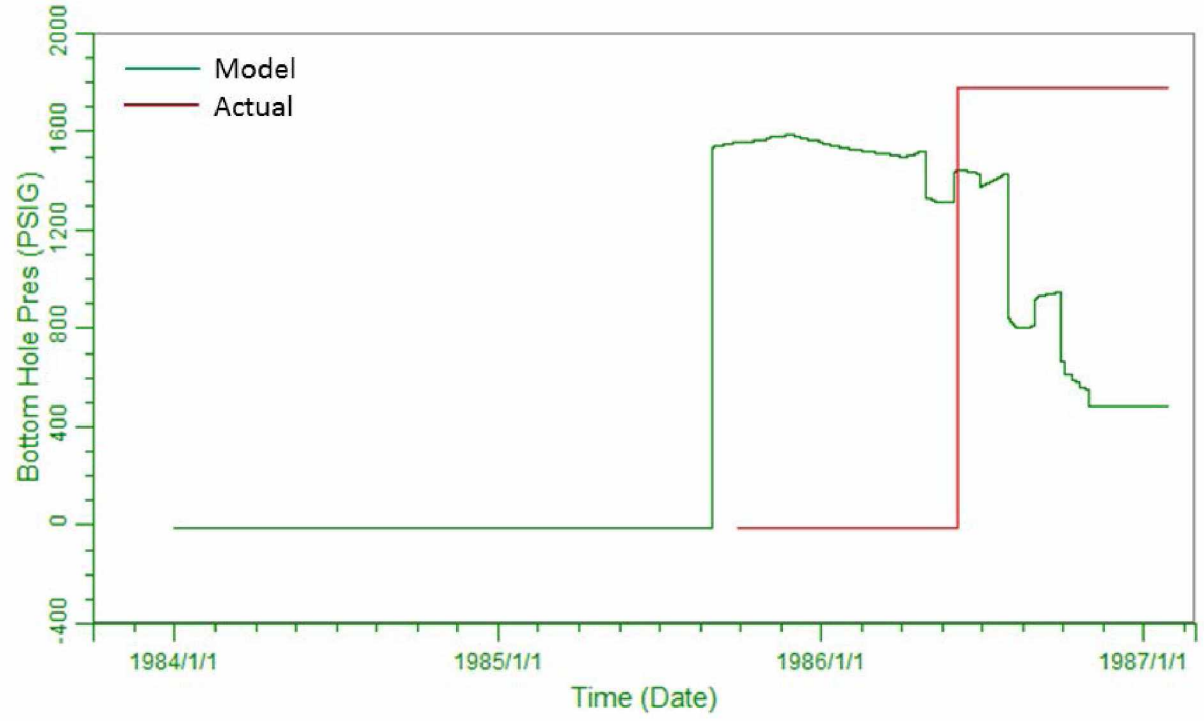

Figure A-40: Comparison of Actual and Calculated Model BHP for West Sak Pilot Producer 20

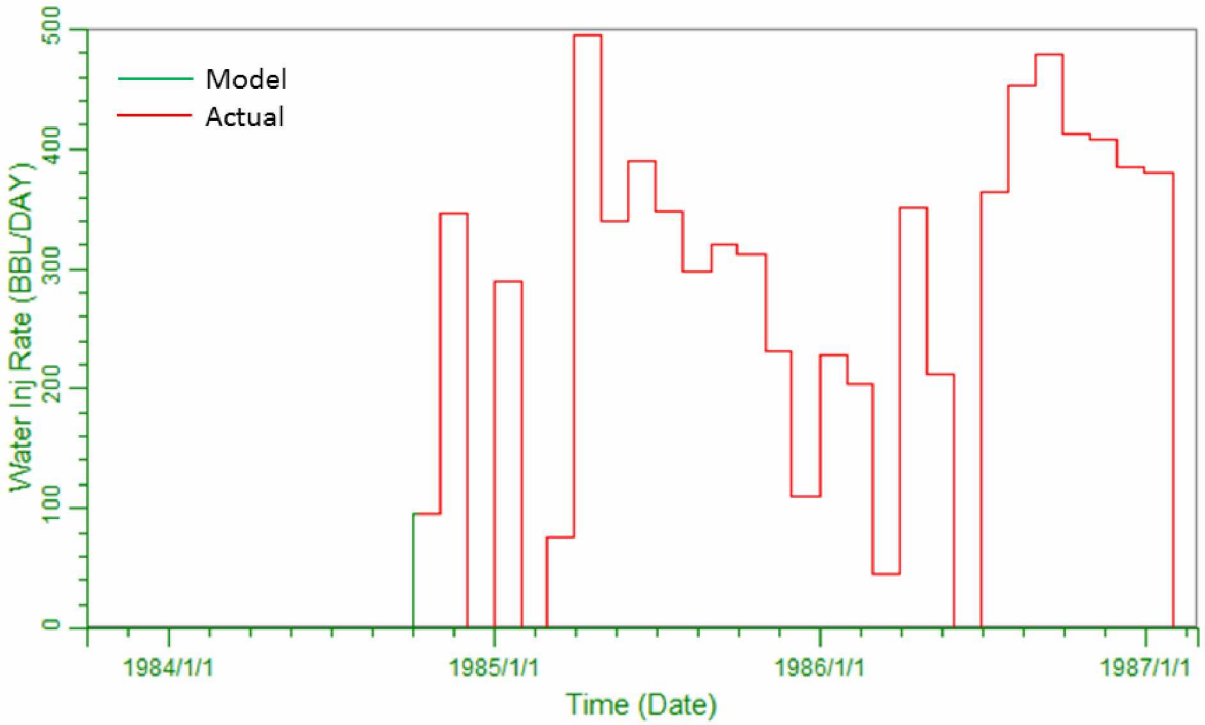

Figure A-41: Comparison of Actual and Calculated Model Water Injection Rates for West Sak Pilot Well 5i

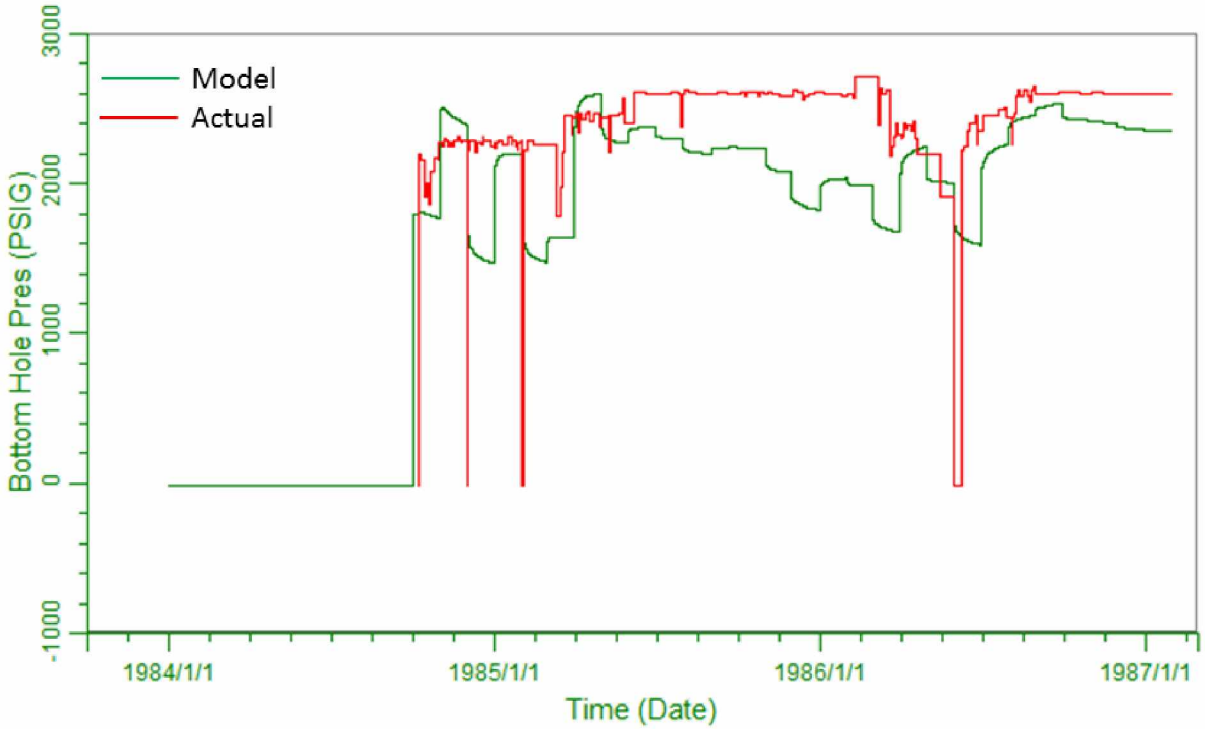

Figure A-42: Comparison of Actual and Calculated Model BHP for West Sak Pilot Injector 5i

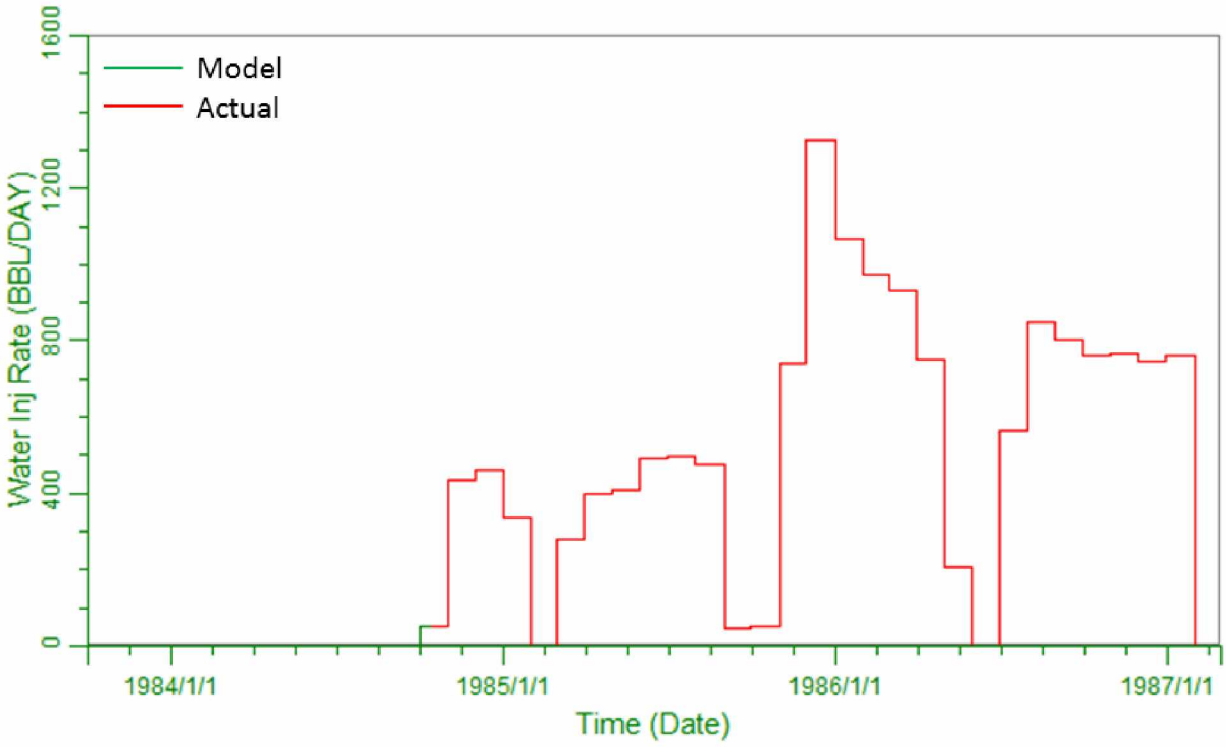

Figure A-43: Comparison of Actual and Calculated Model Water Injection Rates for West Sak Pilot Injector 6i

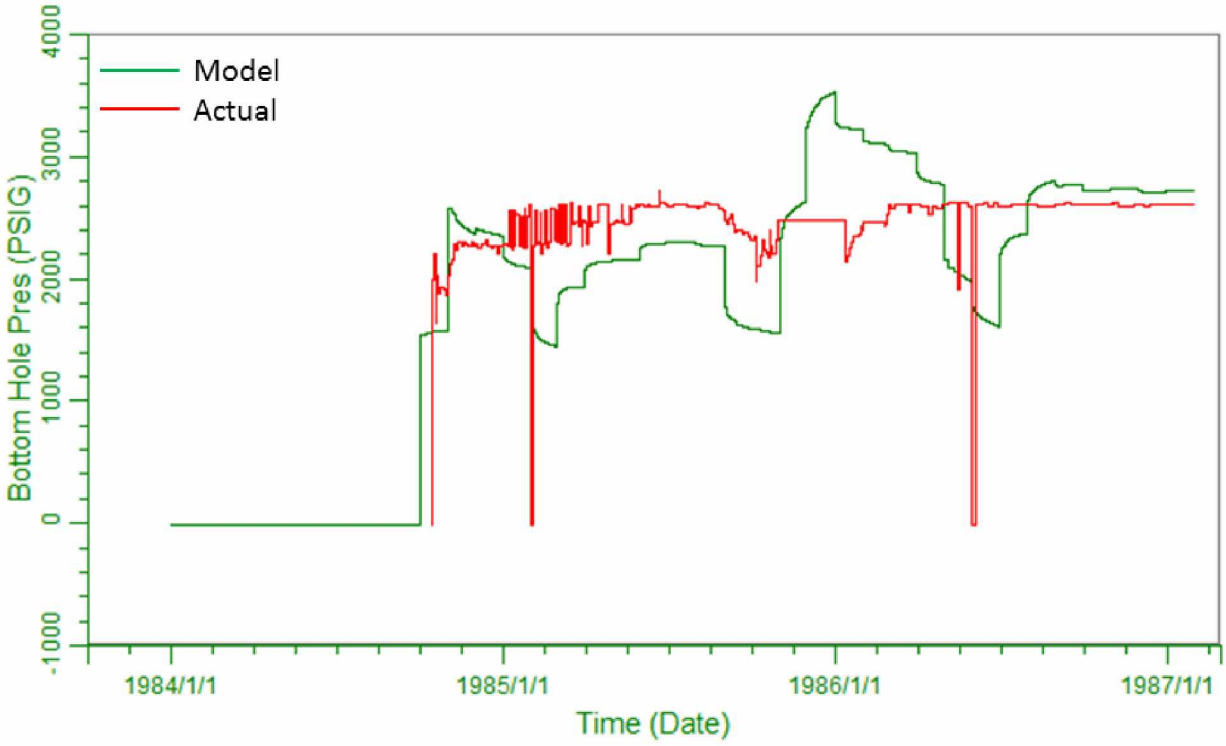

Figure A-44: Comparison of Actual and Calculated Model BHP for West Sak Pilot Injector 6i

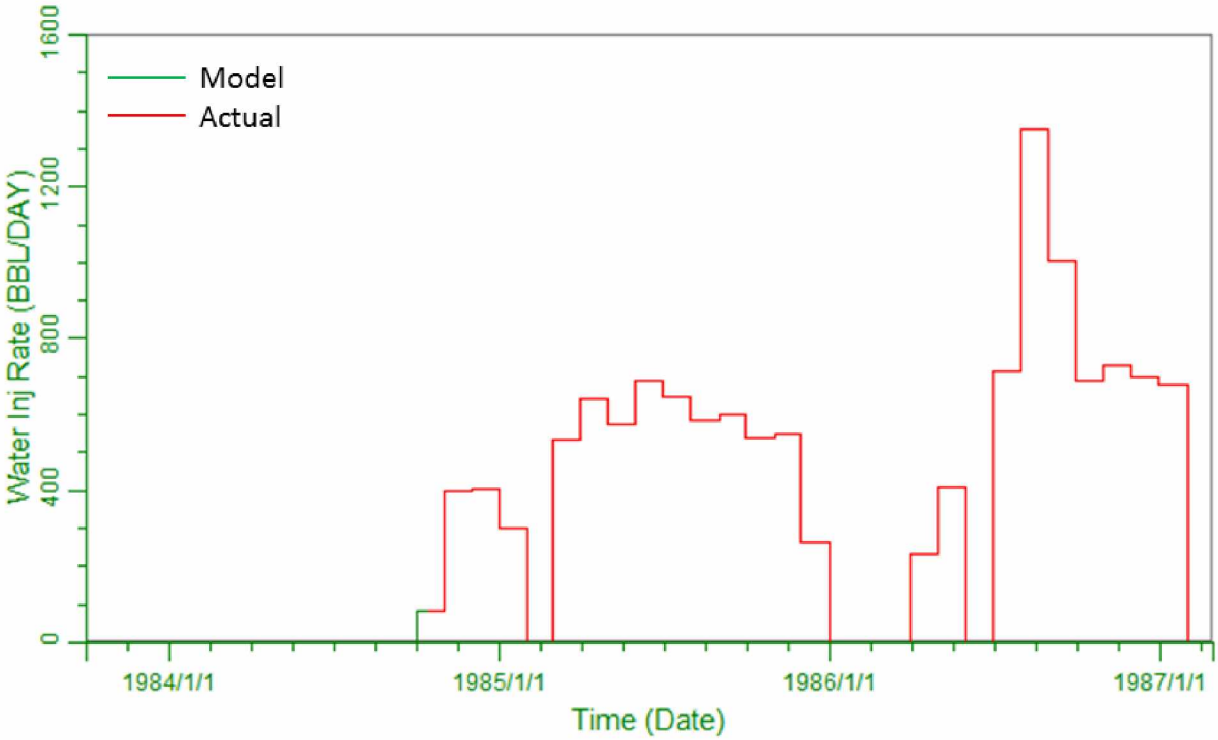

Figure A-45: Comparison of Actual and Calculated Model Water Injection Rates for West Sak Pilot Injector 8i

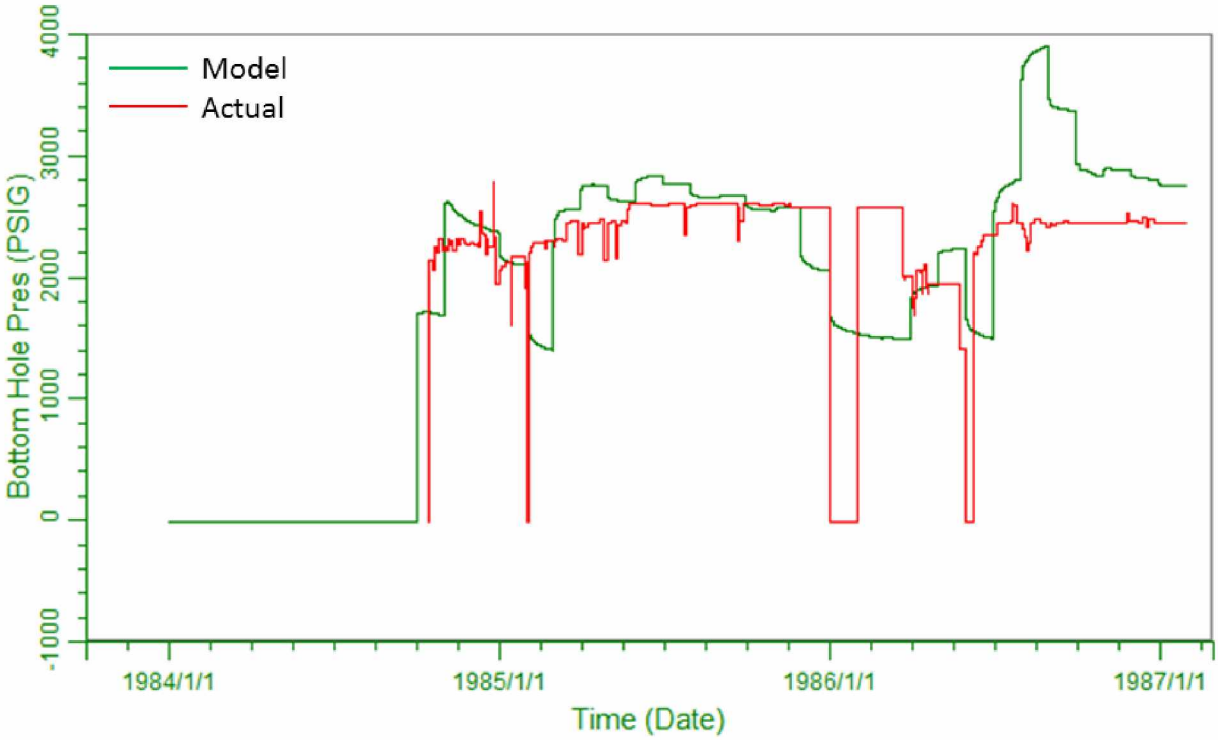

Figure A-46: Comparison of Actual and Calculated Model BHP for West Sak Pilot Injector 8i

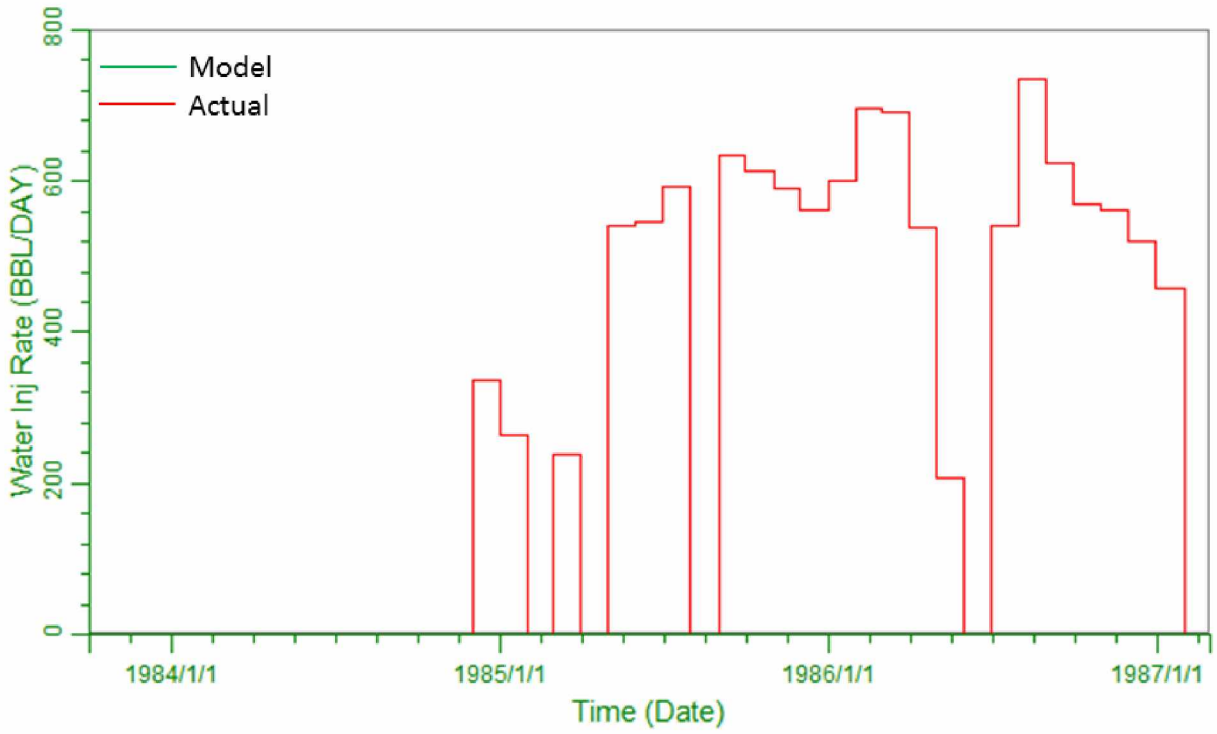

Figure A-47: Comparison of Actual and Calculated Model Water Injection Rates for West Sak Pilot Well 11i

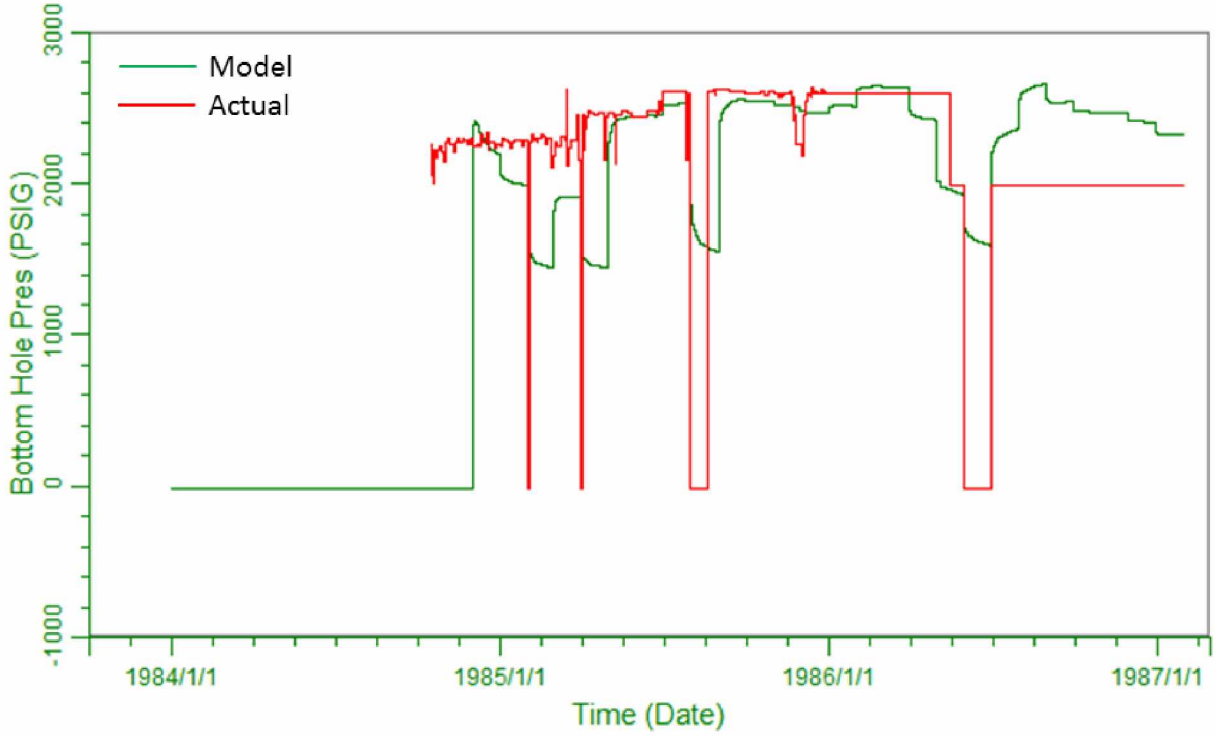

Figure A-48: Comparison of Actual and Calculated Model BHP for West Sak Pilot Injector 11i

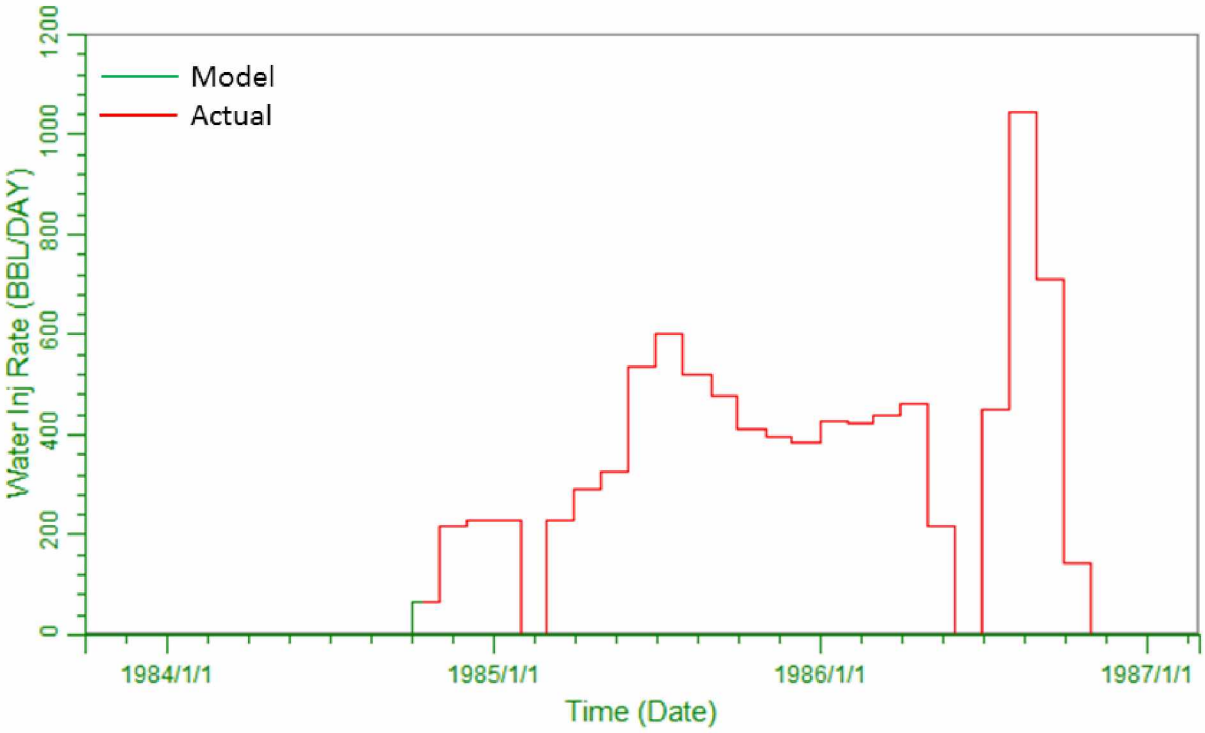

Figure A-49: Comparison of Actual and Calculated Model Water Injection Rates for West Sak Pilot Well 14i

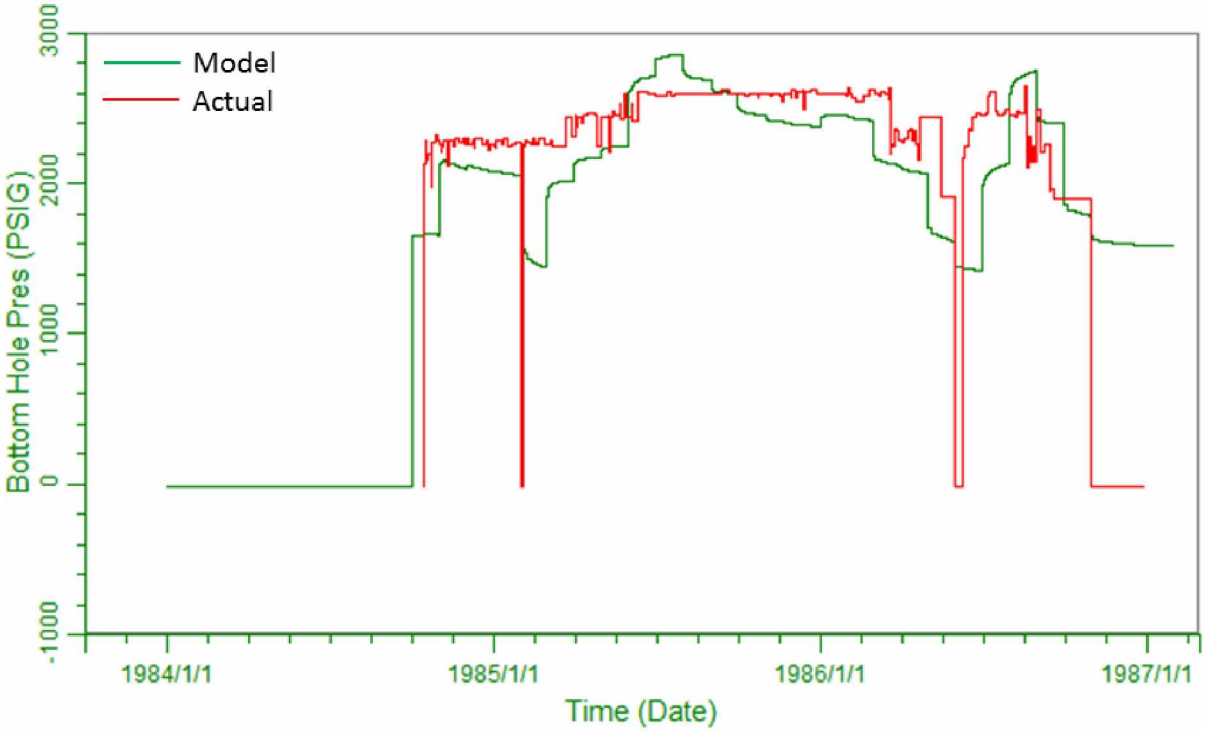

Figure A-50: Comparison of Actual and Calculated Model BHP for West Sak Pilot Injector 14i